ISSN 2410-6593

ТОНКИЕ ХИМИЧЕСКИЕ ТЕХНОЛОГИИ

Fine Chemical Technologies

- Theoretical Bases of Chemical Technology
- Chemistry and Technology of Organic Substances
- Chemistry and Technology of Medicinal Compounds and Biologically Active Substances
- Synthesis and Processing of Polymers and Polymeric Composites
- Chemistry and Technology of Inorganic Materials
- Analytical Methods in Chemistry and Chemical Technology
- Mathematical Methods and Information Systems in Chemical Technology

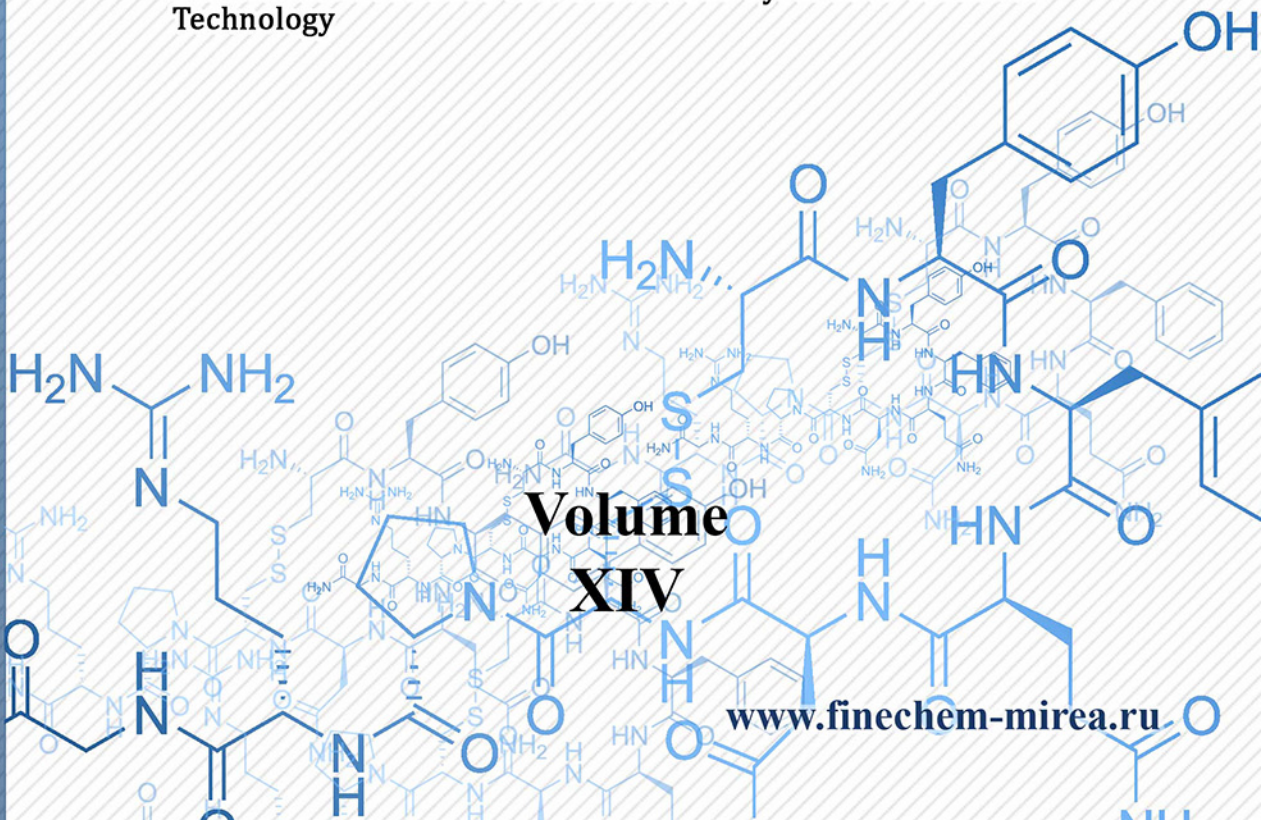

Volume XIV

4

2019

www.finechem-mirea.ru

ТОНКИЕ ХИМИЧЕСКИЕ ТЕХНОЛОГИИ | Fine Chemical Technologies

МИРЭА Российский технологический университет

МИТХТ

www.finechem-mirea.ru

ISSN 2410-6593

DEAR COLLEAGUE!

We invite you to publish articles in the peer-reviewed scientific and technical journal FINE CHEMICAL TECHNOLOGIES.

The peer-reviewed scientific and technical journal Fine Chemical Technologies highlights the modern achievements of fundamental and applied research in the field of fine chemical technologies, including theoretical bases of chemical technology, chemistry and technology of medicinal compounds and biologically active substances, organic substances and inorganic materials, synthesis and processing of polymers and polymeric composites, analytical and mathematical methods and information systems in chemistry and chemical technology.

The journal is included into the List of peer-reviewed science press of the State Commission for Academic Degrees and Titles of the Russian Federation.

- Six issues a year are published
- Publication is free of charge
- Double-blind peer review
- Submission is in English or in Russian

OPEN ACCESS

DOAJ DIRECTORY OF OPEN ACCESS JOURNALS

MAIN TOPICS

- Theoretical Bases of Chemical Technology
- Chemistry and Technology of Organic Substances
- Chemistry and Technology of Medicinal Compounds and Biologically Active Substances
- Synthesis and Processing of Polymers and Polymeric Composites
- Chemistry and Technology of Inorganic Materials
- Analytical Methods in Chemistry and Chemical Technology
- Mathematical Methods and Information Systems in Chemical Technology

INDEXATION

- CAS **Chemical Abstracts**
- **Russian Science Citation Index (RSCI) on WoS platform**
- **Science index**
- ULRICHWEB™ GLOBAL SERIALS DIRECTORY

RSCI Impact Factor (2017) 0.250

Founder and Publisher:
MIREA – Russian Technological University

The journal was founded in 2006 by M.V. Lomonosov Moscow State University of Fine Chemical Technologies and published under the Vestnik MITHT title till 2015.

Website: www.finechem-mirea.ru

Subscription index: 36924

Registration certificate ПИ № ФС 77–74580, December 14, 2018

Editor-in-Chief:
Dr. of Sci. (Engineering), Professor
ALLA K. FROLKOVA

Editorial contacts:

Editor: Galina D. Seredina
+7 (495) 246-05-55 (#2-88), e-mail: vestnik@mitht.ru

Executive Editor: Olga V. Esipova
+7 (495) 246-05-55 (#9-33), e-mail: esipova@mirea.ru

Address: 86, Vernadskogo pr., Moscow 119571, Russia

ISSN 2410-6593

ТОНКИЕ ХИМИЧЕСКИЕ ТЕХНОЛОГИИ

Fine Chemical Technologies

- **Theoretical Bases of Chemical Technology**
- **Chemistry and Technology of Organic Substances**
- **Chemistry and Technology of Medicinal Compounds and Biologically Active Substances**
- **Synthesis and Processing of Polymers and Polymeric Composites**
- **Chemistry and Technology of Inorganic Materials**
- **Analytical Methods in Chemistry and Chemical Technology**
- **Mathematical Methods and Information Systems in Chemical Technology**

Tonkie Khimicheskie Tekhnologii =
Fine Chemical Technologies
Vol. 14, No. 4, 2019

Тонкие химические технологии =
Fine Chemical Technologies
Том 14, № 4, 2019

https://doi.org/10.32362/2410-6593-2019-14-4
www.finechem-mirea.ru

https://doi.org/10.32362/2410-6593 ***www.finechem-mirea.ru***

Tonkie Khimicheskie Tekhnologii = Fine Chemical Technologies 2019, vol. 14, no. 4

The reviewed scientific and technical journal Fine Chemical Technologies highlights the modern achievements of fundamental and applied research in the field of fine chemical technologies, including theoretical bases of chemical technology, chemistry and technology of medicinal compounds and biologically active substances, organic substances and inorganic materials, synthesis and processing of polymers and polymeric composites, analytical and mathematical methods and information systems in chemistry and chemical technology.

Founder and Publisher

Federal State Budget
Educational Institution
of Higher Education
"MIREA – Russian Technological University"
78, Vernadskogo pr., Moscow 119454, Russian Federation.

Six issues a year are published.
The journal was founded in 2006. The name was Vestnik MITHT until 2015 (ISSN 1819-1487).

The journal is included into the List of peer-reviewed science press of the State Commission for Academic Degrees and Titles of the Russian Federation.
The journal is indexed:
DOAJ, Chemical Abstracts, Science Index, RSCI, Ulrich's International Periodicals Directory

Editor-in-Chief:
Alla K. Frolkova – Dr. of Sci. (Engineering), Professor, MIREA – Russian Technological University, Moscow, Russian Federation. Scopus Author ID 35617659200, ResearcherID G-7001-2018, http://orcid.org/0000-0002-9763-4717,
frolkova@mitht.ru

Deputy Editor-in-Chief:
Valery V. Fomichev – Dr. of Sci. (Chemistry), Professor, MIREA – Russian Technological University, Moscow, Russian Federation. Scopus Author ID 57196028937, http://orcid.org/0000-0003-4840-0655,
valeryfom@rambler.ru

Executive Editor:
Olga V. Esipova – Cand. of Sci. (Chemistry), Associate Professor, Deputy Editor-in-Chief of Editorial Department of MIREA – Russian Technological University, Moscow, Russian Federation, Member of the Association of Scientific Editors and Publishers (ASEP)
esipova@mitht.ru

Editorial Staff:
Chief of the Editorial Staff — Galina D. Seredina
Science editors — prof. Tatyana M. Buslaeva, prof. Anatolii V. Markov
Desktop Publishing — Larisa G. Semernya

86, Vernadskogo pr., Moscow, 119571 Russia.
Phone: +7(495) 246-05-55 (#2-88)
E-mail: *vestnik@mitht.ru*

Registration certificate ПИ № ФС 77–74580, issued on December 14, 2018 by the Federal Service for Supervision of Communications, Information Technology, and Mass Media of Russia
The subscription index of «Pressa Rossii»: **36924**

Тонкие химические технологии = Fine Chemical Technologies 2019, том 14, № 4

Научно-технический рецензируемый журнал «Тонкие химические технологии» освещает современные достижения фундаментальных и прикладных исследований в области тонких химических технологий, включая теоретические основы химической технологии, химию и технологию лекарственных препаратов и биологически активных соединений, органических веществ и неорганических материалов, синтез и переработку полимеров и композитов на их основе, аналитические и математические методы и информационные системы в химии и химической технологии.

Учредитель и издатель

федеральное государственное бюджетное
образовательное учреждение
высшего образования
«МИРЭА – Российский технологический университет»
119454, РФ, г. Москва, пр-кт Вернадского, д. 78.

Периодичность: 6 раз в год.
Журнал основан в 2006 году. До 2015 года издавался под названием «Вестник МИТХТ» (ISSN 1819-1487).

Журнал входит в Перечень ведущих рецензируемых научных журналов ВАК РФ.
Индексируется:
DOAJ, Chemical Abstracts, РИНЦ (Science Index), RSCI, Ulrich's International Periodicals Directory

Главный редактор:
Фролкова Алла Константиновна – д.т.н., профессор, МИРЭА – Российский технологический университет, Москва, Российская Федерация. Scopus Author ID 35617659200, ResearcherID G-7001-2018, http://orcid.org/0000-0002-9763-4717,
frolkova@mitht.ru

Заместитель главного редактора:
Фомичёв Валерий Вячеславович – д.х.н., профессор, МИРЭА – Российский технологический университет, Москва, Российская Федерация. Scopus Author ID 57196028937, http://orcid.org/0000-0003-4840-0655,
valeryfom@rambler.ru

Ответственный секретарь:
Есипова Ольга Валерьевна – к.х.н., доцент, зам. главного редактора Редакционно-издательского отдела, МИРЭА – Российский технологический университет, Москва, Российская Федерация, член Ассоциации научных редакторов и издателей (АНРИ)
esipova@mitht.ru

Редакция:
Зав. редакцией — Г.Д. Середина
Научные редакторы — проф. Т.М. Буслаева, проф. А.В. Марков
Компьютерная верстка — Л.Г. Семерня

119571, г. Москва, пр. Вернадского, 86, оф. Л-119.
Тел.: +7(495) 246-05-55 (#2-88)
E-mail: *vestnik@mitht.ru*

Свидетельство о регистрации СМИ: ПИ № ФС 77-74580 от 14.12.2018 выдано Федеральной службой по надзору в сфере связи, информационных технологий и массовых коммуникаций (Роскомнадзор)
Индекс по Объединенному каталогу «Пресса России»: **36924**

© МИРЭА – Российский технологический университет, 2019

Editorial Board

Zinesh S. Abisheva – Corresponding Member of the National Academy of Sciences of Kazakhstan, Dr. Sci. (Eng.), Professor, Institute of Metallurgy and Ore Beneficiation, K.I. Satpaev Kazakh National Research Technical University, Almaty, Kazakhstan. Scopus Author ID 6601954283, ResearcherID O-8453-2017, http://orcid.org/0000-0002-4506-0694, *abisheva_z@mail.ru.*

Sergey P. Verevkin – Dr. Sci. (Eng.), Professor, University of Rostock, Rostock, Germany. Scopus Author ID 7006607848, ResearcherID G-3243-2011, *Sergey.verevkin@uni-rostock.de.*

Dmitry V. Drobot – Dr. Sci. (Chem.), Professor, MIREA – Russian Technological University, Moscow, Russian Federation. Scopus Author ID 35580931100, *dvdrobot@mail.ru* .

Konstantin Yu. Zhizhin – Corresponding Member of the Russian Academy of Sciences, Dr. Sci. (Chem.), Professor, N.S. Kurnakov Institute of General and Inorganic Chemistry of the RAS, Moscow, Russian Federation. Scopus Author ID 6701495620, ResearcherID C-5681-2013, http://orcid.org/0000-0002-4475-124X, *kyuzhizhin@igic.ras.ru.*

Vladimir K. Ivanov– Corresponding Member of the Russian Academy of Sciences, Dr. Sci. (Chem.), Professor, N.S. Kurnakov Institute of General and Inorganic Chemistry of the RAS, Moscow, Russian Federation. Scopus Author ID 56532555100, ResearcherID H-4407-2011, https://orcid.org/0000-0003-2343-2140, *van@igic.ras.ru.*

Igor V. Ivanov – Dr. Sci. (Chem.), Professor, MIREA – Russian Technological University, Moscow, Russian Federation. Scopus Author ID 34770109800, ResearcherID I-5606-2016, http://orcid.org/0000-0003-0543-2067, *ivanov_i@mirea.ru.*

Anatolii A. Ischenko – Dr. Sci. (Chem.), Professor, MIREA – Russian Technological University, Moscow, Russian Federation. Scopus Author ID 6701507307, *aischenko@yasenevo.ru.*

Carlos A. Cardona – PhD (Eng.), Professor, National University of Columbia, Manizales, Colombia. Scopus Author ID 7004278560, ResearcherID G-8554-2016, http://orcid.org/0000-0002-0237-2313, *ccardonaal@unal.edu.co.*

Oskar I. Koifman – Corresponding Member of the Russian Academy of Sciences, Dr. Sci. (Chem.), Professor, Ivanovo University of Chemical Technology, Ivanovo, Russian Federation. Scopus Author ID 6602070468, ResearcherID R-1020-2016, http://orcid.org/0000-0002-1764-0819, *president@isuct.ru.*

Valery F. Kornyushko – Dr. Sci. (Eng.), Professor, MIREA – Russian Technological University, Moscow, Russian Federation, *vfk256@mail.ru.*

Elvira T. Krut'ko – Dr. Sci. (Eng.), Professor, Belarusian State Technological University, Minsk, Belarus. Scopus Author ID 6602297257, *ela_krutko@mail.ru.*

Anatolii I. Miroshnikov – Academician at the Russian Academy of Sciences, Dr. Sci. (Chem.), Professor, M.M. Shemyakin and Yu.A. Ovchinnikov Institute of Bioorganic Chemistry of the RAS, Member of the Presidium of the RAS, Chairman of the Presidium of the RAS Pushchino Research Center, Moscow, Russian Federation. Scopus Author ID 7006592304, ResearcherID G-5017-2017, *aiv@ibch.ru.*

Редакционная коллегия

Абишева Зинеш Садыровна – член-корр. Национальной Академии Наук Республики Казахстан, д.т.н., профессор, Институт металлургии и обогащения, Казахский национальный технический университет имени К. И. Сатпаева, Алматы, Казахстан. Scopus Author ID 6601954283, ResearcherID O-8453-2017, http://orcid.org/0000-0002-4506-0694, *abisheva_z@mail.ru.*

Верёвкин Сергей Петрович – д.т.н., профессор Университета г. Росток, Росток, Германия. Scopus Author ID 7006607848, ResearcherID G-3243-2011, *Sergey.verevkin@uni-rostock.de.*

Дробот Дмитрий Васильевич – д.х.н., проф., МИРЭА – Российский технологический университет, Москва, Российская Федерация. Scopus Author ID 35580931100, *dvdrobot@mail.ru.*

Жижин Константин Юрьевич – член-корр. Российской академии наук, д.х.н., профессор, Институт общей и неорганической химии им. Н.С. Курнакова РАН, Москва, Российская Федерация. Scopus Author ID 6701495620, ResearcherID C-5681-2013, http://orcid.org/0000-0002-4475-124X, *kyuzhizhin@igic.ras.ru.*

Иванов Владимир Константинович – член-корр. Российской академии наук, д.х.н., профессор, Институт общей и неорганической химии им. Н.С. Курнакова РАН, Москва, Российская Федерация. Scopus Author ID 56532555100, ResearcherID H-4407-2011, https://orcid.org/0000-0003-2343-2140, *van@igic.ras.ru.*

Иванов Игорь Владимирович – д.х.н., профессор, МИРЭА – Российский технологический университет, Москва, Российская Федерация. Scopus Author ID 34770109800, ResearcherID I-5606-2016, http://orcid.org/0000-0003-0543-2067, *ivanov_i@mirea.ru.*

Ищенко Анатолий Александрович – д.х.н., профессор, МИРЭА – Российский технологический университет, Москва, Российская Федерация. Scopus Author ID 6701507307, *aischenko@yasenevo.ru.*

Кардона Карлос Ариэль – профессор Национального университета Колумбии, Манизалес, Колумбия. Scopus Author ID 7004278560, ResearcherID G-8554-2016, http://orcid.org/0000-0002-0237-2313, *ccardonaal@unal.edu.co.*

Койфман Оскар Иосифович – член-корр. Российской академии наук, д.х.н., профессор, Ивановский химико-технологический университет, Иваново, Российская Федерация. Scopus Author ID 6602070468, ResearcherID R-1020-2016, http://orcid.org/0000-0002-1764-0819, *president@isuct.ru.*

Корнюшко Валерий Федорович – д.т.н., профессор, МИРЭА – Российский технологический университет, Москва, Российская Федерация, *vfk256@mail.ru.*

Крутько Эльвира Тихоновна – д.т.н., профессор Белорусского государственного технологического университета, Минск, Беларусь. Scopus Author ID 6602297257, *ela_krutko@mail.ru.*

Мирошников Анатолий Иванович – академик Российской академии наук, д.х.н., профессор, Институт биоорганической химии им. академиков М.М. Шемякина и Ю.А. Овчинникова РАН, член Президиума РАН, председатель Президиума Пущинского научного центра РАН, Москва, Российская Федерация. Scopus Author ID 7006592304, ResearcherID G-5017-2017, *aiv@ibch.ru.*

Yuri P. Miroshnikov – Dr. Sci. (Chem.), Professor, MIREA – Russian Technological University Moscow, Russian Federation. Scopus Author ID, 6603349573, *miroshnikov@mirea.ru.*

Aziz M. Muzafarov – Academician at the RAS, Dr. Sci. (Chem.), Professor, A.N. Nesmeyanov Institute of Organoelement Compounds of the RAS, Moscow, Russian Federation. ResearcherID G-1644-2011, https://orcid.org/0000-0002-3050-3253, *aziz@ineos.ac.ru.*

Ivan A. Novakov – Academician at the Russian Academy of Sciences, Dr. Sci. (Chem.), Professor, Volgograd State Technical University, Volgograd, Russian Federation. Scopus Author ID 7003436556, ResearcherID I-4668-2015, http://orcid.org/0000-0002-0980-6591, *president@vstu.ru.*

Alexander N. Ozerin – Corresponding Member of the Russian Academy of Sciences, Dr. Sci. (Chem.), Professor, Enikolopov Institute of Synthetic Polymeric Materials of the RAS, Moscow, Russian Federation. Scopus Author ID 7006188944, ResearcherID J-1866-2018, https://orcid.org/0000-0001-7505-6090, *ozerin@ispm.ru.*

Tapani A. Pakkanen – PhD, Professor, Head of Department of Chemistry, University of Eastern Finland, Joensuu, Finland. Scopus Author ID 7102310323, *tapani.pakkanen@uef.fi.*

Armando J.L. Pombeiro – Academician at the Academy of Sciences of Lisbon, PhD, Professor, Higher Technical Institute of the University of Lisbon, Lisbon, Portugal. Scopus Author ID 57191350501, 7006067269; ResearcherID I-5945-2012, https://orcid.org/0000-0001-8323-888X, *pombeiro@ist.utl.pt.*

Dmitrii V. Pyshnyi – Corresponding Member of the Russian Academy of Sciences, Dr. Sci. (Chem.), Professor, Institute of Chemical Biology and Fundamental Medicine, Siberian Branch of the Russian Academy of Sciences, Novosibirsk, Russian Federation. Scopus Author ID 7006677629, ResearcherID F-4729-2013, https://orcid.org/0000-0002-2587-3719, *pyshnyi@niboch.nsc.ru.*

Alexander S. Sigov – Academician at the Russian Academy of Sciences, Dr. Sci. (Phys. and Math.), Professor, President of MIREA – Russian Technological University, Moscow, Russian Federation. Scopus Author ID 35557510600, ResearcherID L-4103-2017, *sigov@mirea.ru.*

Vladimir A. Tverskoy – Dr. Sci. (Chem.), Professor, MIREA – Russian Technological University, Moscow, Russian Federation. Scopus Author ID 6604012434, 29567701900, ResearcherID H-8042-2017, https://orcid.org/0000-0003-4348-8854, *tverskoy@mitht.ru.*

Alexander M. Toikka – Dr. Sci. (Chem.), Professor, Faculty of Chemistry, Saint Petersburg State University, St. Petersburg, Russian Federation. Scopus Author ID 6603464176, ResearcherID A-5698-2010, http://orcid.org/0000-0002-1863-5528, *a.toikka@spbu.ru.*

Andrzej W. Trochimczuk – Dr. Sci. (Chem.), Professor, Faculty of Chemistry, Wrocław University of Science and Technology, Wroclaw, Poland. Scopus Author ID 7003604847, *andrzej.trochimczuk@pwr.edu.pl.*

Aslan Yu. Tsivadze – Academician at the Russian Academy of Sciences, Dr. Sci. (Chem.), Professor, A.N. Frumkin Institute of Physical Chemistry and Electrochemistry of the RAS, Moscow, Russian Federation. Scopus Author ID 7004245066, ResearcherID G-7422-2014, *tsiv@phyche.ac.ru.*

Мирошников Юрий Петрович – д.х.н., профессор, МИРЭА – Российский технологический университет, Москва, Российская Федерация. Scopus Author ID 6603349573, *miroshnikov@mirea.ru.*

Музафаров Азиз Мансурович – академик Российской академии наук, д.х.н., профессор, Институт элементоорганических соединений им. А.Н. Несмеянова РАН, Москва, Российская Федерация. ResearcherID G-1644-2011, https://orcid.org/0000-0002-3050-3253, *aziz@ineos.ac.ru.*

Новаков Иван Александрович – академик Российской академии наук, д.х.н., профессор, президент Волгоградского государственного технического университета, Волгоград, Российская Федерация. Scopus Author ID 7003436556, ResearcherID I-4668-2015, http://orcid.org/0000-0002-0980-6591, *president@vstu.ru.*

Озерин Александр Никифорович – член-корр. Российской академии наук, д.х.н., профессор, Институт синтетических полимерных материалов им. Н.С. Ениколопова РАН, Москва, Российская Федерация. Scopus Author ID 7006188944, ResearcherID J-1866-2018, https://orcid.org/0000-0001-7505-6090, *ozerin@ispm.ru.*

Пакканен Тапани – профессор, руководитель Департамента химии Университета Восточной Финляндии, Йоенсуу, Финляндия. Scopus Author ID 7102310323, *tapani.pakkanen@uef.fi.*

Помбейро Армандо – академик АН Лиссабона, профессор, президент Центра структурной химии Высшего технического института Университета Лиссабона, Португалия. Scopus Author ID 57191350501, 7006067269; ResearcherID I-5945-2012, https://orcid.org/0000-0001-8323-888X, *pombeiro@ist.utl.pt.*

Пышный Дмитрий Владимирович – член-корр. Российской академии наук, д.х.н., профессор, Институт химической технологии и фундаментальной медицины Сибирского отделения РАН, Новосибирск, Российская Федерация. Scopus Author ID 7006677629, ResearcherID F-4729-2013, https://orcid.org/0000-0002-2587-3719, *pyshnyi@niboch.nsc.ru.*

Сигов Александр Сергеевич – академик Российской академии наук, док.физ.-мат.наук, профессор, президент МИРЭА – Российского технологического университета, Москва, Российская Федерация. Scopus Author ID 35557510600, ResearcherID L-4103-2017, *sigov@mirea.ru.*

Тверской Владимир Аркадьевич – д.х.н., профессор, МИРЭА – Российский технологический университет, Москва, Российская Федерация. Scopus Author ID 6604012434, 29567701900, ResearcherID H-8042-2017, https://orcid.org/0000-0003-4348-8854, *tverskoy@mitht.ru*.

Тойкка Александр Матвеевич – д.х.н., проф., Институт химии, Санкт-Петербургский государственный университет, Санкт-Петербург, Российская Федерация. Scopus Author ID 6603464176, ResearcherID A-5698-2010, http://orcid.org/0000-0002-1863-5528, *a.toikka@spbu.ru.*

Трохимчук Анджей – д.х.н., профессор, Химический факультет Вроцлавского политехнического университета, Вроцлав, Польша. Scopus Author ID 7003604847, *andrzej.trochimczuk@pwr.edu.pl.*

Цивадзе Аслан Юсупович – академик Российской академии наук, д.х.н., профессор, Институт физической химии и электрохимии им. А.Н. Фрумкина РАН, Москва, Российская Федерация. Scopus Author ID 7004245066, ResearcherID G-7422-2014, *tsiv@phyche.ac.ru.*

ТОНКИЕ ХИМИЧЕСКИЕ ТЕХНОЛОГИИ | Fine Chemical Technologies

4

2019

CONTENTS

СОДЕРЖАНИЕ

Fine Chemical Technologies, 2019, Vol. 14, No. 4, pp. 7–23.
Original Russian Text © Mikhail V. Chudinov, published in Tonkie Khimicheskie Tekhnologii, 2019, Vol. 14, No. 4, pp. 7–23

REVIEW ARTICLES

ОБЗОРНЫЕ СТАТЬИ

https://doi.org/10.32362/2410-6593-2019-14-4-7-23
UDC 615.281.8, 615.277.3, 544.165

CC BY

Ribavirin and its analogs: Can you teach an old dog new tricks?

Mikhail V. Chudinov

MIREA – Russian Technological University (M.V. Lomonosov Institute of Fine Chemical Technologies), Moscow 119571, Russia
@Corresponding author, e-mail: chudinov@mirea.ru

The review article focuses on the current state of synthetic and biological studies of ribavirin analogs. Ribavirin is a broad-spectrum nucleoside antiviral drug with a 50-year long history of research and application, but its mechanism of action still remains unclear. This article examines contemporary views on the antiviral and antitumor effects of ribavirin and its analogs and describes the contradictions and gaps that exist in our knowledge. In recent years, new nucleoside analogs of ribavirin have been synthesized. These ribavirin derivatives modified at the heterocyclic base, have the potential to become the antiviral and antitumor agents of the new generation. Thus, this paper presents a systematic review of antiviral activities, antitumor activities and structure–activity relationship (SAR) correlations of 39 ribavirin analogs created in the past 15 years. Biological targets and possible mechanisms of action of these new compounds are also discussed, as well as the prospects and possible directions for further research.

Keywords: *ribavirin, ribavirin analogs, biological mechanism, bioisosterism, antiviral drugs, antitumor drugs.*

Рибавирин и его аналоги: можно ли старую собаку научить новым фокусам

М.В. Чудинов

МИРЭА – Российский технологический университет (Институт тонких химических технологий имени М.В. Ломоносова), Москва 119571, Россия
@Автор для переписки, e-mail: chudinov@mirea.ru

Обзор посвящен современному состоянию синтетических и биологических исследований аналогов рибавирина. Рибавирин – нуклеозидный противовирусный препарат широкого спектра действия с 50-ти-летней историей исследований и применения, но механизмы его действия до сих пор остаются неясными. В обзоре кратко изложены современные взгляды на биологические механизмы противовирусного и противоопухолевого действия рибавирина и его аналогов, существующие в этих взглядах противоречия и пробелы. В течение последних лет получены новые нуклеозидные аналоги – производные рибавирина по гетероциклическому основанию, потенциально представляющие собой противовирусные и противоопухолевые средства нового поколения. В статье дан систематический обзор исследований противовирусной и противоопухолевой активности и корреляций «структура – активность», в общей сложности, для 39 аналогов рибавирина, представленных за последние 15 лет, обсуждаются биологические мишени и возможные механизмы действия этих новых соединений, а также перспективы и направление дальнейших исследований.

Ключевые слова: *рибавирин, аналоги рибавирина, механизмы биологического действия, биоизостеризм, противовирусные препараты, противоопухолевые препараты.*

Introduction

Diseases caused by viral infections are the reality we face. It is no secret that the majority of the available "powerful medicines against colds and the flu" are just costly placebos, whereas the treatment of serious, life-threatening illnesses such as difficult cases of influenza, viral hepatitis and hemorrhagic fever, requires a different approach. Among the drugs that doctors turn to when everything else has been tried, ribavirin occupies a special place. This molecule, 1-(β-D-ribofuranosyl)-1,2,4-triazole-3-carboxamide, is also called virazole (**1**) (Fig. 1).

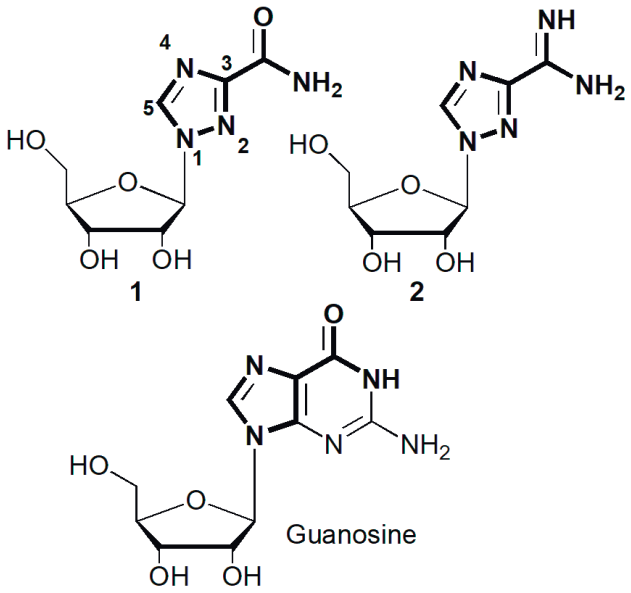

Fig. 1. Ribavirin (**1**) and related compounds, viramidine (**2**) and guanosine (isosteric fragments in heterocycles are highlighted in the bold line).

Having been introduced into clinics almost 50 years ago, ribavirin is still in use, despite several generations of new medications which came after it. All of the drug's drawbacks, such as systemic toxicity, low efficiency of monotherapy for various infections, the significant cost of the course of treatment, are compensated by ribavirin's wide range of antiviral activity. The molecule is active *in vitro* against many RNA- and DNA-containing viruses [1–10], and its *in vivo* activity is just slightly lower. Until recently, the drug was used (in combination with pegylated interferon alfa, INF-α) as the sole effective medication against hepatitis C and in the treatment of severe viral infections, for example, Crimean–Congo hemorrhagic fever, yellow fever, life-threatening cases of influenza. Nonetheless, the introduction of protease inhibitors, such as Sofosbuvir and Simeprevir, seems to have limited the use of ribavirin in hepatitis C treatment – and, fortunately, the other rest of the abovementioned infections are not very common. Does it mean that ribavirin, like many old drugs, is losing its relevance?

According to the Web of Science database, 10 014 articles containing the word "ribavirin" in the title have been published between 1975 and 2019, and 23 480 articles mentioned the drug amongst the keywords. Most of the research was purely medical, and only about 8500 articles were related to chemistry or the molecular biology of the cell. The number of such publications increased every year, from 45 in 1995 to 651 in 2015. After 2015 there was a significant loss of interest to the drug, potentially due to the introduction of protease inhibitors for hepatitis C treatment. Even so, there were 451 publications about it in 2018.

The uniqueness of ribavirin is in its diverse mechanisms of action which are not fully understood even today. So far, multiple attempts to modify the molecule and generate a substance as effective as ribavirin but without its drawbacks, have yielded just

one relatively successful outcome—viramidine (**2**) (1-(β-D-ribofuranosyl)-1,2,4-triazole-3-carboxamidine, taribavirin). This substance (which is less toxic) is a prodrug of ribavirin and is being tested in a Phase IV clinical trial. The research carried out within the last decade opens up new prospects for ribavirin and its derivatives and analogs.

1. Metabolism and mechanism of action of ribavirin and its structural analogs: contemporary concepts

Ribavirin's metabolism and mechanisms of antiviral action are in the focus of multiple review articles [11–21], so less detail of these processes will be presented here. In brief, ribavirin enters the cell through the cytoplasmic membrane with the help of nucleoside transporters CNT3 and ENT1. Then it is phosphorylated in the cytosol by the adenosine kinase, hADK (EC:2.7.1.20) (Fig. 2). Phosphorylation may also occur with the help the cytosolic purine 5'-nucleotidase (EC:3.1.3.5) [22]. Ribavirin 5'-*O*-monophosphate (RMP) (**3**) is processed further by kinases [23] into 5'-di- and triphosphates (**4** and **5**, respectively), which serve as substrates for many enzymes of the host cell and viruses.

Viramidine **2** is also a substrate for hADK, but it is phosphorylated 10–300 times slower than ribavirin, and is 10^4–10^5 times slower than adenosine [22]. Ribavirin's systemic toxicity is explained by the accumulation of its phosphates in erythrocytes, leading to hemolytic anemia in 10% of the patients undergoing a prolonged treatment with it [24]. Other cell types (for example, hepatocytes) remove the metabolites rather quickly ($T_{1/2}$ < 2 h) when the extracellular drug concentration decreases. The metabolites are dephosphorylated back into ribavirin by inosine triphosphate pyrophosphatase (EC:3.6.1.9) [25, 26], then ribavirin undergoes reversible phosphorolysis by purine nucleoside phosphorylase (PNP) (EC:3.6.1.9) [27] and/or hydrolysis of the carboxamide group by adenosine deaminase (ADA) (EC:3.5.4.4) [28, 29]. Thus, the main products of ribavirin's catabolism are 1,2,4-triazole-3-carboxamide (**7**) and 1,2,4-triazole-3-carboxylic acid (**8**), which are released from the body.

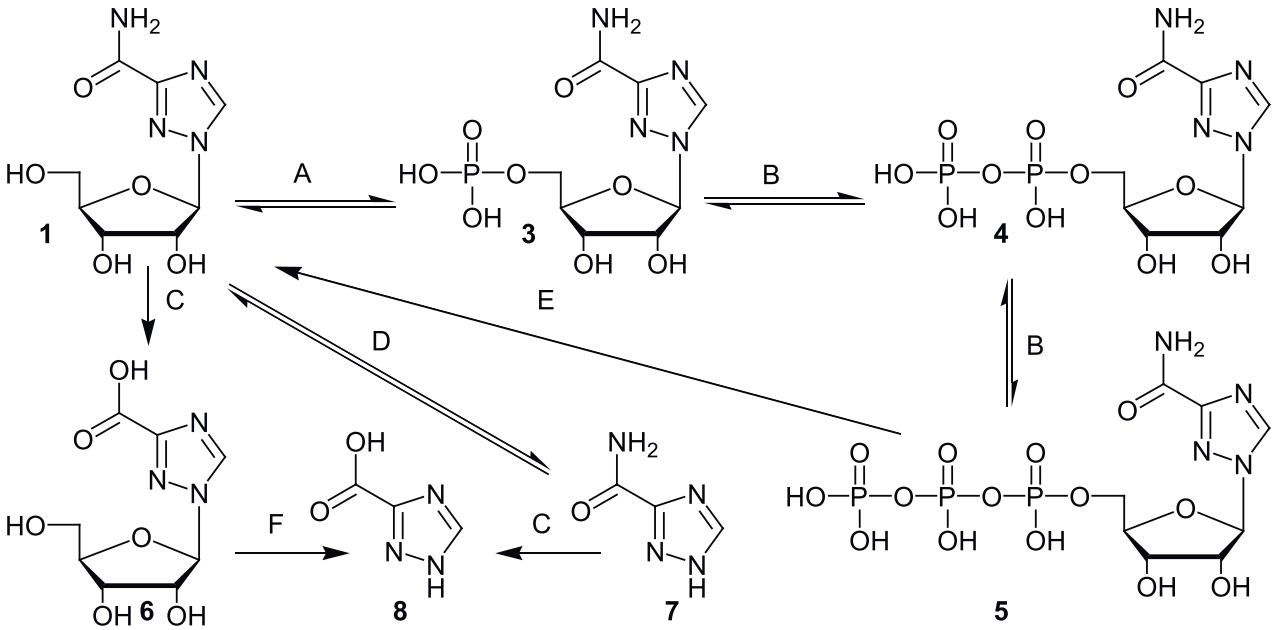

Fig. 2. Metabolism of ribavirin. A – hADK; B – various kinases; C – ADA; D – PNP; E – inosine triphosphate pyrophosphatase; F – various nucleosidases.

Ribavirin is not a substrate or inhibitor for cytochrome P450 (CYP450) and thus is not involved in oxidative catabolism. So, the molecule's metabolic cascade engages the same enzymatic systems as purine nucleosides do. The fact that most of the previously synthesized ribavirin analogs are inactive is often explained by the high substrate specificity of these enzymatic systems. It is usually thought that ribavirin is active against viral

infections only in the 5'-phosphate form [15, 30]. Whereas ribavirin itself, an isostere of guanine and adenosine, is recognized by hADK quite well (phosphorylation rate is only 1200 times lower than for adenosine), other molecules, for example, 1-β-D-ribofuranosyl-1,2,4-triazole-3-carboxylic acid (**6**) and 1-β-D-ribofuranosyl-1,2,4-triazole, are not phosphorylated by kinases at all [31]. It is probably due to this that they exhibit no antiviral activity. According to contemporary concepts, there are six suggested mechanisms of ribavirin's action. Fig. 3, based on review [21], shows the schematic representation of these mechanisms.

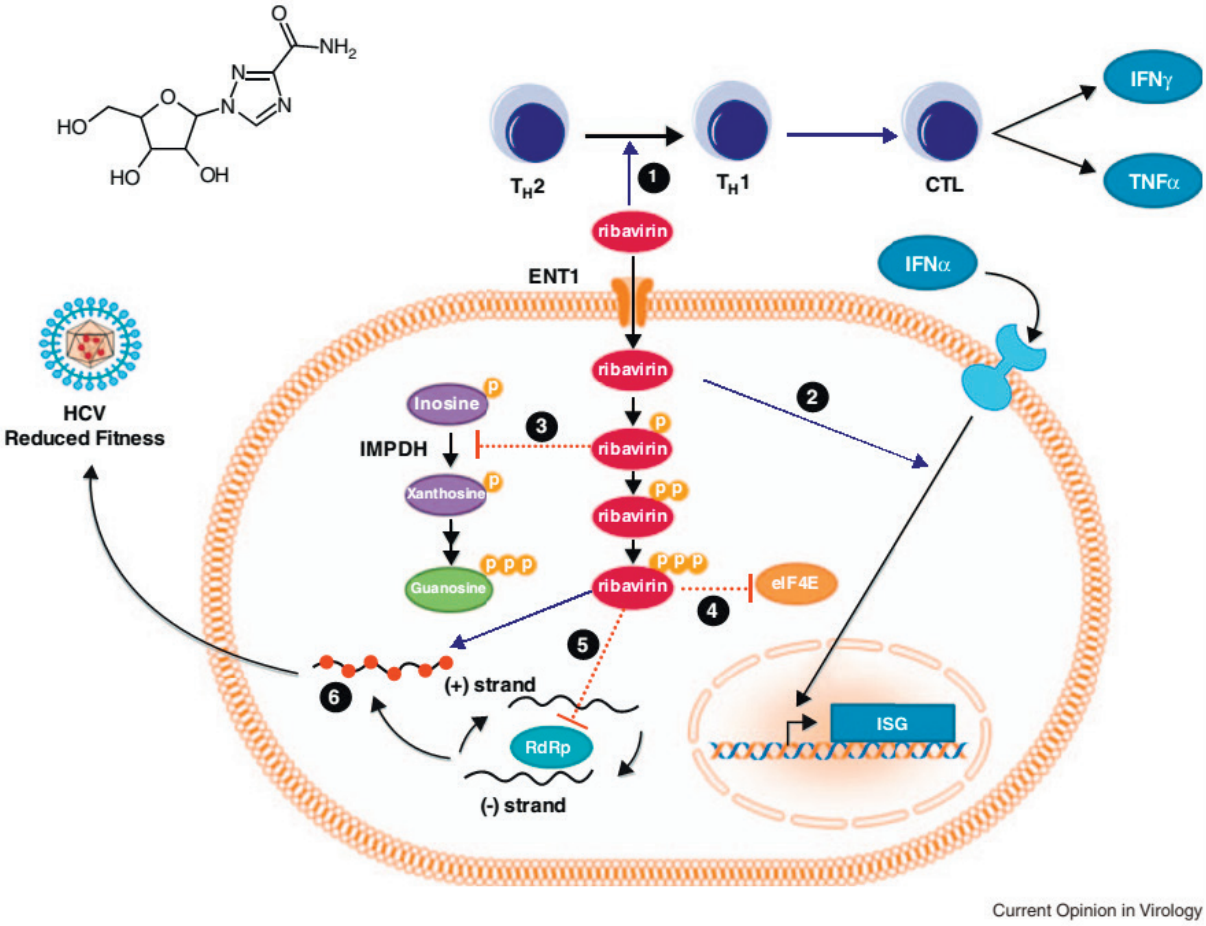

Fig. 3. Mechanisms of ribavirin's action against HCV [21].
1) Modulation of the cell's immune response by lymphocytes Th1 and Th2;
2) modulation of ISG expression; 3) inhibition of inosine monophosphate dehydrogenase (IMPDH);
4) inhibition of eukaryotic translation initiation factor eIF4E;
5) direct inhibition of viral RNA-dependent RNA polymerases (RdRp);
6) viral mutagenesis.

Mechanisms 3–6 are directly related to the phosphorylated metabolites of ribavirin, and the structural bases of the immunomodulating activity in mechanisms 1 and 2 are still unknown. Mechanism 1, related to T lymphocytes, is systemic, and this kind of activity cannot be tested using cell models.

The mechanism which has been studied most (and most proven) is the inhibition of inosine monophosphate dehydrogenase (IMPDH) (EC 1.1.1.205) by RMP (3). IMPDH is a key enzyme in *de novo* synthesis of purine nucleotides. RMP blocks guanosine triphosphate (GTP) synthesis by binding to the enzyme's active site in a reversible manner. This slows down the synthesis of nucleic acids, as well as all other processes in the cell which require GTP as a substrate, including the process of viral genome replication [32]. The change in GTP concentration affects the functioning of the host cell, being the reason behind ribavirin's toxicity.

IMPDH inhibition leads to a decrease in GTP levels to ~60% of the normal level. Afterwards, however, GTP concentration is stabilized and does not decrease further, while ribavirin's concentration increases. At the same time, the dose-dependent manner of the drug's antiviral activity persists [33–36], indicating the presence of other antiviral mechanisms. The change in concentration balance of nucleotide substrates for the viral polymerase may cause the substitution of GTP with other substrates and accumulation of lethal mutations in the viral genome (mechanism 6 in Fig. 3).

Another possible mechanism of action is the direct inhibition of viral polymerases by the "wrong" substrate, ribavirin 5'-*O*-triphosphate (RTP) (5), similar to how azidothymidine terminates elongation of HIV DNA by reverse transcriptase (mechanism 5 in Fig. 3). This mechanism was proved by *in vitro* experiments for hepatitis C virus [37] and influenza virus [38, 39]. There is proof that RTP may be the substrate/inhibitor for other viral fragments [40, 41]. RTP is the substrate for capping enzymes (for example, the D1 of the vaccinia virus) [42], and is able to form a "wrong" RNA cap, containing RMP residues, not 7-*N*-methylguanosine. This cap inhibits the eukaryotic translation initiation factor eIF4E, and the viral RNA cannot be translated (mechanism 4 in Fig. 3).

It is known that ribavirin monotherapy is effective against the Lassa virus [4, 5, 43], human orthopneumovirus (respiratory syncytial virus) [44], but not against chronic hepatitis C. However, when combined with INF-α, a protein which modulates the immune response, ribavirin is an effective medication against hepatitis C [45]. As it turns out, ribavirin switches the phenotype of T lymphocytes produced by the immune system, from Th2 to Th1, thus changing the type of the cell's immune response (mechanism 1 in Fig. 3) [46, 47]. Moreover, the interferon produced by the immune system when binding to receptors on the surface of a cell attacked by a virus, launches a signaling cascade which leads to the expression of interferon stimulated genes (ISG), putting the cell in a "defensive" position (mechanism 2 in Fig. 3). ISG function is a "hot topic" in current research [48–55], but little is known so far. For example, the ISG_{15} protein in human cells is an important part of the innate immune system and is responsible for antiviral activity [56]. Ribavirin has an effect on the signaling cascade of interferon by modulating ISG expression. It was confirmed by *in vitro* [57–60] and *in vivo* [61–63] experiments, but the structural basis of this effect is unknown. There are suggestions [64] that the decrease in GTP levels due to IMDPH inhibition is related to the disruption of the enzymatic cascade, which regulates nitric oxide (NO) levels in the cell (NO is cytotoxic for T lymphocytes, and Th1 cells are less resistant to it).

The immunomodulating activity of ribavirin was discovered in the mid-2000s, when major research on synthesis of the analogs and structure optimization seemed quite complete. The biological properties of most ribavirin analogs had been tested on cheap available cell lines. This is why it is possible to discover immunomodulating activity for the substances which had already been studied and rejected. The diversity of viral infections for which new analogs had been tested also needs to be taken into account; results are difficult to compare since the targets are so different. A substance active against one virus may often be useless against another.

Ribavirin was created as an antiviral drug and is still used as such today, although the idea of utilizing it as a cytostatic agent is quite old [65]. Today, there is information about 28 trials (10 are complete and 6 are in Phase IV) on clinicaltrials.gov [66], where ribavirin is being tested in treatments of cancers of varying kinds. Ribavirin's mechanisms of antitumor activity are quite similar to the antiviral mechanisms described above: the inhibition of enzymatic cascades related to nucleic acids metabolism [67–69], the violation of translation mechanisms [70, 71], immune response modulation [72].

Of all 1,2,4-triazole nucleosides, including those with antiviral activity, almost none have been studied in order to uncover their mechanisms of action, apart from ribavirin itself and a couple of prospective drugs, e.g. viramidine. None of the suggested mechanisms can fully explain ribavirin's biological activity, or the structure–activity relationship for the drug's analogs and derivatives. All theories collided with facts that did not fit sooner or later; there is a number of unresolved issues with each suggested mechanism. IMPDH inhibition, as mentioned before, only leads to lower GTP levels in the cell, which could explain the antiviral effect by the disruption of viral genome replication. However, the comparison of the spectrum and intensity of antiviral activity of ribavirin and other known IMPDH inhibitors shows that, despite the fact that equal inhibition is achieved, the antiviral effects are rather different [32]. Actual interaction with viral enzymes is usually observed in *in vitro* experiments, where ribavirin concentrations are 10–1000 times higher than clinically relevant [16, 73]. Immunomodulating activity is also characteristic for levovirine, or 1-(β-L-ribofuranosyl)-1,2,4-triazole-3-carboxamide, which is the L-enantiomer of ribavirin [74]. This substance cannot be a substrate for hADK because of the configuration of the glycoside fragment, and is, perhaps, not phosphorylated in the body.

There have been quite a few attempts to understand the relationship between the structures of ribavirin analogs and their metabolism and activity [12, 31, 75–77]. However, obvious correlations have not been found. For example, there was an attempt to explain why there is almost no activity in analogs with pentose glycoside residues, other than D-ribose. It could be due to the fact that such compounds do not interact with the human nucleoside diphosphate kinase (hNDKA) (EC:2.7.4.6), an enzyme which catalyzes the reversible transition of nucleoside diphosphates into triphosphates [23]. In this scenario, the dose-dependent manner of the antiviral activity of ribavirin's acyclic analogs, demonstrated using the *in vitro* adenovirus model [78], could not be explained. The attempt to explain the activity of such compounds by their non-specific hydrolysis, followed by the transition from 1,2,4-triazole-3-carboxamide (**7**) into ribavirin with the help of PNP, does not seem very convincing. This is because hydrolysis in cell models is not very likely, and the rate of glycoside bond rupture in a specialized model system correlates weakly with the observed activity [79]. We can conclude that almost 50 years of research have produced more questions than answers.

The molecule of ribavirin has, roughly speaking, three places where modification is possible: glycoside fragment, carboxamide group and the 5-position of the heterocyclic base. Another possible modification route is the change from the 1,2,4-triazole heterocyclic system to another azole, for example, imidazole or 1,2,3-triazole. All these possibilities were reported in the early days of research on synthesis [80, 81], but they did not produce a lot of interesting results. Ribavirin itself has remained the best one amongst its structural analogs, in terms of activity and spectrum of action. Even small changes in the molecule would lead to either complete loss of activity or significant decrease in efficacy and increase in selectivity. For example, 2'-deoxyribavirin is inactive [79]; 5-methylribavirin is inactive as well, according to some data [82]. However, other research suggests that it inhibits reproduction of certain viruses *in vitro*, i.e. the Tahyna virus, the Dhori virus and the vaccinia virus [83], but the effect is much lower than that of ribavirin. The substitution of oxygen with sulfur in the carboxamide group results in the narrower spectrum of action; 1-(β-D-ribofuranosyl)-1,2,4-triazole-3-thiocarboxamide inhibits herpes simplex virus *in vitro*, with 80% efficacy compared to ribavirin, but it is inactive to other viruses that were tested: adenovirus, parainfluenza virus and rhinovirus [84]. Many compounds related to ribavirin but with a different heterocyclic system, such as 5-amino-1-β-D-ribofuranosylimidazole-4-carboxamide (AICAR, acadesine) and 5-hydroxy-1-β-D-ribofuranosylimidazole-4-carboxamide (mizoribine), also have pharmacological prospects, but their biological activity is different [85]. So is there any need to search further when there seems to be no higher peak to reach?

2. New analogs of ribavirin: synthesis and biological properties

2.1. Isosteric analogs for carboxamide group

The only "old" compound which has prospects for use is viramidine **2**, where the carboxamide is replaced with the isosteric amidine group. This molecule's metabolism is different from that of ribavirin [86–88]; it is phosphorylated much slower, and active metabolites do not accumulate in erythrocytes. Viramidine is transformed into ribavirin by ADA in liver cells, where its antiviral activity is supposed to manifest. Moreover, viramidine inhibits PNP [89], blocking one of the pathways of ribavirin's catabolism [90]. Various substituents, such as alkyl groups and amino acid residues (Fig. 4), have been introduced into the amidine group of viramidine [91]. Some of these substances exhibit significant antiviral activity *in vitro* (Table 1).

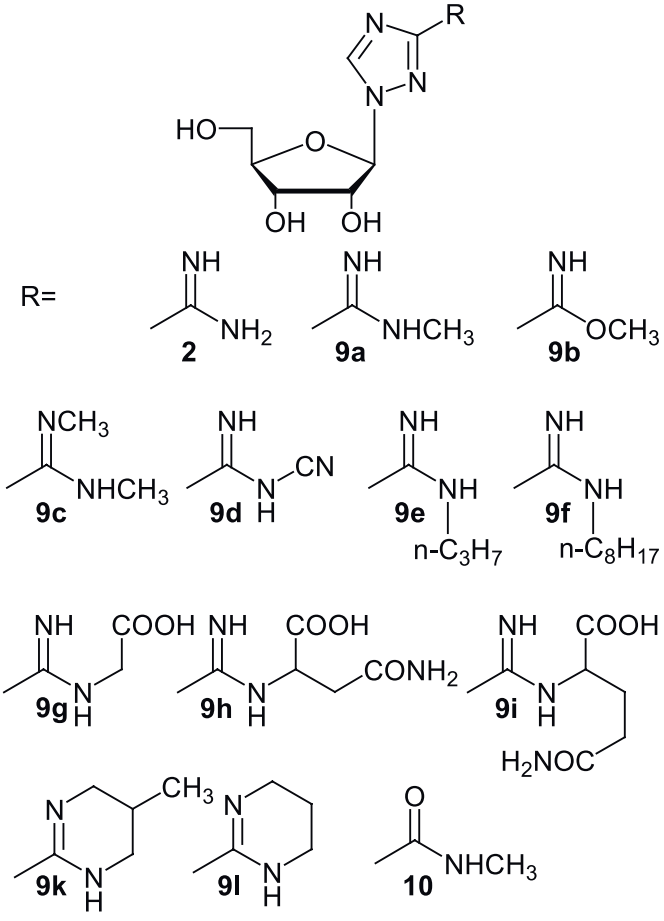

Fig. 4. Viramidine analogs with different substituents [91].

Substituents alter the antiviral activity quite a lot. At the same time, it is hard to explain it by metabolic transition into ribavirin – by deamination or hydrolysis of the amidine group. Compound **9a** is very active, but its hydrolysis product **10** is not. We can see that activity and toxicity decrease with the growing size of the substituent, although this rule has exceptions. Molecule **9e** (homolog of **9a**) is more active and toxic than **9a**, while having a longer alkyl chain, but the spectrum of activity is smaller.

Another isosteric analog of ribavirin is ETAR, 1-(β-D-ribofuranosyl)-3-ethynyl-1,2,4-triazole (**11**) (Fig. 5) [92], in which the carboxamide is replaced with the ethynyl group. The molecule exhibits strong inhibitory properties, better than ribavirin, towards a number of flaviviruses, for example Dengue virus, in cell models [93]. The research suggests that its mechanism of action involves IMPDH inhibition. However, the prospects of this drug are low due to its high toxicity.

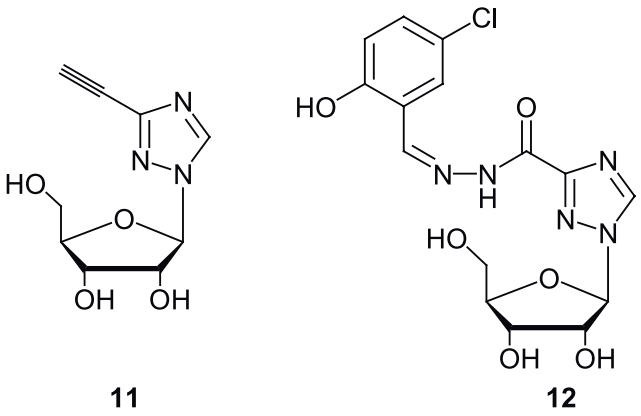

Fig. 5. Active isosteric analogs of ribavirin.

Table 1. Antiviral activity and cytotoxicity of viramidine and its analogs with substituents, measured *in vitro* using Vero cell line

IC_{50}, μg/ml	Compound												
	2	**9a**	**9b**	**9c**	**9d**	**9e**	**9f**	**9g**	**9h**	**9i**	**9k**	**9l**	**10**
SFSV	36	104	98	94	*	73	339	566	484	547	*	*	*
PTV	83	250	201	181	*	41	*	**	1600	2690	*	*	*
DGV4	100	n	76	162	250	n	n	n	n	n	n	n	n
RSV	16	24	n	n	n	n	n	n	n	n	n	n	n
VV	59	198	n	184	n	n	n	n	n	n	n	n	n
IFAV	48	n	63	n	n	n	n	n	n	n	n	n	n
IFBV	48	n	n	n	n	n	n	n	n	n	n	n	n
PIFV3	n	125	n	n	n	n	n	n	n	n	n	n	n
CC_{50}, μg/ml	250–1000	>1000	250–840	250–1000	250–1000	660–1000	>1000	1000–3200	>3200	>3200	>1000	>3200	>320

SFSV – Sandfly fever Sicilian virus; PTV – Punta Toro virus; DGV4 – Dengue 4 virus; RSV – human orthopneumovirus (respiratory syncytial virus); VV – vaccinia virus; IFAV – influenza A virus; IFBV – influenza B virus; PIFV3 – parainfluenza virus type 3.

* inactive; ** inhibition does not reach 50%; n – not tested.

Viramidine inhibits PNP, an enzyme which is targeted in chemotherapy of diseases like cancer [94]. The work of Liu et al. [95] investigates cytotoxic properties of ribavirin analogs, where the carboxamide group is replaced with a hydrazone group. One of the suggested compounds, (*Z*)-*N*'-(1-(5-chloro-2-hydroxyphenyl)ethylidene)-1-(β-D-ribofuranosyl)-1,2,4-triazole-3-carbohydrazide (**12**), inhibits lung cancer (line A549) growth at the concentration of 20 μM.

The research focusing on hADK specificity for ribavirin analogs, where the carboxamide is replaced with an isostere, and potentially related antiviral activity, has not shown a clear correlation between the kinase's ability to phosphorylate a molecule and the activity of the latter [77]. For example, hADK activity towards compounds **9a** and **9b** is 5% and less than 2%, respectively, compared to the enzyme's activity towards ribavirin. At the same time, the inactive methyl amide **10** is phosphorylated only 10 times slower than ribavirin. The patent application [96], where some ribavirin isosteres for the carboxamide group are described as "inhibitors of viral polymerases", has not been approved, and no data on the activity of those compounds were shown in this patent application or elsewhere.

There are alternative phosphorylation pathways which are not dependent on hADK, as well as other types of pharmacological activity. In the studies on

the substrate specificity of the genetically engineered PNP from *E. coli* [97, 98], a number of ribavirin analogs were obtained, with the *N*-alkylated amide group. As it turned out, even bulky substituents in the carboxamide fragment did not affect transglycosylation, which is catalyzed by PNP (Fig. 6).

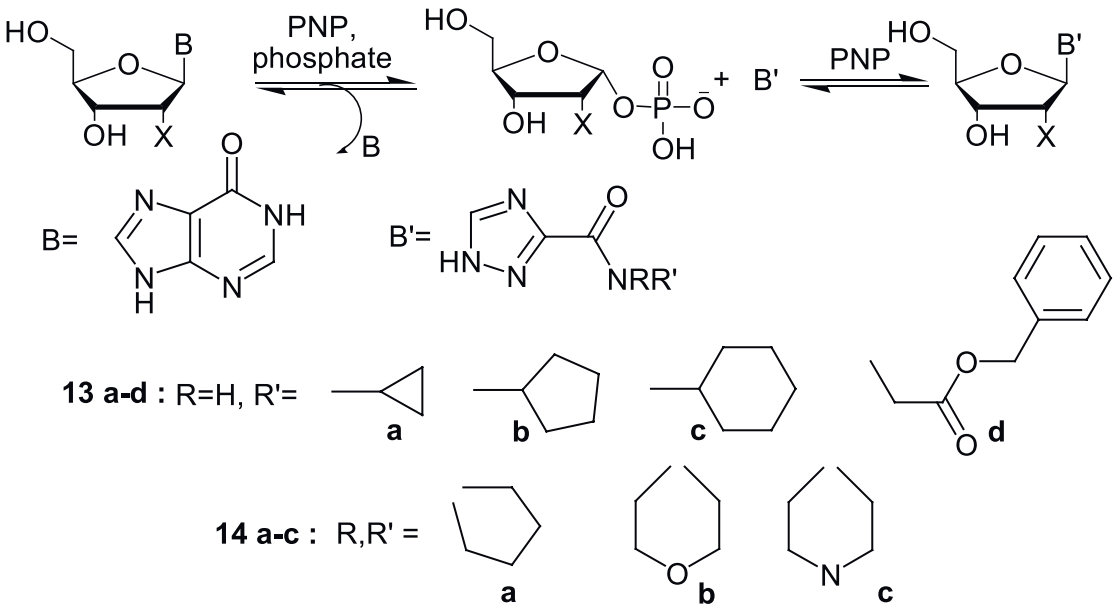

Fig. 6. Synthesis of *N*-alkylamide analogs of ribavirin by chemo-enzymatic transglycosylation.

Alkylamide analogs of ribavirin, **13b** and **13c**, have shown a relatively high *in vitro* activity against influenza A virus and herpes simplex virus (an RNA and a DNA virus, respectively) in different cell lines. Interestingly, according to the existing concepts [99], metabolism of such compounds should not lead to ribavirin, but rather to the inactive 1-β-D-ribofuranosyl-1,2,4-triazole-3-carboxylic acid. It is impossible to explain the observed activity by a metabolic transformation into an active compound, as in the case of molecules **9a** and **10**. It's important to note that, when ribavirin in all its roles (maybe apart from that of the immunomodulating molecule) imitates natural purine nucleosides and participates in their enzymatic cascades, the analogs **13b–c** can hardly partake in the majority of these processes, because of steric factors. This indicates the existence of yet unknown mechanisms of antiviral activity for compounds of this type.

The research paper [100] suggests using another approach to modify the carboxamide group (Fig. 7). The 3-position in the designed molecules contains 1,2,4-oxadiazole instead of the carboxamide, the former being the heterocyclic bioisostere of the latter.

The 3-(1,2,4-triazolyl)-1,2,4-oxadiazoles, as it was discovered, are perfect substrates for PNP; that is why nucleosides **14a–d** can be synthesized by ribavirin

[1]Galegov G.A., Deryabin P.G., Andronova V.L. (in press).

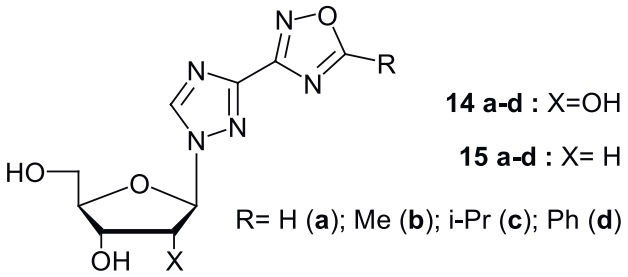

Fig. 7. 3-Oxadiazole analogs of ribavirin.

modification, as well as by chemo-enzymatic methods from natural nucleoside substrates, that allows to produce 2'-deoxy analogs **15a–d**. The most active compound (against hepatitis C virus *in vitro*), amongst the isosteres **14** and **15**, is molecule **14d** (IC_{50} = 8.8 μg/ml; 12.5 μg/ml for ribavirin). At the same time, its toxicity for the tested cell line is much lower than ribavirin's. Substances **14a** and **14b** also exhibit some activity against herpes simplex virus and influenza A virus, respectively. Compounds of this type cannot be metabolized into ribavirin, and the structure of the most active molecule **14d** contains a bulky aromatic substituent, that sterically prevents it from participating in processes such as replication.

2.2. Ribavirin analogs with substitutions at the 5-position of the heterocycle

Of the publications within the past 10 years dedicated to structural analogs of ribavirin, the majority focus on derivatives of 1,2,4-triazole-3-carboxylic acids, with substituents at the 5-position. Most of these works, especially aspects of synthesis, are carefully summarized in the review by Xia et al. [101]. A significant number of the described compounds contain D-ribose or an acyclic methoxyethanol residue as the glycoside fragment, and the substituent in the 3- or 5-position of the triazole cycle (depending on the glycoside position) contains an aryl fragment, attached to the triazole by spacers of various nature (Fig. 8). The structural similarity, to a great extent, is related to the methodology of these research papers based on a serial modification of the sole nucleoside precursor by one or two chemical reactions (most commonly, Pd-catalyzed cross-coupling).

Compounds containing a substituted 1,2,3-triazole in the 5-position, **16–24** (Fig. 9), have been found effective against the tobacco mosaic virus (TMV) [102–104]. The experiments involved the "half-leaf juice rubbing" model, wherein 50% of the surface of a tobacco plant leaf were treated with the tested substance, and then the plant was infected with TMV. The comparison of the affected areas

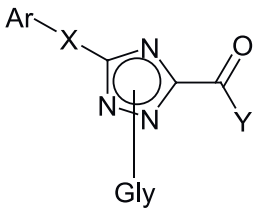

Fig. 8. The general structure of ribavirin analogs substituted at the 5-position. X – spacer group (ethynyl, vinyl, 1,2,3-triazolyl, NH, S); Y – NH_2, OEt; Gly – glycoside fragment (ribose, methoxyethanol, H).

on treated and untreated surfaces showed the level of antiviral activity. The antiviral effect is exhibited not only by nucleosides or acyclic nucleoside analogs, but also by their protected derivatives and by heterocyclic bases themselves (which have the highest activity). In this case, it is hard to suggest a mechanism that would include synthesis of a nucleoside from the base, with the help of PNP, because such a bulky substituent in the 5-position limits the substrate specificity of the enzyme [97, 105]. We can speculate that antiviral activity is determined by the heterocyclic base and the glycoside fragment has a transport function.

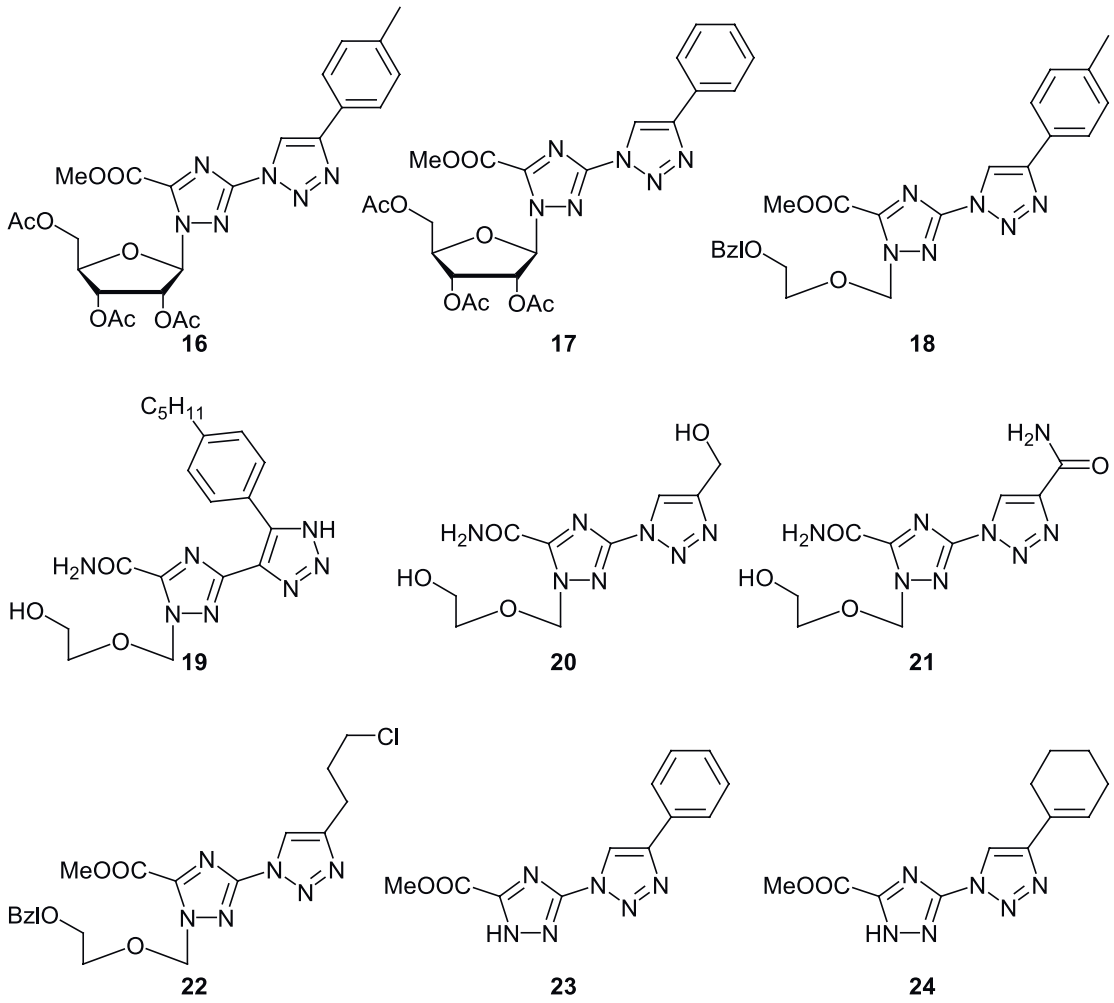

Fig. 9. Ribavirin analogs active against TMV.

Compounds **25–28** (Fig. 10) with an ethynyl spacer are quite active against hepatitis C virus (HCV) (Table 2) in cell models which contain the viral replicon [106–108].

In this case, there is a similar and consistent pattern: the carbohydrate fragment seems not to be too critical for activity, although it has influence on the toxicity of the compound. The authors of the study have analyzed the structure–activity relationship (SAR) by synthesizing a number of compounds and demonstrating that the important part is the rigid spacer group in the 5-position of the 1,2,4-triazole ring, as well as the position and type of the substituent in the arylethynyl fragment. When the triple bond in compound **28** is replaced with a single bond, activity is lost. This indicates the importance of the molecule's geometry and/or the presence of π-conjugation between aromatic fragments in the base, for the substance to be active against HCV. Derivatives with a substituent in the 4-position of the aryl ring are active, and the antiviral activity increases with the growth of lipophilicity and the substituent size. However, it is difficult to suggest a mechanism in this case. One of the most active compounds is not a nucleoside, but a protected derivative **25**, which is unable to participate in metabolic cascades. Also, it is the only active derivative without an aryl ring.

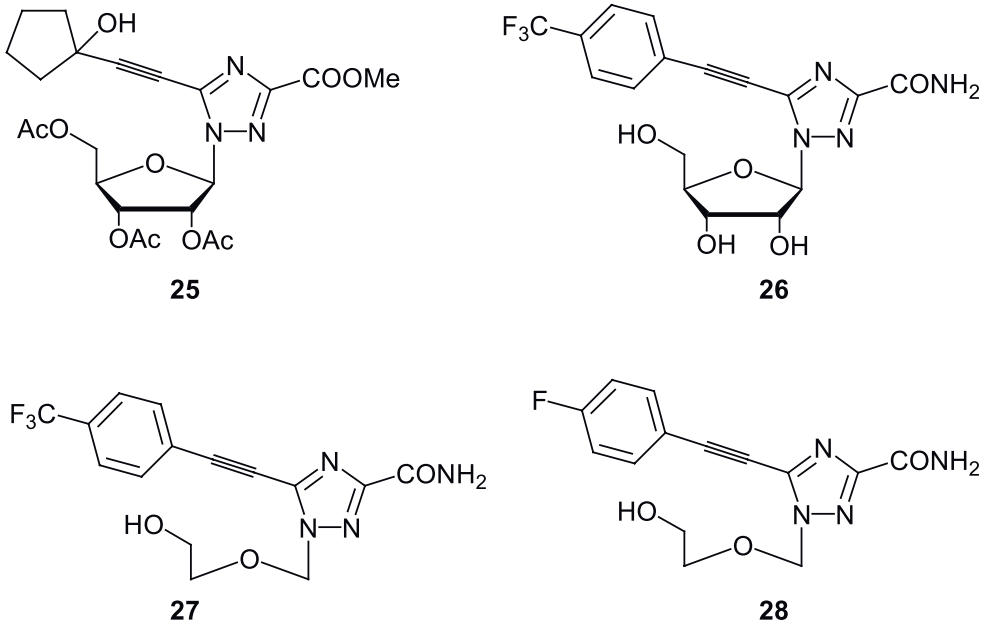

Fig. 10. Ribavirin analogs active against HCV.

Table 2. Activity of arylethynyl analogs of ribavirin against HCV virus *in vitro*

Cell line / Compound	Huh-5-2		Huh-9-13		Huh-6	
	EC_{50}	CC_{50}	EC_{50}	CC_{50}	EC_{50}	CC_{50}
25	52.3±3.1	>105	54.3±18	>105	25.1±4.8	>105
26	17.7±1.9	82.5±9.7	19.4±7.0	>120	43.7±20	>120
27	14.1±3.7	56.5±14	36.7±23	79.0±19	50.8±21	87.5±14
28	72.3±9.9	>160	125±6.6	>160	95.3±3.3	132±18
Ribavirin	28.7±8.2	86.0±45	84.0±15	229	33.0	>100

EC_{50} (μM) – concentration at which inhibition occurs with 50% efficiency; inhibition of replication of subgenome replicon of HCV in a respective cell line;
CC_{50} (μM) – concentration at which 50% cells die.

Nucleoside analogs with simple alkyl substituents in the 5-position of the triazole cycle are almost inactive against hepatitis C virus in cell models *in vitro* [105]. Analogs of compound **26** (Fig. 11) that have a double bond are active in the *trans* configuration (EC_{50} = 9 μM, CC_{50} > 30 μM) and inactive in the *cis* configuration [109].

For ribavirin analogs substituted at the 5-position, antitumor activity is observed for compounds **30–37**, which are structurally similar to the anti-HCV and anti-TMV substances described earlier; although there are compounds of other types in the series (Fig. 12) [108, 110–115].

Fig. 11. Active (**29a**) and inactive (**29b**) vinyl analogs of compound **26**.

Xia et al. [111, 113, 116] have shown that the anticancer activity of 5-arylethynyl analogs is due to the induced caspase-dependent apoptosis. The antitumor effect was demonstrated using a cell line of pancreatic cancer, MiaPaCa-2, which is drug resistant. Apoptosis is launched since the expression of the heat shock protein Hsp27 is suppressed because of these nucleoside compounds. Other mechanisms have been suggested as well: the inhibition of androgen receptors [116] and immunomodulating activity of derivatives with a 1,2,3-triazole spacer [114].

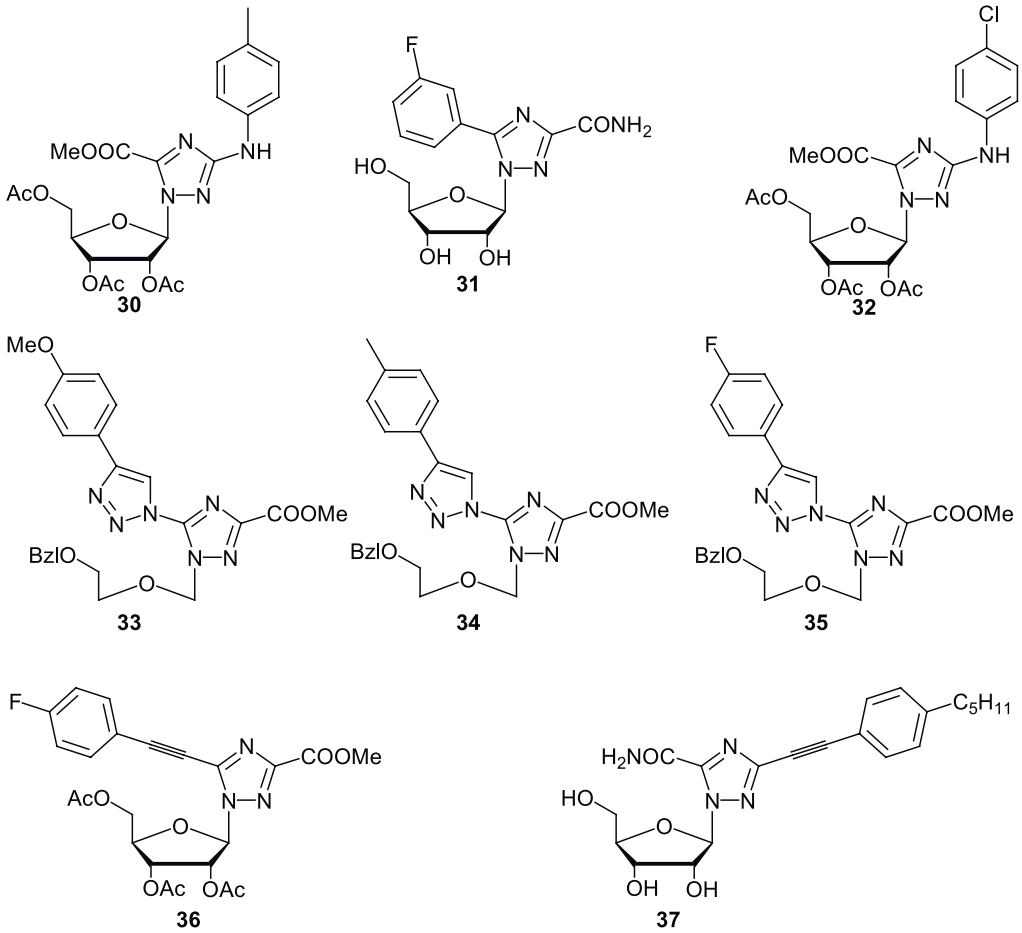

Fig. 12. Ribavirin analogs with a substituent at the 5-position that have antitumor activity.

Interestingly, the SAR parameters obtained for some analogs of compound **37** show almost the same consistent pattern as the anti-HCV derivatives do. A rigid spacer group and a lipophilic substituent in the 4-position of the aromatic ring are needed. At the same time, the roles of the glycoside fragment and the carboxamide group in the 3-position are unclear. Computer modeling of the structures of the active compounds and X-ray crystallography demonstrate the coplanarity of the connected aromatic fragments in the base. Researchers are of the opinion that this structural motif imitates planar conjugated aromatic systems in natural purine bases and is required for the activity of the compound [115].

Conclusions

The majority of the publications summarized here focus on biological properties of large libraries of target compounds. Some conclusions can be made regarding the structure–activity relationship (SAR) for ribavirin

analogs of the last generation, compounds **16–37**, which contain bulky substituents in the 5- (or 3-) position of the heterocyclic base. The first and most important observation is that these substances, while having structures quite different from the parent molecule, cannot have the same mechanisms of biological activity as ribavirin itself. This is because they do not imitate the structure of a purine base and cannot be substrates for the enzymes of the purine metabolic cascade. Inhibition of IMPDH or viral polymerases by these compounds is also not very likely, due to the high substrate specificity of these enzymes; at least, the possible mechanism of such inhibition would be very different from ribavirin's. The isosteres of ribavirin **13**–**15**, on the contrary, may be supposed to imitate the purine structure, and their possible mechanisms of action may be the same as for ribavirin. Our second conclusion is that compounds **16–37**, which exhibit various types of activity, are very similar in structure, and the presence of the glycoside fragment (that makes the molecule a nucleoside analog) is not required. It is possible that the structural basis for mechanisms of activity is not connected to the nucleoside structure of the molecule, but only to the heterocyclic base, 1,2,4-triazole, which is attached to an aromatic lipophilic fragment by a rigid spacer group. This idea is supported by multiple facts: the abovementioned, high anti-TMV activity of bitriazole bases **23** and **24**; the varying activity of the analogs, with substituents at the N1 and N2 atoms of the triazole and acyclic derivatives; the high activity of many protected precursors. However, there is no direct proof of this hypothesis, because antiviral and anticancer activity of aglycones has not been studied.

In line with these conclusions, a significant antiviral activity of compound AMP-006, 5-(tetrahydrofuran-2-yl)-1,2,4-triazole-3-carboxamide (**38**) (Fig. 13) has been reported [118]. This molecule, while being a close structural analog of ribavirin, is not at all a nucleoside. It has no hydroxy groups and it is not hydrolyzed by enzymes, but the molecule has very low cytotoxicity, and is active *in vitro* against the influenza A virus and the herpes virus, being just a little bit less effective than ribavirin. Nucleoside **39**, which is obtained from it synthetically, does not have antiviral activity[2].

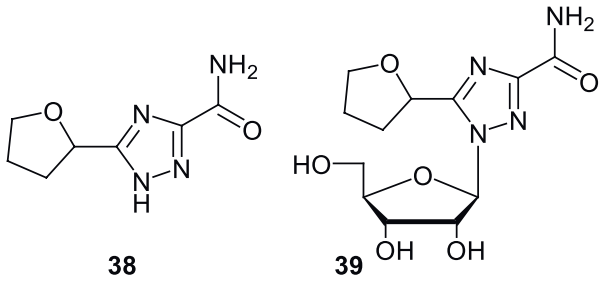

Fig. 13. AMP-006 (**38**) and its inactive nucleoside derivative **39**.

Given the fact that mechanisms of ribavirin's activity are not known in detail, the role of this drug (and its new structural analogs) in the fight against viral diseases and tumors is still very promising. It seems that in near future these molecules will still be playing an important part.

The author declares no conflict of interest.

References:

1. Sidwell R.W., Huffman J.H., Khare L.G P., Allen B., Witkowski R.J.T., Robins K. Broad-spectrum antiviral activity of virazole: 1-β-D-Ribofuranosyl-1,2,4-triazole-3-carboxamide. *Science.* 1972;177(4050):705-706. https://doi.org/10.1126/science.177.4050.705

2. Oxford J.S. Inhibition of the replication of influenza A and B viruses by a nucleoside analogue (ribavirin). *J. Gen. Virol.* 1975;28(3):409-14. https://doi.org/10.1099/0022-1317-28-3-409

3. Hruska J.F., Bernstein J.M., Douglas R.G. Jr., Hall C.B. Effects of ribavirin on respiratory syncytial virus *in vitro*. *Antimicrob. Agents Chemother.* 1980;17(5):770-775. https://doi.org/10.1128/AAC.17.5.770

4. McCormick J.B., King I.J., Webb P.A., Scribner C.L., Craven R.B., Johnson K.M., Elliott L.H., Belmont-Williams R. Lassa fever. Effective therapy with ribavirin. *N. Engl. J. Med.* 1986;314(1):20-26. https://doi.org/10.1056/NEJM198601023140104

5. Huggins J.W. Prospects for treatment of viral hemorrhagic fevers with ribavirin, a broad-spectrum antiviral drug. *Rev. Infect. Dis.* 1989;11(Suppl_4):S750-S761. https://doi.org/10.1093/clinids/11.Supplement_4.S750

6. Shigeta S., Mori S., Baba M., Ito M., Honzumi K., Nakamura K., Oshitani H., Numazaki Y., Matsuda A., Obara T. Antiviral activities of ribavirin, 5-ethynyl-1-β-D-ribofuranosyl-imidazole-4-carboxamide, and 6'-(R)-6'-C-methylneplanocin A against several ortho- and paramyxoviruses. *Antimicrob. Agents Chemother.* 1992;36(2):435-439. https://doi.org/10.1128/AAC.36.2.435

7. Jordan I., Briese T., Fischer N., Lau J.Y., Lipkin W.I. Ribavirin inhibits West Nile virus replication and cytopathic effect in neural cells. *J. Infect. Dis.* 2000;182(4):1214-1217. https://doi.org/10.1086/315847

8. Kim Y., Lee C. Ribavirin efficiently suppresses porcine nidovirus replication. *Virus Res.* 2013;171(1):44-53. https://doi.org/10.1016/j.virusres.2012.10.018

9. Kihira S., Uematsu J., Kawano M., Itoh A., Ookohchi A., Satoh S., Maeda Y., Sakai K., Yamamoto H., Tsurudome M., O'Brien M., Komada H. Ribavirin inhibits human parainfluenza virus type 2 replication *in vitro*. *Microbiology and Immunology.* 2014;58(11):628-635. https://doi.org/10.1111/1348-0421.12192

10. Ramirez-Olivencia G., Estebanez M., Membrillo F.J.,

[2]Prutkov A.N., Chudinov M.V., Galegov G.A., Deryabin P.G., Andronova V.L. (in press).

Ybarra M.D.C. Use of ribavirin in viruses other than hepatitis C. A review of the evidence. *Enferm. Infect. Microbiol. Clin.* 2018. (in press). https://doi.org/10.1016/j.eimc.2018.05.008

11. Streeter D.G., Witkowski J.T., Khare G.P., Sidwell R.W., Bauer R.J., Robins R.K., Simon L.N. Mechanism of action of 1-D-ribofuranosyl-1,2,4-triazole-3-carboxamide (Virazole), a new broad-spectrum antiviral agent. *Proc. Natl. Acad. Sci. USA.* 1973;70(4):1174-1178. https://doi.org/10.1073/pnas.70.4.1174

12. Miller J.P., Kigwana L.J., Streeter D.G., Robins R.K., Simon L.N., Roboz J. The relationship between the metabolism of ribavirin and its proposed mechanism of action. *Ann. N. Y. Acad. Sci.* 1977;284(1):211-229. https://doi.org/10.1111/j.1749-6632.1977.tb21953.x

13. Crotty S., Cameron C., Andino R. Ribavirin's antiviral mechanism of action: Lethal mutagenesis? *J. Mol. Med.* (Berl.). 2002;80(2):86-95. https://doi.org/10.1007/s00109-001-0308-0

14. Hong Z., Cameron C.E. Pleiotropic mechanisms of ribavirin antiviral activities. *Progr. Drug Res.* Basel: Birkhäuser Basel. 2002;59:41-69. https://doi.org/10.1007/978-3-0348-8171-5_2

15. Parker W.B. Metabolism and antiviral activity of ribavirin. *Virus Res.* 2005;107(2):165-171. https://doi.org/10.1016/j.virusres.2004.11.006

16. Dixit N.M., Perelson A.S. The metabolism, pharmacokinetics and mechanisms of antiviral activity of ribavirin against hepatitis C virus. *Cell. Mol. Life Sci.* 2006;63(7-8):832-842. https://doi.org/10.1007/s00018-005-5455-y

17. Graci J.D., Cameron C.E. Mechanisms of action of ribavirin against distinct viruses. *Rev. Med. Virol.* 2006;16(1):37-48. https://doi.org/10.1002/rmv.483

18. Te H.S., Randall G., Jensen D.M. Mechanism of action of ribavirin in the treatment of chronic hepatitis C. *Gastroenterol. Hepatol.* (N. Y.). 2007;3(3):218-225. http://www.ncbi.nlm.nih.gov/pmc/articles/PMC3099343

19. Chung R.T., Gale M.Jr., Polyak S.J., Lemon S.M., Liang T.J., Hoofnagle J.H. Mechanisms of action of interferon and ribavirin in chronic hepatitis C: Summary of a workshop. *Hepatology* (Baltimore, Md.). 2008;47(1):306-320. https://doi.org/10.1002/hep.22070

20. Shiffman M.L. What future for ribavirin? *Liver Int.* 2009;29(Suppl 1):68-73. https://doi.org/10.1111/j.1478-3231.2008.01936.x

21. Paeshuyse J., Dallmeier K., Neyts J. Ribavirin for the treatment of chronic hepatitis C virus infection: A review of the proposed mechanisms of action. *Curr. Opin. Virol.* 2011;1(6):590-598. https://doi.org/10.1016/j.coviro.2011.10.030

22. Wu J.Z., Larson G., Walker H., Shim J. H., Hong Z. Phosphorylation of ribavirin and viramidine by adenosine kinase and cytosolic 5'-nucleotidase II: Implications for ribavirin metabolism in erythrocytes. *Antimicrob. Agents Chemother.* 2005;49(6):2164-2171. https://doi.org/10.1128/AAC.49.6.2164-2171.2005

23. Gallois-Montbrun S., Chen Y., Dutartre H., Sophys M., Morera S., Guerreiro C., Schneider B., Mulard L., Janin J., Veron M., Deville-Bonne D., Canard B. Structural analysis of the activation of ribavirin analogs by NDP kinase: Comparison with other ribavirin targets. *Mol. Pharmacol.* 2003;63(3):538-546. https://doi.org/10.1124/mol.63.3.538

24. Russmann S., Grattagliano I., Portincasa P., Palmieri V., Palasciano G. Ribavirin-induced anemia: Mechanisms, risk factors and related targets for future research. *Cur. Med. Chem.* 2006;13(27):3351-3357. https://doi.org/10.2174/092986706778773059

25. Nystrom K., Pettersson G., Wanrooij P.H., Brunet S., Said J., Ortolani G., Waldenstrom J., Adamek L., Tang K.W., Norberg P., Chabes A., Hellstrand K., Norder H., Lagging M. Inosine triphosphate pyrophosphatase enhances the effect of ribavirin on hepatitis C virus cell culture infection. *J. Hepatol.* 2017;66(1):321. http://dx.doi.org/10.1016/S0168-8278(17)30965-0

26. Nystrom K., Wanrooij P. H., Waldenstrom J., Adamek L., Brunet S., Said J., Nilsson S., Wind-Rotolo M., Hellstrand K., Norder H., Tang K.W., Lagging M. Inosine triphosphate pyrophosphatase dephosphorylates ribavirin triphosphate and reduced enzymatic activity potentiates mutagenesis in hepatitis C virus. *J. Virol.* 2018; 92(19):e01087-18. https://doi.org/10.1128/JVI.01087-18

27. Furihata T., Kishida S., Sugiura H., Kamiichi A., Iikura M., Chiba K. Functional analysis of purine nucleoside phosphorylase as a key enzyme in ribavirin metabolism. *Drug Metabolism and Pharmacokinetics.* 2014;29(2):211-214. https://doi.org/10.2133/dmpk.DMPK-13-NT-065

28. Page T., Connor J.D. The metabolism of ribavirin in erythrocytes and nucleated cells. *Int. J. Biochem.* 1990;22(4):379-383. https://doi.org/10.1016/0020-711X(90)90140-X

29. Wu J.Z., Walker H., Lau J.Y.N., Hong Z. Activation and deactivation of a broad-spectrum antiviral drug by a single enzyme: Adenosine deaminase catalyzes two consecutive deamination reactions. *Antimicrob. Agents Chemother.* 2003;47(1):426-431. https://doi.org/10.1128/AAC.47.1.426-431.2003

30. Martin P., Jensen D.M. Ribavirin in the treatment of chronic hepatitis C. *J. Gastroenterol. Hepatol.* 2008;23(6):844-855. https://doi.org/10.1111/j.1440-1746.2008.05398.x

31. Drabikowska A.K., Dudycz L., Shugar D. Studies on the mechanism of antiviral action of 1-(β-D-ribofuranosyl)-1,2,4-triazole-3-carboxamide (ribavirin). *J. Med. Chem.* 1979;22(6):653-657. https://doi.org/10.1021/jm00192a009

32. Nair V., Shu Q. Inosine monophosphate dehydrogenase as a probe in antiviral drug discovery. *Antivir. Chem. & Chemother.* 2007;18(5):245-258. https://doi.org/10.1177%2F095632020701800501

33. Wray S.K., Gilbert B.E., Noall M.W., Knight V. Mode of action of ribavirin: Effect of nucleotide pool alterations on influenza virus ribonucleoprotein synthesis. *Antiviral Res.* 1985; 5(1):29-37. https://doi.org/10.1016/0166-3542(85)90012-9

34. Crotty S., Maag D., Arnold J.J., Zhong W., Lau J.Y., Hong Z., Andino R., Cameron C.E. The broad-spectrum antiviral ribonucleoside ribavirin is an RNA virus mutagen. *Nat. Med.* 2000; 6(12):1375-1379. https://doi.org/10.1038/82191

35. Lanford R.E., Chavez D., Guerra B., Lau J.Y., Hong Z., Brasky K.M., Beames B. Ribavirin induces error-prone replication of GB virus B in primary tamarin hepatocytes. *J. Virol.* 2001;75(17):8074-8081. https://doi.org/10.1128/jvi.75.17.8074-8081.2001

36. Olschlager S., Neyts J., Gunther S. Depletion of GTP pool is not the predominant mechanism by which ribavirin exerts its antiviral effect on Lassa virus. *Antiviral Res.* 2011;91(2):89-93. https://doi.org/10.1016/j.antiviral.2011.05.006

37. Vo N.V., Young K.C., Lai M.M. Mutagenic and inhibitory effects of ribavirin on hepatitis C virus RNA polymerase. *Biochemistry.* 2003;42(35):10462-10471. https://doi.org/10.1021/bi0344681

38. Wray S.K., Gilbert B.E., Knight V. Effect of ribavirin triphosphate on primer generation and elongation during

influenza virus transcription *in vitro*. *Antiviral Res.* 1985;5(1):39-48. https://doi.org/10.1016/0166-3542(85)90013-0

39. Eriksson B., Helgstrand E., Johansson N.G., Larsson A., Misiorny A., Noren J.O., Philipson L., Stenberg K., Stening G., Stridh S., Oberg B. Inhibition of influenza virus ribonucleic acid polymerase by ribavirin triphosphate. *Antimicrob. Agents Chemother.* 1977;11(6):946-951. https://doi.org/10.1128/aac.11.6.946

40. Heck J.A., Lam A.M.I., Narayanan N., Frick D.N. Effects of mutagenic and chain-terminating nucleotide analogs on enzymes isolated from hepatitis C virus strains of various genotypes. *Antimicrob. Agents Chemother.* 2008;52(6):1901-1911. https://dx.doi.org/10.1128%2FAAC.01496-07

41. Benarroch D., Egloff M.P., Mulard L., Guerreiro C., Romette J.L., Canard B. A structural basis for the inhibition of the NS5 Dengue virus mRNA 2'-O-methyltransferase domain by ribavirin 5'-triphosphate. *J. Biol. Chem.* 2004;279(34):35638-35643. https://doi.org/10.1074/jbc.M400460200

42. Goswami B.B., Borek E., Sharma O.K., Fujitaki J., Smith R.A. The broad spectrum antiviral agent ribavirin inhibits capping of mRNA. *Biochem. Biophys. Res. Commun.* 1979;89(3):830-836. https://doi.org/10.1016/0006-291X(79)91853-9

43. Carrillo-Bustamante P., Nguyen T.H.T., Oestereich L., Günther S., Guedj J., Graw F. Determining Ribavirin's mechanism of action against Lassa virus infection. *Scientific Reports.* 2017;7(1):11693. https://doi.org/10.1038/s41598-017-10198-0

44. Hall C., Walsh E.E., Hruska J.F., Betts R.F., Hall W.J. Ribavirin treatment of experimental respiratory syncytial viral infection: A controlled double-blind study in young adults. *JAMA.* 1983;249(19):2666-2670. https://doi.org/10.1001/jama.1983.03330430042027

45. Reichard O., Schvarcz R., Weiland O. Therapy of hepatitis C: Alpha interferon and ribavirin. *Hepatology.* 2003;26(S3):108S-111S. https://doi.org/10.1002/hep.510260719

46. Hultgren C., Milich D.R., Weiland O., Sallberg M. The antiviral compound ribavirin modulates the T helper (Th) 1/Th2 subset balance in hepatitis B and C virus-specific immune responses. *J. Gen. Virol.* 1998;79(10):2381-2391. https://doi.org/10.1099/0022-1317-79-10-2381

47. Tam R.C., Pai B., Bard J., Lim C., Averett D.R., Phan U.T., Milovanovic T. Ribavirin polarizes human T cell responses towards a Type 1 cytokine profile. *J. Hepatol.* 1999;30(3):376-382. https://doi.org/10.1016/S0168-8278(99)80093-2

48. Metz P., Reuter A., Bender S., Bartenschlager R. Interferon-stimulated genes and their role in controlling hepatitis C virus. *J. Hepatol.* 2013;59(6):1331-1341. https://doi.org/10.1016/j.jhep.2013.07.033

49. Schneider W.M., Chevillotte M.D., Rice C.M. Interferon-stimulated genes: A complex web of host defenses. *Ann. Rev. Immunol.* 2014;32:513-545. https://doi.org/10.1146/annurev-immunol-032713-120231

50. Schoggins J.W. Interferon-stimulated genes: Roles in viral pathogenesis. *Curr. Opin. Virol.* 2014;6:40-46. https://doi.org/10.1016/j.coviro.2014.03.006

51. Sun J., Rajsbaum R., Yi M. Immune and non-immune responses to hepatitis C virus infection. *World J. Gastroenterol.* 2015;21(38):10739-10748. https://doi.org/10.3748/wjg.v21.i38.10739

52. Wong M.T., Chen S.S. Emerging roles of interferon-stimulated genes in the innate immune response to hepatitis C virus infection. *Cell Mol. Immunol.* 2016;13(1):11-35. https://doi.org/10.1038/cmi.2014.127

53. Hayes C.N., Chayama K. Interferon stimulated genes and innate immune activation following infection with hepatitis B and C viruses. *J. Med. Virol.* 2017;89(3):388-396. https://doi.org/10.1002/jmv.24659

54. Niedzwiedzka-Rystwej P., Ratajczak W., Tokarz-Deptula B., Deptula W. Mechanisms of type I interferon action and its role in infections and diseases transmission in mammals. *Acta Biochim. Pol.* 2017;64(2):199-205. https://doi.org/10.18388/abp.2016_1403

55. Wang W., Xu L., Su J., Peppelenbosch M.P., Pan Q. Transcriptional regulation of antiviral interferon-stimulated genes. *Trends. Microbiol.* 2017;25(7):573-584. https://doi.org/10.1016/j.tim.2017.01.001

56. Morales D.J., Lenschow D.J. The antiviral activities of ISG15. *J. Mol. Biol.* 2013;425(24):4995-5008. https://doi.org/10.1016/j.jmb.2013.09.041

57. Thomas E., Feld J.J., Li Q., Hu Z., Fried M.W., Liang T.J. Ribavirin potentiates interferon action by augmenting interferon-stimulated gene induction in hepatitis C virus cell culture models. *Hepatology.* 2011;53(1):32-41. https://doi.org/10.1002/hep.23985

58. Meier V., Burger E., Mihm S., Saile B., Ramadori G. Ribavirin inhibits DNA, RNA, and protein synthesis in PHA-stimulated human peripheral blood mononuclear cells: Possible explanation for therapeutic efficacy in patients with chronic HCV infection. *J. Med. Virol.* 2003;69(1):50-8. https://doi.org/10.1002/jmv.10264

59. Taylor M.W., Grosse W.M., Schaley J.E., Sanda C., Wu X., Chien S.C., Smith F., Wu T.G., Stephens M., Ferris M.W., McClintick J.N., Jerome R.E., Edenberg H.J. Global effect of PEG-IFN-alpha and ribavirin on gene expression in PBMC *in vitro*. *J. Interferon Cytokine Res.* 2004;24(2):107-18. https://doi.org/10.1089/107999004322813354

60. Stevenson N.J., Murphy A.G., Bourke N.M., Keogh C.A., Hegarty J.E., O'Farrelly C. Ribavirin enhances IFN-alpha signalling and MxA expression: A novel immune modulation mechanism during treatment of HCV. *PLoS One.* 2011;6(11):e27866. https://doi.org/10.1371/journal.pone.0027866

61. Feld J.J., Lutchman G.A., Heller T., Hara K., Pfeiffer J.K., Leff R.D., Meek C., Rivera M., Ko M., Koh C., Rotman Y., Ghany M.G., Haynes-Williams V., Neumann A.U., Liang T.J., Hoofnagle J.H. Ribavirin improves early responses to peginterferon through improved interferon signaling. *Gastroenterology.* 2010;139(1):154-162.e4. https://doi.org/10.1053/j.gastro.2010.03.037

62. Conte E., Modica A., Cacopardo B., Messina L., Nigro L., Messina A. Ribavirin up-regulates IL-12 p40 gene expression and restores IL-12 levels in Leishmania-treated PBMCs. *Parasite Immunol.* 2005;27(12):447-51. https://doi.org/10.1111/j.1365-3024.2005.00796.x

63. Tokumoto Y., Hiasa Y., Uesugi K., Watanabe T., Mashiba T., Abe M., Kumagi T., Ikeda Y., Matsuura B., Onji M. Ribavirin regulates hepatitis C virus replication through enhancing interferon-stimulated genes and interleukin 8. *J. Infect. Dis.* 2012;205(7):1121-1130. https://doi.org/10.1093/infdis/jis025

64. Kast R.E. Ribavirin in cancer immunotherapies - Controlling nitric oxide helps generate cytotoxic lymphocyte. *Cancer Biology & Therapy.* 2002;1(6):626-630. https://doi.org/10.4161/cbt.310

65. Müller W.E.G., Maidhof A., Taschner H., Zahn R.K. Virazole (1-β-D-ribofuranosyl-1,2,4-triazole-3-carboxamide); A cytostatic agent. *Biochem. Pharmacol.* 1977;26(11):1071-1075. https://doi.org/10.1016/0006-2952(77)90246-5

66. https://clinicaltrials.gov/ct2/results?term=ribavirin&cond=cancer

67. Petrelli R., Torquati I., Felczak K., Wilson D.J., Cappellacci L. Novel inhibitors of inosine monophosphate dehydrogenase as potential anti-cancer drugs: A patent review (2002-2014). In: Topics in Anti-Cancer Research. V. 3. *Bentham Publ.*, 2014:37-102. https://doi.org/10.2174/978160805090891140301

68. Ochiai Y., Sano E., Okamoto Y., Yoshimura S., Makita K., Yamamuro S., Ohta T., Ogino A., Tadakuma H., Ueda T., Nakayama T., Hara H., Yoshino A., Katayama Y. Efficacy of ribavirin against malignant glioma cell lines: Follow-up study. *Oncol. Rep.* 2018;39(2):537-544. https://doi.org/10.3892/or.2017.6149

69. Pankiewicz K.W., Felczak K. From ribavirin to NAD analogues and back to ribavirin in search for anticancer agents. *Heterocyclic Commun.* 2015;21(5):249-257.

70. Shi F., Len Y., Gong Y., Shi R., Yang X., Naren D., Yan T. Ribavirin inhibits the activity of mTOR/eIF4E, ERK/Mnk1/eIF4E signaling pathway and synergizes with tyrosine kinase inhibitor Imatinib to impair Bcr-Abl mediated proliferation and apoptosis in Ph+ leukemia. *PLoS One.* 2015;10(8):e0136746. https://doi.org/10.1371/journal.pone.0136746

71. De la Cruz-Hernandez E., Medina-Franco J.L., Trujillo J., Chavez-Blanco A., Dominguez-Gomez G., Perez-Cardenas E., Gonzalez-Fierro A., Taja-Chayeb L., Duenas-Gonzalez A. Ribavirin as a tri-targeted antitumor repositioned drug. *Oncol. Rep.* 2015;33(5):2384-2392. https://doi.org/10.3892/or.2015.3816

72. Shelton J., Lu X., Hollenbaugh J.A., Cho J.H., Amblard F., Schinazi R.F. Metabolism, biochemical actions, and chemical synthesis of anticancer nucleosides, nucleotides, and base analogs. *Chem. Rev.* 2016;116(23):14379-14455. https://doi.org/10.1021/acs.chemrev.6b00209

73. Naik G.S., Tyagi M.G. A pharmacological profile of ribavirin and monitoring of its plasma concentration in chronic hepatitis C infection. *J. Clin. Exp. Hepatol.* 2012;2(1):42-54. https://doi.org/10.1016/S0973-6883(12)60090-5

74. Ramasamy K.S., Tam R.C., Bard J., Averett D.R. Monocyclic l-nucleosides with type 1 cytokine-inducing activity. *J. Med. Chem*. 2000;43(5):1019-1028. https://doi.org/10.1021/jm9905514

75. Harris S., Robins R.K. Ribavirin: Structure and Antiviral Activity Relationships. Ribavirin – A Broad Spectrum Antiviral Agent. New York: Academic Press, 1980:1-21.

76. Streeter D.G., Miller J.P., Robins R.K., Simon L.N. The enzymic conversion of 1,2,4-triazole-3-carboxamide to ribavirin-5'-phosphate and its relationship to the proposed mechanism of action. *Ann. N. Y. Acad. Sci.* 1977;284(1):201-210. https://doi.org/10.1111/j.1749-6632.1977.tb21952.x

77. Kumarapperuma S.C., Sun Y., Jeselnik M., Chung K., Parker W.B., Jonsson C.B., Arterburn J.B. Structural effects on the phosphorylation of 3-substituted 1-β-D-ribofuranosyl-1,2,4-triazoles by human adenosine kinase. *Bioorg. Med. Chem. Lett.* 2007;17(11):3203-3207. https://doi.org/10.1016/j.bmcl.2007.03.018

78. Tsilevich T.L., Schaveleva I.L., Nosach N.L., Govtnovataya V.L., Smirnov I.P., Kochetkova S.V., Gottich B.P., Florent'ev V.L. Acyclic ribavirin analogues. Synthesis and antiviral activity. *Bioorganicheskaya Khimiya (Russian Journal of Bioorganic Chemistry).* 1988;14(5):689-693 (in Russ.).

79. Witkowski J.T., Robins R.K. N-Substituted 1,2,4-triazoles : Pat. US 3991078. Appl. 03/18/1974; publ. 11/09/1976. 5 p.

80. Witkowski J.T., Robins R.K. Synthesis and Chemistry of Certain Azole Nucleosides. In: Chemistry and Biology of Nucleosides and Nucleotides. Eds. R.E.Harmon, R.K. Robins, L.B. Townsend. New York: Academic Press, 1978:267-286. https://doi.org/10.1016/B978-0-12-326140-3.50023-1

81. Preobrazhenskaya M.N., Korbukh I.A. The Synthesis and Reactions of Pyrrole, Pyrazole, Triazole, Indole, Indazole, and Benzotriazole Nucleosides and Nucleotides. In: Chemistry of Nucleosides and Nucleotides. Ed. L.B. Townsend. V. 3. New York: Springer US, 1994:1-105. https://doi.org/10.1007/978-1-4757-9667-4_1

82. Naik S.R., Witkowski J.T., Robins R.K. Synthesis of nucleosides of 5-substituted 1,2,4-triazole-3-carboxamides. *J. Het. Chem.* 1974;11(1):57-61. https://doi.org/10.1002/jhet.5570110112

83. Konstantinova I.D., Fateev I.V., Muzyka I.S., Galkina I.V., Butenko A.M., Galegov G.A., Belov A.V., Larichev V.F., Deryabin P.G., Shvets V.I., L'vov D.K., Miroshnikov A.I. A biotechnological method for obtaining of ribavirin 5-methyl substitutes and study on their antiviral activity. *Biotechnology in Russia.* 2008;(4):98-112. Translated from Biotechnologiya, 2008;(4):69-79.

84. Witkowski J.T., Robins R.K., Khare G.P., Sidwell R.W. Synthesis and antiviral activity of 1,2,4-triazole-3-thiocarboxamide and 1,2,4-triazole-3-carboxamidine ribonucleosides. *J. Med. Chem.* 1973;16(8):935-937. https://doi.org/10.1021/jm00266a014

85. Zeidler J., Baraniak D., Ostrowski T. Bioactive nucleoside analogues possessing selected five-membered azaheterocyclic bases. Eur. *J. Med. Chem.* 2015;97:409-418. https://doi.org/10.1016/j.ejmech.2014.11.057

86. Lin C.-C., Lourenco D., Xu G., Yeh L.-T. Disposition and metabolic profiles of [^{14}C]viramidine and [^{14}C]ribavirin in rat and monkey red blood cells and liver. *Antimicrob. Agents Chemother.* 2004;48(5):1872-1875. https://doi.org/10.1128/aac.48.5.1872-1875.2004

87. Lin C.-C., Luu K., Lourenco D., Yeh L.-T. Pharmacokinetics and metabolism of [^{14}C]viramidine in rats and cynomolgus monkeys. *Antimicrob. Agents Chemother.* 2003;47(8):2458-2463. https://dx.doi.org/10.1128%2FAAC.47.8.2458-2463.2003

88. Lin C.C., Philips L., Xu C., Yeh L.T. Pharmacokinetics and safety of viramidine, a prodrug of ribavirin, in healthy volunteers. *J. Clin. Pharmacol.* 2004;44(3):265-275. https://doi.org/10.1177/0091270004262974

89. Sanghvi Y.S., Hanna N.B., Larson S.B., Fujitaki J.M., Willis R.C., Smith R.A., Robins R.K., Revankar G.R. Synthesis and evaluation of 5-amino-1-β-D-ribofuranosyl-1,2,4-triazole-3-carboxamidine and certain related nucleosides as inhibitors of purine nucleoside phosphorylase. *J. Med. Chem.* 1988;31(2):330-335. https://doi.org/10.1021/jm00397a010

90. Wu J.Z., Larson G., Hong Z. Dual-action mechanism of viramidine functioning as a prodrug and as a catabolic inhibitor for ribavirin. *Antimicrob. Agents Chemother.* 2004;48(10):4006-4008. https://dx.doi.org/10.1128%2FAAC.48.10.4006-4008.2004

91. Gabrielsen B., Phelan M.J., Barthel-Rosa L., See C., Huggins J.W., Kefauver D.F., Monath T.P., Ussery M.A., Chmurny G.N. Synthesis and antiviral evaluation of *N*-carboxamidine-substituted analogs of 1-β-D-ribofuranosyl-1,2,4-triazole-3-carboxamidine hydrochloride. *J. Med. Chem.* 1992;35(17):3231-3238. https://doi.org/10.1021/jm00095a020

92. Arterburn J., Kumarapperuma S., Jeselnik M., Chung D.-H., Sun Y., Parker W., Chu Y.K., Jonsson C. Design, synthesis and evaluation of 3-ethynyl-azole nucleosides with antiviral

activity against hantaviruses. *Antiviral Res.* 2008;78(2):A33. http://dx.doi.org/10.1016/j.antiviral.2008.01.057

93. McDowell M., Gonzales S.R., Kumarapperuma S. C., Jeselnik M., Arterburn J.B., Hanley K.A. A novel nucleoside analog, 1-β-D-ribofuranosyl-3-ethynyl-[1,2,4]-triazole (ETAR), exhibits efficacy against a broad range of flaviviruses *in vitro*. *Antiviral Res.* 2010;87(1):78-80. https://doi.org/10.1016/j.antiviral.2010.04.007

94. Bzowska A., Kulikowska E., Shugar D. Purine nucleoside phosphorylases: properties, functions, and clinical aspects. *Pharmacology & Therapeutics.* 2000;88(3):349-425. https://doi.org/10.1016/S0163-7258(00)00097-8

95. Liu W.Y., Li H.Y., Zhao B.X., Shin D.S., Lian S., Miao J.Y. Synthesis of novel ribavirin hydrazone derivatives and anti-proliferative activity against A549 lung cancer cells. *Carbohydr. Res.* 2009;344(11):1270-1275. https://doi.org/10.1016/j.carres.2009.05.017

96. Arterburn J.B., Jonsson C.B., Parker W.B. Azole nucleosides and use as inhibitors of RNA and DNA viral polymerases. Int. Pat. Appl. WO2008067002A2. Appl. 09/11/2006; publ. 06/05/2008. 64 p.

97. Konstantinova I.D., Chudinov M.V., Fateev I.V., Matveev A.V., Zhurilo N.I., Shvets V.I., Miroshnikov A.I. Chemoenzymatic method of 1,2,4-triazole nucleoside synthesis: Possibilities and limitations. *Russ. J. Bioorg. Chem.* 2013;39(1):53-71. https://doi.org/10.1134/S1068162013010056

98. Smirnova O.S., Konstantinova I.D., Fateev I.V., Zhurilo N.I., Chudinov M.V., Miroshnikov A.I. Biotechnological process for the preparation of an antiviral drug ribavirin analogues substituted on the amide group. *FEBS J.* 2013; 280 (Suppl):369. https://doi.org/10.1111/febs.12340

99. Goswami A., Van Lanen S.G. Enzymatic strategies and biocatalysts for amide bond formation: Tricks of the trade outside of the ribosome. *Mol. Biosyst.* 2015;11(2):338-353. https://doi.org/10.1039/c4mb00627e

100. Zhurilo N.I., Chudinov M.V., Matveev A.V., Smirnova O.S., Konstantinova I.D., Miroshnikov A.I., Prutkov A.N., Grebenkina L.E., Pulkova N.V., Shvets V I. Isosteric ribavirin analogues: Synthesis and antiviral activities. *Bioorg. Med. Chem. Lett.* 2018;28(1):11-14. https://doi.org/10.1016/j.bmcl.2017.11.029

101. Xia Y., Qu F., Peng L. Triazole nucleoside derivatives bearing aryl functionalities on the nucleobases show antiviral and anticancer activity. *Mini-Reviews in Med. Chem.* 2010;10(9):806-821. https://doi.org/10.2174/138955710791608316

102. Xia Y., Fan Z., Yao J., Liao Q., Li W., Qu F., Peng L. Discovery of bitriazolyl compounds as novel antiviral candidates for combating the tobacco mosaic virus. *Bioorg. Med. Chem. Lett.* 2006;16(10):2693-2698. https://doi.org/10.1016/j.bmcl.2006.02.023

103. Wang M., Zhu R., Fan Z., Fu Y., Feng L., Yao J., Maggiani A., Xia Y., Qu F., Peng L. Bitriazolyl acyclonucleosides synthesized via Huisgen reaction using internal alkynes show antiviral activity against tobacco mosaic virus. *Bioorg. Med. Chem. Let*t. 2011; 21(1): 354-357. https://doi.org/10.1016/j.bmcl.2010.10.141

104. Xia Y., Li W., Qu F., Fan Z., Liu X., Berro C., Rauzy E., Peng L. Synthesis of bitriazolyl nucleosides and unexpectedly different reactivity of azidotriazole nucleoside isomers in the Huisgen reaction. *Org. Biomol. Chem.* 2007;5(11):1695-1701. https://doi.org/10.1039/b703420b

105. Chudinov M.V., Matveev A.V., Prutkov A.N., Konstantinova I.D., Fateev I.V., Prasolov V.S., Smirnova O.A., Ivanov A.V., Galegov G.A., Deryabin P.G. Novel 5-alkyl(aryl)-substituted ribavirine analogues: synthesis and antiviral evaluation. *Mendeleev Commun.* 2016;26(3):214-216. https://doi.org/10.1016/j.mencom.2016.04.012

106. Zhu R., Wang M., Xia Y., Qu F., Neyts J., Peng L. Arylethynyltriazole acyclonucleosides inhibit hepatitis C virus replication. *Bioorg. Med. Chem. Lett.* 2008;18(11):3321-3327. https://doi.org/10.1016/j.bmcl.2008.04.026

107. Neyts J., Peng L., Que F., Zhu R. Novel viral replication inhibitors: Int. Pat. Appl. WO2009015446A2. Appl. 07/27/2007; publ. 02/05/2009. 50 p.

108. Wan J., Xia Y., Liu Y., Wang M., Rocchi P., Yao J., Qu F., Neyts J., Iovanna J. L., Peng L. Discovery of novel arylethynyltriazole ribonucleosides with selective and effective antiviral and antiproliferative activity. *J. Med. Chem.* 2009;52(4):1144-1155. https://doi.org/10.1021/jm800927r

109. Chudinov M.V., Prutkov A.N., Matveev A.V., Grebenkina L.E., Konstantinova I.D., Berezovskaya Y.V. An alternative route to the arylvinyltriazole nucleosides. *Bioorg. Med. Chem. Lett.* 2016;26(14):3223-3225. https://doi.org/10.1016/j.bmcl.2016.05.072

110. Peng L., Rocchi P., Iovanna J., Xia Y., Qu F., Wan J., Liu Y., Wang M. Novel triazole derivatives, their preparation and their application in therapeutics: US Pat. Appl. 2011136754A1; appl. 02/14/2011; publ. 06/09/2011. 26 p.

111. Xia Y., Liu Y., Wan J., Wang M., Rocchi P., Qu F., Iovanna J.L., Peng L. Novel triazole ribonucleoside down-regulates heat shock protein 27 and induces potent anticancer activity on drug-resistant pancreatic cancer. *J. Med. Chem.* 2009;52(19):6083-6096. https://doi.org/10.1021/jm900960v

112. Liu Y., Xia Y., Fan Y., Maggiani A., Rocchi P., Qu F., Iovanna J.L., Peng L. N-Aryltriazole ribonucleosides with potent antiproliferative activity against drug-resistant pancreatic cancer. *Bioorg. Med. Chem. Lett.* 2010;20(8):2503-2507. https://doi.org/10.1016/j.bmcl.2010.02.104

113. Xia Y., Liu Y., Rocchi P., Wang M., Fan Y., Qu F., Iovanna J. L., Peng L. Targeting heat shock factor 1 with a triazole nucleoside analog to elicit potent anticancer activity on drug-resistant pancreatic cancer. *Cancer Lett.* 2012;318(2):145-153. https://doi.org/10.1016/j.canlet.2011.09.043

114. Xia Y., Wang M., Demaria O., Tang J., Rocchi P., Qu F., Iovanna J. L., Alexopoulou L., Peng L. A novel bitriazolyl acyclonucleoside endowed with dual antiproliferative and immunomodulatory activity. *J. Med. Chem.* 2012;55(11):5642-5646. https://doi.org/10.1021/jm300534u

115. Chen M.M., Zhou Z.W., Suo Y.X., Li M.Y., Yao J.H., Peng L., Xia Y. Acyclonucleosides bearing coplanar arylethynyltriazole nucleobases: synthesis, structural analysis, and biological evaluation. *New Journal of Chemistry.* 2017;41(16):8509-8519. https://doi.org/10.1039/C7NJ01406F

116. Xia Y., Wang M., Beraldi E., Cong M., Zoubeidi A., Gleave M., Peng L. A novel triazole nucleoside suppresses prostate cancer cell growth by inhibiting heat shock factor 1 and androgen receptor. *Anticancer Agents Med. Chem.* 2015;15(10):1333-1340. https://doi.org/10.2174/1871520615666150617110943

117. Konstantinova I.D., Chudinov M.V., Prutkov A.N., Matveev A.V., Grebenkina L.E., Dorofeeva E.V. 5-(Tetrahydrofuran-2-yl)-1,2,4-triazole-3-carboxylic acid amide with antiviral activity, and method for production: pat. RU 2624018. Appl. 09/26/2016; publ. 06/30/2017. 8 p. (in Russ.).

About the author:

Mikhail V. Chudinov, Cand. of Sci. (Chemistry), Associate Professor of the Chair of Biotechnology and Industrial Pharmacy, M.V. Lomonosov Institute of Fine Chemical Technologies, MIREA – Russian Technological University (86, Vernadskogo pr., Moscow 119571, Russia). E-mail: chudinov@mirea.ru. ResearcherID L-5728-2016, https://orcid.org/0000-0001-9735-9690

Об авторе:

Чудинов Михаил Васильевич, кандидат химических наук, доцент кафедры биотехнологии и промышленной фармации Института тонких химических технологий им. М.В. Ломоносова ФГБОУ ВО «МИРЭА – Российский технологический университет» (119571, Россия, Москва, пр-т Вернадского, д. 86). E-mail: chudinov@mirea.ru. ResearcherID L-5728-2016, https://orcid.org/0000-0001-9735-9690

For citation: Chudinov M.V. Ribavirin and its analogs: Can you teach an old dog new tricks? *Tonkie Khimicheskie Tekhnologii = Fine Chemical Technologies.* 2019;14(4):7-23 (in Russ.). https://doi.org/10.32362/2410-6593-2019-14-4-7-23

Для цитирования: Чудинов М.В. Рибавирин и его аналоги: можно ли старую собаку научить новым фокусам? // Тонкие химические технологии. 2019. Т. 14. № 4. С. 7–23. https://doi.org/10.32362/2410-6593-2019-14-4-7-23

Translated by R. Trikin

Fine Chemical Technologies, 2019, Vol. 14, No. 4, pp. 24–32.
Original Russian Text © Valentina M. Raeva, Olga V. Gromova, published in Tonkie Khimicheskie Tekhnologii, 2019, Vol. 14, No. 4, pp. 24–32

THEORETICAL BASES OF CHEMICAL TECHNOLOGY

ТЕОРЕТИЧЕСКИЕ ОСНОВЫ ХИМИЧЕСКОЙ ТЕХНОЛОГИИ

https://doi.org/10.32362/2410-6593-2019-14-4-24-32
UDC 66.048.625

CC BY

Separation of water – formic acid – acetic acid mixtures in the presence of sulfolane

Valentina M. Raeva[@], Olga V. Gromova

MIREA – Russian Technological University (M.V. Lomonosov Institute of Fine Chemical Technologies), Moscow 119571, Russia
[@] Corresponding author, e-mail: raevalentina1@gmail.com

In this paper, extractive distillation flowsheets for water–formic acid–acetic acid mixtures were designed. Flowsheets not involving preliminary dehydration were considered, and the relative volatilities of the components in the presence of sulfolane were analyzed. The result of extractive distillation depends on the amount of sulfolane. The structure of the flowsheet is determined by the results of the basic ternary mixture extractive distillation. In three-column flowsheets (schemes I, II), water is isolated in the distillate of the extractive distillation column. In the second column, distillation of the formic acid–acetic acid–sulfolane mixture is carried out, yielding formic acid (90 wt %) and acetic acid (80 wt %). The recycled flow is returned to the first column. Dilution of the formic acid–acetic acid–sulfolane mixture with sulfolane (second column of flowsheet II) allows for acids of higher quality (main substance content equal to or more than 98.5 wt %) to be obtained. Flowsheet III includes four columns and two recycling stages. First, the water–formic acid mixture is isolated in the distillate of the extractive distillation column. Then, water and formic acid are separated in a two-column complex by extractive distillation, also with sulfolane. We were carrying out calculations for column working pressure 101.32 and 13.33 kPa. To prevent thermal decomposition of sulfolane, working pressure for regeneration columns was always 13.33 kPa. The extractive distillation column of the basic three-component mixture is the main factor contributing to the total energy consumption for separation (in all schemes).

Keywords: *formic acid, acetic acid, water, sulfolane, extractive distillation, separation flowsheet.*

Разделение смеси вода – муравьиная кислота – уксусная кислота в присутствии сульфолана

В.М. Раева[@], О.В. Громова

МИРЭА – Российский технологический университет (Институт тонких химических технологий имени М.В. Ломоносова), Москва 119571, Россия
[@] Автор для переписки, e-mail: raevalentina1@gmail.com

При экстрактивной ректификации (ЭР) водных смесей низших карбоновых кислот (муравьиной и уксусной), в зависимости от выбора селективного агента, возможно выделение в дистиллате воды или смеси вода – муравьиная кислота. Однако обычно задача выделения всех практически чистых компонентов не рассматривается. Здесь предлагаются схемы выделения муравьиной (МК) и уксусной (УК) кислот из водной смеси экстрактивной ректификацией (ЭР) с сульфоланом, не предусматривающие предварительное обезвоживание. Анализ рядов относительных летучестей компонентов в присутствии сульфолана показал, что в зависимости от количества вводимого агента возможны три варианта организации ЭР. В схемах, состоящих из трех колонн, в дистиллате колонны ЭР базовой смеси вода–МК–УК выделяют воду, в последней колонне схемы УК отделяют от агента, возвращаемого в первую колонну схемы. Во второй колонне схемы I проводят ректификацию смеси МК–УК–сульфолан с получением МК (90% масс.) и УК (80% масс.), в схеме II смесь МК–УК разбавляют сульфоланом, что позволяет получать кислоты более высокого качества: МК (УК) с содержанием основного вещества не менее 98.5% масс. Схема III состоит из двух двухколонных комплексов ЭР: сначала выделяют смесь воды и муравьиной кислоты, которую затем разделяют ЭР также с сульфоланом. Расчеты схем проведены для рабочих давлений колонн 101.32 и 13.33 кПа. Для предотвращения термического разложения сульфолана колонны регенерации всегда работают при давлении 13.33 кПа. Максимальный вклад в суммарные энергозатраты на разделение во всех схемах вносит колонна ЭР базовой трехкомпонентной смеси.

Ключевые слова: *муравьиная кислота, уксусная кислота, вода, сульфолан, экстрактивная ректификация, схема разделения.*

Introduction

It is often necessary to separate aqueous mixtures of carboxylic acids with low molecular weights (C_1–C_4) for the purposes of fine organic synthesis and in pulp manufacturing [1–3]. For example, the oxidation of C_9–C_{20} paraffins results in a mixture of C_1–C_6 carboxylic acids (wt %): formic acid (FA) – 35–40, acetic acid (AA) – 30–35, propionic and butyric acids – 20–30, valeric and caproic acids – up to 2–6. Having removed the C_4–C_6 acids, the next step is to separate the water–FA–AA mixture of different compositions.

The use of reactive distillation has been proposed, namely esterification with low molecular weight alcohols, in order to purify waste waters [4–7]. The latter, when resulting from the liquid-phase oxidation of solid paraffins, contain on average 8–10 wt % of C_1–C_4 carboxylic acids [2]. Reactive distillation experimental tests have been carried out for the undilluted solutions of acids [7]. In the column distillate, it is possible to obtain a mixture of esters (methyl formate–methyl acetate) by reactive distillation, using water–FA–AA mixtures with 10:80:10 and 30:60:10 wt %. The methanol:AA ratio is 2.4:1 (mol/mol) and the reflux ratio is 10. The bottom product contains water and acetic acid.

Results of extractive distillation in industrial conditions have also been published [8, 9]. In these experiments, the periodic operation mode was used at a pressure of 101.32 kPa. Water–FA–AA mixtures with 40:32:28 wt %, with various added agents, were analyzed. When pelargonic acid was introduced, the distillate composition of water–FA–AA mixture was 75:14:11 wt %, and the bottom product of the column contained an FA–AA–agent mixture with the ratio of 12:15:73 wt % [8]. The addition of an acetylsalicylic acid/heptanoic acid mixture (50:50 wt %) led to the following composition of the distillate and bottom product: 78:18:4 wt % and 10:14:76 wt %, respectively [9].

Extractive distillation in the presence of *N*-methyl-2-pyrrolidone was performed for the mixture water–FA–AA–admixtures. The ratio of the components was 27.8:5.5:64.7:2 wt %, and atmospheric pressure (1.013 bar) was applied. The bottom product in this case also contained mostly acetic acid and added agent; water–FA–AA–agent = 0.1:2.0:28.6:69.6 wt %. The distillate contained water and formic acid, with no more than 0.2 wt % total admixtures [10]. The regeneration of *N*-methyl-2-pyrrolidone in the industrial setting was performed at 0.3 bar (60 theoretical plates; R≈1). This produced rather pure *N*-methyl-2-pyrrolidone; 0.1:0.4:4.7:94.9 wt %. The distillate of the regeneration column was as follows: water–FA–AA = 0.4:7.6:92.0 wt %.

Another goal, was set in [11], namely the generation of almost pure water by extractive distillation of basic mixtures with *N*-methyl-2-pyrrolidone. Extractive distillation was performed for mixtures containing formic acid at 10÷80 wt % with an increment of 10 wt %. The pressure was 101.3 kPa and *N*-methyl-2-pyrrolidone was used at

a 2:1 (mol/mol) ratio with feed. The result showed that extractive distillation with *N*-methyl-2-pyrrolidone could be done for mixtures containing: 10 wt % formic acid and more than 50 wt % water; 20 (30) wt % formic acid and more than 40 wt % water. The rate of agent was selected, without any further reasoning, as the economically stipulated limit, with anything above it leading to a dramatically higher consumption of energy used for separation. This is why it is recommended to use Pressure Swing Distillation (PSD) for mixtures that contain less than 30 wt % water [11].

Thus, the choice of the additive for extractive distillation of the basic three-component mixture dictates the need to further separate water–FA or FA–AA mixtures, for instance, by extraction [12, 13] or extractive distillation.

In order to choose the selective solvents in an industrial setting (based on vapor–liquid equilibrium (VLE) data from Othmer Still), the influence of various chemical substances on the VLE for water–FA [14–20] and FA–AA [21, 22] mixtures has been investigated.

The increase in the volatility of water (W) compared to FA at atmospheric pressure has been observed in the presence of individual or mixed solvents, of different compositions. They can be based on:

- sulfolane or adiponitrile with added acetophenone, acetylsalicylic acid, sulfones, etc. ($3.2 \le \alpha_{W/FA} \le 5$) [14];
- cyclohexanone or isophorone with added aliphatic monocarboxylic acids and acetophenone ($2 \le \alpha_{W/FA} \le 3$) [15];
- ethylene carbonate or propylene carbonate with added carboxylic acids (various structures) and isophorone ($2.5 \le \alpha_{W/FA} \le 2.9$) [16];
- dicarboxylic acids with added monocarboxylic acids, 2-hydroxyacetone and other substances with a high boiling point ($2.8 \le \alpha_{W/FA} \le 3.1$) [17];
- sulfolane, adiponitrile, dimethylformamide, *N,N*-dimethylacetamide, *N*-mehtyl-2-pyrrolidone, acetophenone and their mixtures with other organic substances ($3 \le \alpha_{W/FA} \le 11$) [18].

Batch extractive distillation for water–FA mixtures shows that the distillate may contain almost pure water if the following agents are used: heptanoic and azelaic acids (ratio 80:20 wt %); heptanoic, azelaic acids and 2-hydroxyacetone (ratio 67:16:17 wt %) [17]; sulfolane [14]; adiponitrile [18]; *N*-formylmorpholine [19]. The use of isophorone leads to the accumulation of FA in the distillate (89 wt %) [15].

According to experimental data, the choice of a selective agent for extractive distillation of FA–AA mixtures is rather complicated [8, 9, 21–23]. Certain binary extractive agents have been suggested, in which acetylsalicylic acid is paired with an organic solvent: amyl acetate, ethylene carbonate, propylene carbonate, diisobutyl ketone, 2-(4-)hydroxyacetophenone, methyl (ethyl, butyl) benzoates, cyclohexanone, and aromatic nitro compounds. The majority of these substances have been found to be not selective enough, with the highest values of $1.5 \le \alpha_{FA/AA} \le 2.2$ observed for the mixed agents which contain carboxylic acids, nitrobenzene or acetophenone [8].

This work focuses on extractive distillation of the three-component water–FA–AA mixture with sulfolane (S). The latter is an industrial solvent, which fits the standard requirements for extractive agents [24, 25], and sulfolane was previously suggested for extractive distillation of water–FA [18], water–AA [26] mixtures. The use of sulfolane allows for the expectation that separation of water from carboxylic acids will occur.

Methods

Calculations were conducted using Aspen ONE Engineering V9.0 software. The NRTL equation was utilized to simulate VLE. The nonideal behavior of the vapor phase was taken into account by the NRTL-HOC model.

Results and Discussion

The VLE simulation for the water–FA–AA mixture corresponds to the existing data [27, 28]: at pressure of 101.32 kPa and lower than 26.66 kPa the curvature of the separatrix is different (Fig. 1). The selection of 13.33 kPa pressure is determined by the need to prevent the decomposition of the agent [25].

According to the data from [11], the highest energy consumption (for PSD) is observed when water–FA–AA mixtures contain 10–20 wt % FA. To evaluate the

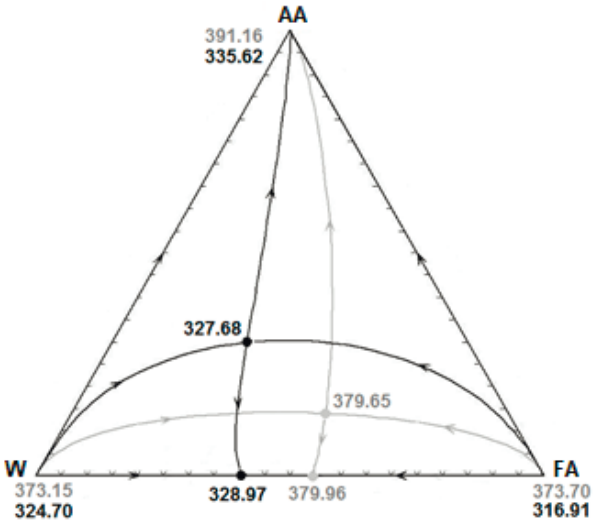

Fig. 1. The diagram of the vapor–liquid equilibrium (VLE) for the water (W)–formic acid (FA)–acetic acid (AA) system.
——— 13.33 kPa ——— 101.32 kPa

feasability of extractive distillation with sulfolane, we have selected the equimolar mixture (water:FA:AA = 14.5:37.0:48.5 wt %). This mixture has been considered in previous publications, and the separation options take into account the changes in separatrix position and shape with changing pressure [11, 27, 28].

We have calculated the relative volatilities $\alpha_{W\text{-}FA}$, $\alpha_{W\text{-}AA}$, $\alpha_{FA\text{-}AA}$ for the basic equimolar mixture and for the derived system, water−FA−AA−S, with various amounts of sulfolane (S). Two different pressure values were used (Tables 1, 2). Since the $\alpha_{FA\text{-}AA}$ values are the lowest, it is predicted that a water-enriched distillate will be obtained at extractive distillation of the equimolar water−FA−AA mixture. The calculations for extractive distillation of this mixture are presented in Table 3 (column I). The distillate contains almost pure water.

Table 1. The relative volatilities of the substances and selectivity of sulfolane at 101.32 kPa

F_S	$\alpha_{W\text{-}FA}$	$\alpha_{W\text{-}AA}$	$\alpha_{FA\text{-}AA}$	$S_{W\text{-}FA}$	$S_{W\text{-}AA}$	$S_{FA\text{-}AA}$
0	1.17	1.26	1.08	–	–	–
50	1.99	2.90	1.46	1.70	2.30	1.35
100	2.67	4.23	1.585	2.28	3.35	1.47
150	3.25	5.29	1.63	2.77	4.19	1.51
200	3.73	6.14	1.65	3.19	4.87	1.53
250	4.14	6.82	1.65	3.54	5.41	1.53
300	4.48	7.37	1.64	3.84	5.84	1.53
350	4.77	7.81	1.64	4.07	6.19	1.52
400	5.00	8.16	1.63	4.27	6.47	1.51
450	5.20	8.45	1.62	4.44	6.695	1.51
500	5.37	8.68	1.62	4.56	6.88	1.50

Table 2. The relative volatilities of the substances and selectivity of sulfolane at 13.33 kPa

F_S	$\alpha_{W\text{-}FA}$	$\alpha_{W\text{-}AA}$	$\alpha_{FA\text{-}AA}$	$S_{W\text{-}FA}$	$S_{W\text{-}AA}$	$S_{FA\text{-}AA}$
0	0.86	0.955	1.115	–	–	–
50	1.68	2.53	1.50	1.96	2.645	1.36
100	2.44	3.99	1.64	2.845	4.18	1.40
150	3.14	5.31	1.695	3.66	5.57	1.52
200	3.77	6.50	1.72	4.41	6.81	1.54
250	4.35	7.54	1.73	5.10	7.90	1.55
300	4.86	8.45	1.74	5.67	8.85	1.56
350	5.31	9.24	1.74	6.20	9.67	1.56
400	5.71	9.92	1.74	6.67	10.4	1.56
450	6.071	10.5	1.73	7.09	11.0	1.555
500	6.389	11.05	1.73	7.46	11.6	1.55

We have considered the separation of 100 kmol/h of the water−FA−AA equimolar mixture at two different pressure values. To prevent reagent decomposition, the columns whose bottom products contain almost pure sulfolane, work at reduced pressure.

Extractive distillation flowsheets for the basic water−FA−AA mixture are shown in Fig. 2. Flowsheets I, II result in the production of water in the distillate, flowsheet III results in the water−FA mixture in the distillate.

According to empirically substantiated guidelines, $S \geq 2$ for selective agents in extractive distillation of binary mixtures. The sulfolane selectivity relative to water for the basic three-component mixture is determined as follows:

$$S_{W-FA} = \frac{\alpha_{W-FA}^{(S)}}{\alpha_{W-FA}}, \quad S_{W-AA} = \frac{\alpha_{W-AA}^{(S)}}{\alpha_{W-AA}}$$

abovementioned condition of the amount of sulfolane being less than 100 kmol/h (Tables 1, 2).

The calculations for extractive distillation are shown in Table 3 (column I). The lowest amount of the agent which allows for the separation of almost pure water (99.5 wt %) is 150 and 170 kmol/h at atmospheric and

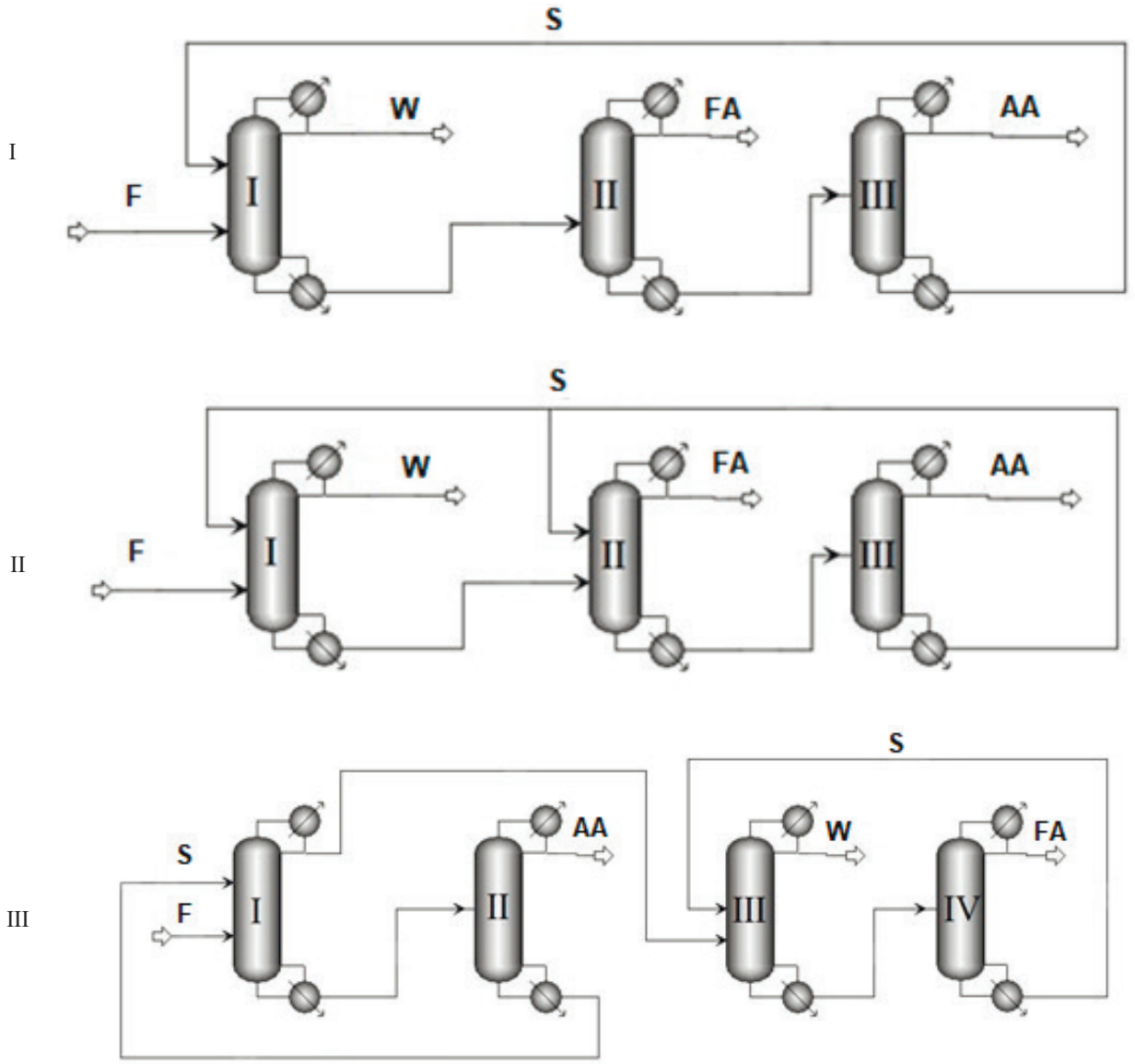

Fig. 2. Principal flowsheets of extractive distillation.
Flowsheets **I, II:** I − extractive distillation column; flowsheet **III:** I, III − extractive distillation columns.
F − basic mixture: water (W)−formic acid (FA)−acetic acid (AA).

reduced pressure, respectively. Further sequential selection of carboxylic acids is possible (flowsheet **I**, Fig. 2).

Table 4 shows the quality of acids where the content of the main component is no less than 86.5 wt % for formic acid (GOST 1706-78, mark B) and no less than 80 wt % for acetic acid (GOST 19814-74, 3rd grade).

Sulfolane is not selective in the separation of binary mixtures of carboxylic acids. For example, at 101.32 kPa, $\alpha_{FA\text{-}AA}$ is 1.49 (addition of 50 kmol agent) and 1.45 (addition of 400 kmol agent) when the amount of FA−AA is 100 kmol. The selectivity of the agent

$$S_{FA-AA} = \frac{\alpha^{(S)}_{FA-AA}}{\alpha_{FA-AA}}$$

is close to 1 at both pressure values and is almost independent of the amount of the agent.

Flowsheet **II** suggests the additional introduction of sulfolane into column II (flowsheet **II**, Fig. 2). Dilution with this agent leads to the weakening of interactions between the molecules of the acids [29], thus helping to separate them. Upon the addition of 120 kmol sulfolane to the FA−AA−S mixture (bottom flow of the extractive distillation column), the selectivity S_{FA-AA} is 0.987 (101.32 kPa) and 0.977 (13.33 kPa), indicating the absence of auto-extractive distillation.

Calculations for flowsheet **II** are shown in Table 5. Dilution of the FA−AA−S mixture with sulfolane gives purer acids (compared with data in Table 4) − no less than 98.5 wt % of the main component (formic acid, GOST 1706-78, mark A; acetic acid, GOST

Table 3. Static parameters for distillation columns in flowsheet **I**

Column		I	II	III	I	II	III
Pressure, kPa		101.32	101.32	13.33	13.33	13.33	13.33
N, N_S/N_F		40, 5/25	50, 18	5, 4	40, 3/12	50, 8	5, 4
R		1	6.6	0.01	0.05	8	0.05
Feed flow F, kmol/h		100	216.7	183.4	100	236.7	203.4
Feed flow composition, mol. fract.	W	0.3330	0.0003	0	0.333	0.0002	0
	FA	0.3330	0.1534	0.0140	0.333	0.1405	0.0126
	AA	0.3340	0.1541	0.1681	0.334	0.1411	0.1516
	S	–	0.6922	0.8179	–	0.7182	0.8358
Feed temperature T_F, K		379.86	437.78	397.45	327.49	373.36	400.98
Sulfolane flow F_S, kmol/h		150	–	–	170	–	–
Sulfolane temperature T_S, K		353.15	–	–	303.15	–	–
Distillate flow D, kmol/h		33.3	33.3	33.4	33.3	33.3	33.4
Distillate composition, mol. fract.	W	0.9983	0.0017	0	0.9984	0.0017	0
	FA	0.0017	0.9210	0.0742	0.0016	0.9216	0.0736
	AA	0	0.0773	0.8491	0	0.0767	0.8487
	S	0	0	0.0767	0	0	0.0777
Distillate temperature T_D, K		373.21	374.54	336.51	324.73	317.89	336.56
Bottom product flow W, kmol/h		216.7	183.4	150	236.7	203.4	170
Its composition, mol. fract.	W	0.0003	0	0	0.0002	0	0
	FA	0.1534	0.0140	0.0007	0.1405	0.0126	0.0006
	AA	0.1541	0.1681	0.0164	0.1411	0.1516	0.0147
	S	0.6922	0.8179	0.9829	0.7182	0.8358	0.9847
Bottom flow temperature T_W, K		437.78	469.42	460.93	373.36	400.98	462.64
Reboiler duty Q, MW		1.62	1.85	0.98	1.17	2.10	1.05
ΣQ, MW		4.45			4.32		

Abbreviations (here and throughout): N – total number of theoretical plates in the column; N_S – number of the plate where sulfolane is introduced; N_F – number of the theoretical plate with feed (numbering starts from the top of the column); R – reflux ratio.

Table 4. The quality of the obtained products

Scheme	I		II		III	
Pressure, kPa	101.32	13.33	101.32	13.33	101.32	13.33
W, wt %	99.58	99.54	99.58	99.59	99.63	99.51
FA, wt %	90.06	90.14	98.53	98.60	98.53	98.62
AA, wt %	80.14	80.03	99.17	99.21	99.00	99.02

Table 5. Static parameters for distillation columns in flowsheet **II**

Column		I	II	III	I	II	III
Pressure, kPa		101.32	101.32	13.33	13.33	13.33	13.33
N, N_S/N_F		40, 5/25	45, 5/26	15,10	40, 3/12	45, 5/21	15, 10
R		1	5	1.3	0.05	3	1.4
Feed flow F, kmol/h		100	216.7	303.4	100	236.7	323.4
Feed flow composition, mol. fract.	W	0.3330	0.0003	0	0.333	0.0002	0
	FA	0.3330	0.1534	0.0012	0.333	0.1405	0.0011
	AA	0.3340	0.1541	0.1089	0.334	0.1411	0.1022
	S	–	0.6922	0.8899	–	0.7182	0.8967
Feed temperature T_F, K		379.86	437.78	415.28	327.49	373.36	417.30
Sulfolane flow F_S, kmol/h		150	120	–	170	120	–
Sulfolane temperature T_S, K		353.15	353.15	–	303.15	303.15	–

Table 5. Continued

Column		I	II	III	I	II	III
Distillate flow D, kmol/h		33.3	33.3	33.4	33.3	33.3	33.4
Distillate composition, mol. fract.	W	0.9983	0.0017	0	0.9984	0.0016	0
	FA	0.0017	0.9875	0.0108	0.0016	0.9882	0.0097
	AA	0	0.0108	0.9892	0	0.0102	0.9903
	S	0	0	0	0	0	0
Distillate temperature T_D, K		373.21	373.85	335.30	324.73	317.10	335.33
Bottom product flow W, kmol/h		216.7	303.4	270	236.7	323.4	290
Bottom flow composition, mol. fract.	W	0.0003	0	0	0.0002	0	0
	FA	0.1534	0.0012	0	0.1405	0.0011	0
	AA	0.1541	0.1089	0.0004	0.1411	0.1022	0.0004
	S	0.6922	0.8899	0.9996	0.7182	0.8967	0.9996
Bottom flow temperature T_W, K		437.78	491.17	479.82	373.36	417.30	479.84
Reboiler duty Q, MW		1.62	2.77	1.49	1.17	2.01	1.55
ΣQ, MW		5.88			4.73		

19814-74, "synthetic acetic acid", 2nd grade). Evidently, the generation of purer products requires more energy.

Flowsheet **III** (Fig. 2) uses a variant of extractive distillation where water–FA is separated in the first column, thus eliminating the need to separate carboxylic acids at any further steps.

Energy consumption of the extractive distillation column for the basic mixture at 101.32 kPa (Table 6) is

Table 6. Static parameters for distillation columns in flowsheet **III**

Column		I	II	III	IV
Pressure, kPa		101.32	13.33	101.32	13.33
N, N_S/N_F		40, 5/28	30, 20	30, 5/10	20, 10
R		3	0.8	1	1
Feed flow F, kmol/h		100	133.4	66.6	133.3
Feed flow composition, mol. fract.	W	0.3333	0	0.5000	0.0004
	FA	0.333	0.0032	0.4935	0.2462
	AA	0.334	0.2472	0.0065	0.0032
	S	–	0.7496	0	0.7502
Feed temperature T_F, K		379.86	387.68	379.87	369.76
Sulfolane flow F_S, kmol/h		100	–	100	–
Sulfolane temperature T_S, K		353.15	–	353.15	–
Distillate flow D, kmol/h		66.6	33.4	33.3	33.3
Distillate composition, mol. fract.	W	0.5000	0	0.9986	0.0014
	FA	0.4935	0.0130	0.0014	0.9856
	AA	0.0065	0.9870	0.0000	0.0130
	S	0	0	0	0
Distillate temperature T_D, K		379.87	335.24	373.21	317.11
Bottom product flow W, kmol/h		133.4	100	133.3	100
Bottom flow composition, mol. fract.	W	0	0	0.0004	0
	FA	0.0032	0	0.2462	0
	AA	0.2472	0.0010	0.0032	0.0001
	S	0.7496	0.9990	0.7502	0.9999
Bottom flow temperature T_W, K		456.92	478.97	439.42	480.32
Reboiler duty Q, MW		3.19	0.89	1.32	1.03
ΣQ, MW		6.43			

twice as high as the values for flowsheets **I** and **II**. At 13.33 kPa the total energy consumption in flowsheet **III**, with unchanging static parameters of the columns (N, N_S/N_F), remains largely unchanged: ΣQ = 6.5 MW, Q for columns I−IV is 3.08; 0.94; 1.19; and 1.29 MW, respectively.

Conclusions

Sulfolane can be used to separate water − formic acid − acetic acid mixtures. The rate of the agent determines the results of the extractive distillation for the basic mixture. When less sulfolane is used, the distillate contains water and formic acid (flowsheet **III**). When more sulfolane is used, the distillate contains only water (flowsheets **I**, **II**).

The highest energy consumption is observed for those distillation columns where acids are distributed in various product flows: water − FA (distillate), AA – bottom product (column I in flowsheet **III**) and FA − distillate, AA − bottom product (column II in flowsheets **I**, **II**). The energy consumption of the extractive distillation column for the basic mixture in flowsheet III is twice as high as the values for schemes **I** and **II**, thus making flowsheet **III** inefficient.

The dilution of the formic acid−acetic acid mixture with sulfolane for distillation (column II, flowsheet **II**) allows for the production of acids of higher quality and purity. Flowsheet I is recommended for the production of "mark B" formic acid (GOST 1706-78) and 3rd grade acetic acid (GOST 19814-74). Yet higher quality of acids can be achieved in flowsheet II − "mark A" formic acid and 2nd grade acetic acid. The operation distillation columns I, II is recommended, with the working pressure in flowsheet **I** set at 101.32 kPa, and in flowsheet **II** – at 13.33 kPa.

It is necessary to search for ways to lower energy consumption during the separation of aqueous mixtures with formic and acetic acids. This necessity determines the next steps in research, in particular, finding selective agents for the extractive distillation of formic acid−acetic acid mixtures.

Acknowledgments

This work was carried out with the financial support of the Russian Foundation for Basic Research (RFBI), grant No. 1803-01224-a.

The authors declare no conflict of interest.

References:

1. Kushner T.M., Tatsiyevskaya G.I., Serafimov L.A., L'vov S.V. Isolation of lower carboxylic acids from the fraction of straight-run gasoline oxide. *Khimicheskaya promyshlennost' = Chemical Industry.* 1969;1:20-23 (in Russ.).

2. Frolov G.M., Shaburov M.A. Acetic acid production. Moscow: Lesnaya promyshlennost' Publ., 1978. 240 p. (in Russ.).

3. Muurinen E.I., Solo J.K. Solvent recovery in peroxyacid pulping. In: Proceed. of the First European Congress on Chemical Engineering. Florence, Italy. May 4-7, 1997; 1:543-552.

4. Painer D., Lux S., Grafschafter A., Toth A., Siebenhofen M. Isolation of carboxylic acids from biobased feedstock. *Chem. Ing. Tech.* 2017;89(1-2):161-171. https://doi.org/10.1002/cite.201600090

5. Patil K.D., Kulkarni B.D. Review of recovery methods for acetic acid from industrial waste streams by reactive distillation. J. Water Pollut. Purif. Res. 2014;1(2):13-18. https://www.researchgate.net/publication/263327618

6. Saha B., Chopade S., Mahajan S. Recovery of dilute acetic acid through esterification in a reactive distillation column. *Catal. Today.* 2000;60(1):147-157. http://dx.doi.org/10.1016/S0920-5861(00)00326-6

7. Painer D., Lux S., Siebenhofen M. Recovery of formic acid and acetic acid from waste water using reactive distillation. *Separation Science and Technology.* 2015;50(18):2930-2936. https://doi.org/10.1080/01496395.2015.1085407

8. Berg L. Separation of formic acid from acetic acid by extractive distillation: pat. 4,692,219 US; filed 12/03/1986; publ. 09/08/1987.

9. Berg L. Separation of formic acid from acetic acid by extractive distillation with acetyl salicylic acid: pat. 4,909,907 US; filed 01/17/1989; publ. 03/20/1990.

10. Cohen L.R. Method for separating carboxylic acids from mixtures with non-acids: pat. 4,576,683 US; filed 06/06/1984; publ. 03/18/1986.

11. Muuriner E. A review and distillation study related to peroxyacid pulping. Organosolv pulping. Oulu, Finland: Publ. House Oulu Yliopisto, 2000. 314 p. http://herkules.oulu.fi/isbn9514256611/isbn9514256611.pdf)

12. Sprakel L.M.J., Schuur B. Solvent developments for liquid-liquid extraction of carboxylic acids in perspective. *Separation and Purification Technology.* 2019; 211:935-957. https://doi.org/10.1016/j.seppur.2018.10.023

13. Behroozi M., Vahedpour M., Shardi Manaheji M. Separation of formic acid from aqueous solutions by liquid extraction technique at different temperatures. *Phys. Chem. Res.* 2019;7(1):201-215. https://dx.doi.org/10.22036/pcr.2019.154646.1557

14. Berg L., Yeh An-I. Dehydration of formic acid by extractive distillation: pat. 4,642,166 US; filed 02/10/1986; publ. 02/10/1987.

15. Berg L., Kraig M., Szabados R. J. Dehydration of formic acid by extractive distillation: pat. 5,173,156 US; filed 12/09/1991; publ. 12/22/1992.

16. Berg L. Dehydration of formic acid by extractive distillation: pat. 4,786,370 US; filed 01/04/1988; publ. 11/22/1988.

17. Berg L. Dehydration of formic acid by extractive distillation with dicarboxylic acids; pat. 4,877,490 US; filed 01/23/1989; publ. 10/31/1989.

18. Berg L., Yeh An-I. Dehydratation of impure formic acid by extractive distillation; pat. 4,735,690 US; filed 04/28/1986; publ. 04/05/1988.

19. Buelow H., Hohenschutz H., Schmidt J.E., Sachsze W. Purification of formic acid by extractive distillation; pat. 4,076,594 US; filed 10/04/1976; publ. 02/28/1978.

20. Prajapati Chintan, Bhatt R.P. Separation of azeotropic

mixture of formic acid − water by using Li-Br as a salt by extractive distillation. *IJARIIE.* 2016;2(3):607-612 (available from http://www.ijariie.com).

21. Berg L. Separation of formic acid from acetic acid by extractive distillation: pat. 54,692,219. US; filed 03/12/1986; publ. 08/09/1987.

22. Berg L. Separation of formic acid from acetic acid by extractive distillation; pat. 5,227,029 US; filed 01/29/1993; publ. 07/13/1993.

23. Berg L. Separation of formic acid from acetic acid by extract separation of formic acid from acetic acid by extractive distillation; pat. 4,909,907 US; filed 01/17/1989; publ. 03/20/1990.

24. Kirk-Othmer Encyclopedia of Chemical Technology. V. 8. Online ISBN: 9780471238966 Copyright © 1999-2014 by John Wiley and Sons, Inc.

25. Gayle A.A., Somov V.Ye., Varshavskiy O.M., Semenov L.V. Sulfolan: Properties and use as a selective solvent. Saint-Petersburg: Khimizdat Publ., 1998. 144 p. (in Russ.).

26. Berg L. Dehydration of acetic acid by extractive distillation; pat. 5,167,774 US; filed 02/06/1992; publ. 12/01/1992.

27. Raeva V.M. Features of the behavior of azeotropic mixtures and their separation with varying pressure: thesis ... Cand. of Sci. (Engineering). Moscow, 1998. 168 p. (in Russ.).

28. Raeva V.M., Frolkova A.K. Separation of azeotropic mixtures using pressure-based complexes. *Russian Journal of General Chemistry.* 1998;XLII(6):76-88 (in Russ.).

29. Bates R.G., Pawlak Z. Solvent effects on acid-base behavior: Five uncharged acids in water-sulfolane solvents. *J. Solution Chem.* 1976;5(3):213-222. https://doi.org/10.1007/BF00654338

About the authors:

Valentina M. Raeva, , Cand. of Sci. (Engineering), Associate Professor of the Chair of Chemistry and Technology of Basic Organic Synthesis, M.V. Lomonosov Institute of Fine Chemical Technologies, MIREA − Russian Technological University (86, Vernadskogo pr., Moscow, 119571, Russia). E-mail: raevalentina1@gmail.com. Scopus Author ID 6602836975, ResearcherID C-8812-2014, https://orcid.org/0000-0002-5664-4409

Olga V. Gromova, Master, Chair of Chemistry and Technology of Basic Organic Synthesis, M.V. Lomonosov Institute of Fine Chemical Technologies, MIREA − Russian Technological University (86, Vernadskogo pr., Moscow, 119571, Russia).

Об авторах:

Раева Валентина Михайловна, кандидат технических наук, доцент кафедры химии и технологии основного органического синтеза Института тонких химических технологий им. М.В. Ломоносова ФГБОУ ВО «МИРЭА − Российский технологический университет» (119571, Россия, Москва, пр-т Вернадского, д. 86). E-mail: raevalentina1@gmail.com. Scopus Author ID 6602836975, ResearcherID C-8812-2014, https://orcid.org/0000-0002-5664-4409

Громова Ольга Владимировна, магистр, кафедра химии и технологии основного органического синтеза Института тонких химических технологий им. М.В. Ломоносова ФГБОУ ВО «МИРЭА − Российский технологический университет» (119571, Россия, Москва, пр-т Вернадского, д. 86).

Для цитирования: Раева В.М., Громова О.В. Разделение смеси вода – муравьиная кислота – уксусная кислота в присутствии сульфолана // Тонкие химические технологии. 2019. Т. 14. № 4. С. 24–32. https://doi.org/10.32362/2410-6593-2019-14-4-24-32

For citation: Raeva V.M., Gromova O.V. Separation of the water – formic acid – acetic acid mixture with sulfolane. *Tonkie Khimicheskie Tekhnologii = Fine Chemical Technologies.* 2019;14(4):24-32 (in Russ.). https://doi.org/10.32362/2410-6593-2019-14-4-24-32

Translated by R. Trikin

Fine Chemical Technologies, 2019, Vol. 14, No. 4, pp. 33–38.
Original Russian Text © Polina E. Ignatieva, Elena S. Zhavoronok, Olga A. Legonkova, Stanislav A. Kedik,
published in Tonkie Khimicheskie Tekhnologii, 2019, Vol. 14, No. 4, pp. 33–38

CHEMISTRY AND TECHNOLOGY OF MEDICINAL COMPOUNDS AND BIOLOGICALLY ACTIVE SUBSTANCES

ХИМИЯ И ТЕХНОЛОГИЯ ЛЕКАРСТВЕННЫХ ПРЕПАРАТОВ И БИОЛОГИЧЕСКИ АКТИВНЫХ СОЕДИНЕНИЙ

https://doi.org/10.32362/2410-6593-2019-14-4-33-38

UDC 616.1

CC BY

On the use of aqueous solutions of polyvinyl methyl ether for the embolization of blood vessels

Polina E. Ignatieva[1,@], Elena S. Zhavoronok[1], Olga A. Legonkova[2], Stanislav A. Kedik[1]

[1]MIREA – Russian Technological University (M.V. Lomonosov Institute of Fine Chemical Technologies), Moscow 119571, Russia
[2]A.V. Vishnevsky National Medical Research Center of Surgery, Ministry of Health of the Russian Federation, Moscow 117997, Russia
[@]Corresponding author, e-mail: ignateva.polly@mail.ru

Aqueous solutions of polyvinyl methyl ether were investigated in order to test whether it is possible to utilize them as bases for embolic agents used to deliberately block blood vessels. This may be necessary in the course of treatment of vascular abnormalities, tumors, as well as during the preparation of patients for surgery. The right branch of the binodal curve for the binary system "polyvinyl methyl ether–water" was drawn using the cloud point method and the lower critical mixing temperature (35.5 °C) was calculated. Furthermore, the exact concentration of polyvinyl methyl ether in aqueous solutions at which phase transition occurs (given the temperature of 35.5° C) was found to be 30 wt %. The viscosity–velocity curves for the 30% solution of polyvinyl methyl ether, obtained by rheoviscometry in the temperature range of 5 to 36 °C, indicate that this aqueous solution has a low viscosity and behaves like a Newtonian fluid. However, at the temperature of 35 °C and higher, close to the phase transition, a significant deviation from its Newtonian behavior is observed due to precipitation of polyvinyl methyl ether as it forms a solid white mass. Through the use of the Arrhenius–Frenkel–Eyring equation, the activation energy of the viscous flow for polyvinyl methyl ether solutions was found to be 31 kJ/mol. Based on refractometry data, it was demonstrated that phase transition in aqueous solutions of polyvinyl methyl ether is reversible. This feature can facilitate medical equipment cleaning before introducing the embolic agent into a patient's bloodstream. Finally, the investigation determined some parameters, in which the formation of embolic agents from a 30% polyvinyl methyl ether aqueous solution occurs (in situ in a blood vessel at a temperature of 35.5 °C).

Keywords: *embolization, embolic agent, viscosity, polyvinyl methyl ether, aqueous solution.*

О возможности применения водных растворов поливинилметилового эфира для эмболизации кровеносных сосудов

П.Е. Игнатьева[1,@], Е.С. Жаворонок[1], О.А. Легонькова[2], С.А. Кедик[1]

[1]МИРЭА – Российский технологический университет (Институт тонких химических технологий имени М.В. Ломоносова), Москва 119571, Россия
[2]Национальный медицинский исследовательский центр хирургии имени А.В. Вишневского Министерства здравоохранения Российской Федерации, Москва 117997, Россия
[@]Автор для переписки, e-mail: ignateva.polly@mail.ru

Статья посвящена исследованию водных растворов поливинилметилового эфира с целью определения возможности их использования в качестве основы эмболизирующего состава для преднамеренной закупорки кровеносных сосудов при терапии сосудистых аномалий, опухолей и предоперационной подготовке пациентов. На основании экспериментальных данных, полученных с помощью метода точек помутнения, построена правая ветвь бинодальной кривой бинарной системы поливинилметиловый эфир – вода и определено значение нижней критической температуры смешения (35.5 °C). Определена концентрация поливинилметилового эфира в водном растворе, при которой фазовый переход происходит при температуре 35.5 °C – она составляет 30% мас. Вязкостно-скоростные кривые 30%-го водного раствора поливинилметилового эфира, полученные с помощью метода реовискозиметрии в широком диапазоне температур 5–36 °C, свидетельствуют, что исследуемые растворы низковязки и проявляют ньютоновское поведение при течении. Однако уже при 35 °C и выше в области фазового перехода наблюдается значительное отклонение от ньютоновского поведения вследствие выпадения поливинилметилового эфира из раствора в виде белой твердой массы. В рамках уравнения Аррениуса–Френкеля–Эйринга оценена энергия активации вязкого течения водных растворов поливинилметилового эфира, которая составляет 31 кДж/моль. С помощью рефрактометрии было показано, что фазовый переход в исследуемых растворах имеет обратимый характер, что, в частности, облегчает очистку оборудования для введения эмболизирующего состава в организм пациента. В результате работы определены некоторые параметры, при которых формирование эмбола в кровеносном сосуде in situ происходит из 30%-го водного раствора поливинилметилового эфира при температуре 35.5 °C.

Ключевые слова: *эмболизация, эмболизирующий агент, вязкость, поливинилметиловый эфир, водный раствор.*

Introduction

Today, the treatment of major issues in blood vessels by embolization has become rather popular. It is a virtually noninvasive procedure wherein vessels are intentionally blocked [1–4]. Embolization is used to treat various conditions such as aneurysms, cases of angiodysplasia, uterine fibroids, various cancers, injuries with severe blood loss, as well as for the preparation of patients for surgery (to limit blood loss) [1]. To perform embolization, a catheter is used to deliver substances into the blood vessel. These substances may be different in nature, structure and composition; they may be liquid or solid, but their role is to form a thrombus (clot) which prevents free blood flow.

Some of the first materials that were used for blood vessel blockage were fragments of muscle tissue, fat tissue or brain meninges, as well as hemostatic sponges and stainless steel granules [5, 6]. Modern cardiovascular medicine uses embolization based on gelatin sponges, synthetic polymers, and microspheres of various composition, balloons, occluders and coils. However, the development of current treatment standards requires novel embolic agents, based on polymers and co-polymers [5, 6]. It is worth noting that liquid agents, which form solid emboli in blood vessels *in situ*, have some advantages when compared to solid agents [7]. For example, liquids are easier to introduce into a vessel and localize in a certain area; the risk of vessel damage is also lower. Most liquid embolic agents contain

toxic solvents that may affect the human body and cause negative side effects [8]. This can be avoided by using water-based agents; their development is very important [9]. A promising reagent for this purpose is an aqueous solution of polyvinyl methyl ether (PVME) [10]. It is a synthetic polymer with high solubility in cold water, but it precipitates at temperatures above 35 ºC. Materials based on PVME are highly adhesive to various surfaces, particularly plastic and metal, and they are used in production of glues and varnishes, letterpress ink and sealants [11]. The purpose of the current study was to evaluate the possibility of creating PVME-based aqueous embolic agents.

Materials and Methods

We used aqueous solutions of polyvinyl methyl ether (PVME) (Sigma-Aldrich, US) at concentrations ranging from 5 to 50 wt %.

The cloud point temperature for PVME solutions was measured using the following setup. The specimen was fixed between two glass cover slips next to the sensor bulb of a mercury-in-glass thermometer, which was thermostated. The temperature was elevated or decreased gradually at the speed of 1 ºC/min. In the first scenario, the cloud point temperature was determined at the moment when clouding started to occur, and in the second – when the specimen became transparent again. We have analyzed PVME solutions with the following concentrations: 5, 10, 20, 30, 35, 40, 45, 50 wt %.

The dynamic viscosity of PVME aqueous solutions was measured using a Brookfield DV2TLV viscometer (SC4-16 module) at the following temperatures (ºC): 5, 10, 15, 20, 25, 30, 33, 34, 35, 36. The shear rate was in the 25–50 s^{-1} range. We used Rheocalc software to process the data.

The refractive index for 30% and 50% PVME solutions was measured on an URL-1 refractometer in the 25–40 ºC range, with gradual (by 3 ºC) increase/decrease in temperature.

Results and Discussion

The phase transition in aqueous solutions of PVME results in a change from the original liquid fluid into solid matter, which may be used as an embolus. The temperature of this transition highly depends on the polymer's concentration. Thus, to optimize this embolic agent, it is necessary to investigate the phase diagram of the PVME–water system and to determine the concentration at which the phase transition occurs, at 35 ºC or a higher temperature (human body temperature). Based on the data obtained via cloud point method, we have created the binodal curve of the phase diagram for the PVME–water system (Fig. 1).

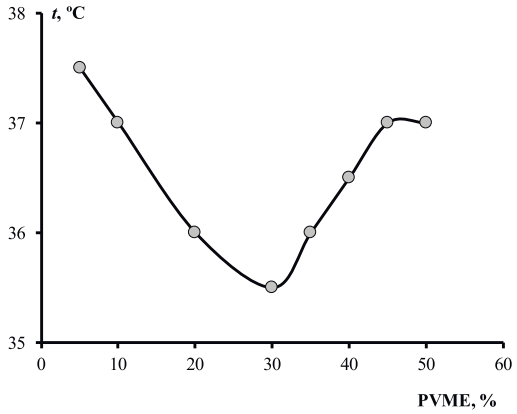

Fig. 1. Phase diagram (binodal) for the binary system PVME–water.

It is evident from this figure that PVME solutions do have the lowest critical mixing temperature, 35.5 ºC. The PVME–water system is a transparent liquid fluid (Fig. 2a) at points below the binodal, and it is a solid white substance (Fig. 2b) when above the binodal. The solid form is able to be lodged in a blood vessel.

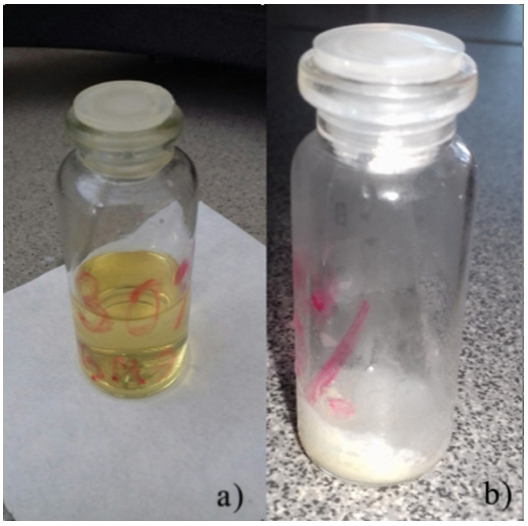

Fig. 2. A typical view of the PVME–water system, below (a) and above (b) the binodal curve.

The lowest critical mixing temperature is observed when the concentration of PVME is 30 wt %, according to the binodal (Fig. 1). If this solution is introduced into a blood vessel, clouding is guaranteed to occur, since the human body temperature is 36.5–37.0 ºC.

One of the most important characteristics of an embolic agent is its viscosity, which determines the embolization technique, particularly the diameter of the catheter and the mode of introduction into the blood system. That is why the next step of this work

sought to investigate the rheological parameters of the 30% PVME solution. Its viscosity was analyzed in a wide range of temperatures, from 5 to 36 ºC. The experimental viscosity–velocity curves (Fig. 3) show that the solutions tested are lowly viscous and almost Newtonian. However, at 35 ºC and 36 ºC, a significant scattering of experimental values was observed. This indicates that the substance deviates from the Newtonian behavior when close to phase transition.

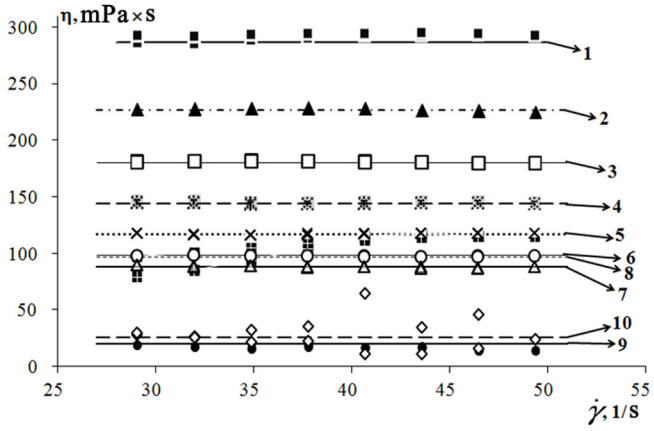

Fig. 3. Viscosity–velocity curves for 30% aqueous solution of PVME at the following temperatures, ºC:
1 – 5, **2** –10, **3** – 15, **4** – 20, **5** – 25,
6 – 30, **7** – 33, **8** – 34, **9** – 35, **10** – 36

The analysis of the data obtained at different temperatures allows for the estimation of the activation energy of viscous flow using the Arrhenius–Frenkel–Eyring equation:

$$\ln \eta = \ln A - \frac{E_{act}}{RT}, \quad (1)$$

where η is the dynamic viscosity coefficient, A – pre-exponential factor, E_{act} – activation energy of viscous flow, R – universal gas constant, T – temperature.

The anamorphosis of the temperature dependency for the dynamic viscosity coefficient of the 30% PVME solution is shown in Fig. 4.

The graph (Fig. 4) shows that at 35–36 ºC, a sharp deviation from equation (1) occurs, clearly due to phase transition. The polymer forms a solid white precipitate (Fig. 2b). However, the data for the temperatures below the phase transition point enables the calculation of the activation energy of viscous flow for the PVME solution. Its level is at 31 kJ/mol, and the pre-exponential factor ln$A$ = –2.71. Knowing these parameters, the viscosity of PVME in a wide range of temperatures – from storage conditions to

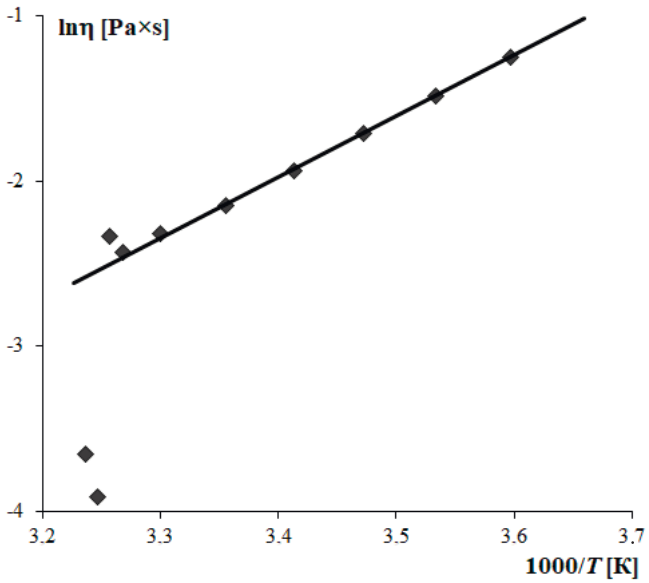

Fig. 4. Temperature dependency of the viscosity for the 30% aqueous solution of PVME based on equation (1).

the phase transition point – can be predicted.

The important feature of embolic agents based on PVME aqueous solutions is the reversibility of phase transition. The temperature dependency of the refractive index (Fig. 5) shows that PVME is dissolved in water in a reversible manner. This may facilitate the cleaning of medical equipment used for the introduction of an embolus into a blood vessel. At the same time, it is safe for the patient as the temperature of a living human body cannot be lower than 35 ºC.

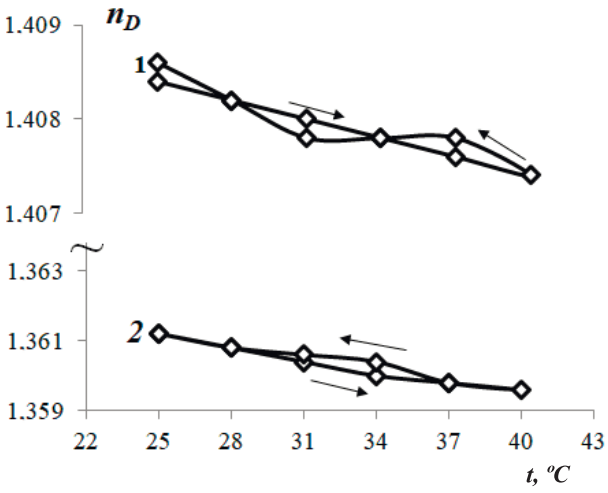

Fig. 5. Refractive index of PVME solutions depends on temperature:
1 – 50% PVME, 2 – 30% PVME.

Conclusion

Rheoviscometry and refractometry were used to analyze aqueous solutions of polyvinyl methyl ether (PVME). The potential of such solutions to be used as embolic agents was demonstrated, as they undergo phase transition at 35–36 ºC. The cloud point method was used to create the right branch of the binodal for the phase diagram of the PVME–water system. This has helped to determine the optimal PVME concentration, 30 wt %, at which the phase transition occurs and an embolus is formed at a temperature of 35 ºC. The reversible character of the clouding–solubilization process in the analyzed system was also demonstrated.

The authors declare no conflict of interest.

References:

1. Kiron Varghese, Srilakshmi Adhyapak. Therapeutic Embolization. Bangalore, 2017. 133 p.
2. Chabrot P., Boyer L. Embolization. Springer, 2013. 472 p.
3. Dan V.N., Sapelkin S.V. Angiodysplasia (congenital vascular malformations). Moscow: Verdun Publ., 2008. 200 p.
4. Dan V.N., Sapelkin S.V., Legonkova O.A., Tsygankov V.N., Varava A.B., Kedik S.A., Lark E.S., Panov A.V. Materials and methods of endovascular treatment of arteriovenous malformations: Opportunities and Challenges. *Voprosy biologicheskoi, meditsinskoi i farmatsevticheskoi khimii. Meditsinskaya khimiya* [Issues of Biological, Medicinal and Pharmaceutical Chemistry. Medicinal Chemistry]. 2016;(7):49-51 (in Russ.).
5. Kedik S.A., Suslov V.V., Malkov A.P., Shnyak E.A., Domnina Yu.M. Gelling polymers to create a liquid embolic agents. *Razrabotka i registratsiya lekarstvennykh sredstv* [Development and Registration of Medicines]. 2017;4(21):38-45 (in Russ.).
6. Ignatieva P.E., Zhavoronok E.S., Legonkova O.A., Kedik S.A. Compositions based on aqueous solutions of chitosan and glutaraldehyde for embolization of blood vessels. *Tonkie khimicheskie tekhnologii = Fine Chemical Technologies.* 2019;14(1):14-20 (in Russ.). https://doi.org/10.32362/2410-6593-2019-14-1-25-31
7. Lu X.-Y., Zhang X. Onyx embolization for an angiographically progressive traumatic pseudoaneurysm of the middle meningeal artery: A case report and literature review. *Exp. Ther. Med.* 2019;17(5):4144-4148. https://doi.org/10.3892/etm.2019.7403
8. Vaidya S., Tozer K.R., Chen J. An overview of embolic agents. *Semin. Intervent. Radiol.* 2008;(25):204-215. https://doi.org/10.1055/s-0028-1085930
9. Jones J.P., Sima M., O'Hara R.G., Stewart R.J. Water-borne endovascular embolics inspired by the undersea adhesive of marine sandcastle worms. *Adv. Healthc. Mater.* 2018;5(7):795-801. https://doi.org/10.1002/adhm.201500825
10. Casalini R., Roland C.M. Dynamic properties of polyvinylmethylether near the glass transition. *J. Chem. Phys.* 2003;119(7):4052-4059.
11. PVME poly(vinyl methyl ether). In: Wypych G. Handbook of Polymers. Chem Tec Publishing, 2016. P. 646-648. https://doi.org/10.1016/C2015-0-01462-9

Список литературы:

1. Kiron Varghese, Srilakshmi Adhyapak. Therapeutic Embolization. Bangalore, 2017. 133 p.
2. Chabrot P., Boyer L. Embolization. Springer, 2013. 472 p.
3. Дан В.Н. Сапелкин С.В. Ангиодисплазии (врожденные пороки развития сосудов). М.: Вердана, 2008. 200 с.
4. Дан В.Н., Сапелкин С.В., Легонькова О.А., Цыганков В.Н., Варава А.Б., Кедик С.А., Жаворонок Е.С., Панов А.В. Материалы и методы эндоваскулярного лечения артериовенозных мальформаций: возможности и проблемы // Вопросы биологической, медицинской и фармацевтической химии. Медицинская химия. 2016. № 7. С. 49–51.
5. Кедик С.А., Суслов В.В., Малкова А.П., Шняк Е.А., Домнина Ю.М. Гелеобразующие полимеры для создания жидких эмболизатов // Разработка и регистрация лекарственных средств. 2017. № 4 (21). С. 38–45.
6. Игнатьева П.Е., Жаворонок Е.С., Легонькова О.А., Кедик С.А. Композиции на основе водных растворов хитозана глутарового альдегида для эмболизации кровеносных сосудов// Тонкие химические технологии. 2019. Т. 19. № 1. С. 14–20. https://doi.org/10.32362/2410-6593-2019-14-1-25-31
7. Lu X.-Y., Zhang X. Onyx embolization for an angiographically progressive traumatic pseudoaneurysm of the middle meningeal artery: A case report and literature review // Exp. Ther. Med. 2019. V. 17. № 5. P. 4144–4148. https://doi.org/10.3892/etm.2019.7403.
8. Vaidya S., Tozer K.R., Chen J. An overview of embolic agents // Semin. Intervent. Radiol. 2008. № 25. P. 204–215. https://doi.org/10.1055/s-0028-1085930
9. Jones J.P., Sima M., O'Hara R.G., Stewart R.J. Water-borne endovascular embolics inspired by the undersea adhesive of marine sandcastle worms // Adv. Healthc. Mater. 2018. V. 5. № 7. P. 795–801. https://doi.org/10.1002/adhm.201500825
10. Casalini R., Roland C.M. Dynamic properties of polyvinylmethylether near the glass transition // J. Chem. Phys. 2003. V. 119. № 7. P. 4052–4059.
11. PVME poly(vinyl methyl ether) / In: Wypych G. Handbook of Polymers. Chem Tec Publishing, 2016. P. 646–648. https://doi.org/10.1016/C2015-0-01462-9

About the authors:

Polina E. Ignatieva, Student of the Chair of Biotechnology and Industrial Pharmacy, M.V. Lomonosov Institute of Fine Chemical Technologies, MIREA – Russian Technological University (86, Vernadskogo pr., Moscow 119571, Russia).

Elena S. Zhavoronok, Cand. of Sci. (Chemistry), Associate Professor, Chair of Biotechnology and Industrial Pharmacy, M.V. Lomonosov Institute of Fine Chemical Technologies, MIREA – Russian Technological University (86, Vernadskogo pr., Moscow 119571, Russia). Scopus Author ID 7801409746, ResearcherID H-9420-2013, https://orcid.org/0002-7235-3361

Olga A. Legonkova, Dr. of Sci. (Engineering), Head of the Department of Dressings, Suture and Polymeric Materials in Surgery, A.V. Vishnevsky National Medical Research Center of Surgery, Ministry of Health of the Russian Federation (27, Bolshaya Serpukhovskaya ul., Moscow 117997, Russia). Scopus Author ID 18437207900

Stanislav A. Kedik, Dr. of Sci. (Engineering), Professor, Head of the Chair of Biotechnology and Industrial Pharmacy, M.V. Lomonosov Institute of Fine Chemical Technologies, MIREA – Russian Technological University (86, Vernadskogo pr., Moscow 119571, Russia). https://orcid.org/0003-2610-8493

Об авторах:

Игнатьева Полина Евгеньевна, студент кафедры биотехнологии и промышленной фармации Института тонких химических технологий имени М.В. Ломоносова ФГБОУ ВО «МИРЭА – Российский технологический университет» (119571, Россия, Москва, пр-т Вернадского, д. 86).

Жаворонок Елена Сергеевна, кандидат химических наук, доцент кафедры биотехнологии и промышленной фармации Института тонких химических технологий имени М.В. Ломоносова ФГБОУ ВО «МИРЭА – Российский технологический университет» (119571, Россия, Москва, пр-т Вернадского, д. 86). Scopus Author ID 7801409746, ResearcherID H-9420-2013, https://orcid.org/0002-7235-3361

Легонькова Ольга Александровна, доктор технических наук, руководитель отдела перевязочных, шовных и полимерных материалов в хирургии ФГБУ «Национальный медицинский исследовательский центр хирургии имени А.В. Вишневского» Министерства здравоохранения Российской Федерации (117997, Россия, Москва, ул. Большая Серпуховская, д. 27). Scopus Author ID 18437207900

Кедик Станислав Анатольевич, доктор технических наук, профессор, заведующий кафедрой биотехнологии и промышленной фармации Института тонких химических технологий имени М.В. Ломоносова ФГБОУ ВО «МИРЭА – Российский технологический университет» (119571, Россия, Москва, пр-т Вернадского, д. 86). Scopus Author ID 7801632547, https://orcid.org/0003-2610-8493.

For citation: Ignatieva P.E., Zhavoronok E.S., Legonkova O.A., Kedik S.A. On the use of aqueous solutions of polyvinyl methyl ether for the embolization of blood vessels. *Tonkie Khimicheskie Tekhnologii = Fine Chemical Technologies.* 2019;14(4):33-38 (in Russ.). https://doi.org/10.32362/2410-6593-2019-14-4-33-38

Для цитирования: Игнатьева П.Е., Жаворонок Е.С., Легонькова О.А., Кедик С.А. О возможности применения водных растворов поливинилметилового эфира для эмболизации кровеносных сосудов // Тонкие химические технологии. 2019. Т. 14. № 4. С. 33–38. https://doi.org/10.32362/2410-6593-2019-14-4-33-38

Translated by R. Trikin

Fine Chemical Technologies, 2019, Vol. 14, No. 4, pp. 39–44.
Original Russian Text © Artyom B. Baranov, Tatyana I. Andreeva, Igor D. Simonov-Emely'anov, Oleg E. Peksimov,
published in Tonkie Khimicheskie Tekhnologii, 2019, Vol. 14, No. 4, pp. 39–44

СИНТЕЗ И ПЕРЕРАБОТКА ПОЛИМЕРОВ И КОМПОЗИТОВ НА ИХ ОСНОВЕ
SYNTHESIS AND PROCESSING OF POLYMERS AND POLYMERIC COMPOSITES

https://doi.org/10.32362/2410-6593-2019-14-4-39-44
UDC 691.175.2

CC BY

The structure, composition and preparation of injection-molded composite materials based on glass-filled polysulfone

Artyom B. Baranov[1], Tatyana I. Andreeva[2], Igor D. Simonov-Emely'anov[1], Oleg E. Peksimov[2]

[1]MIREA – Russian Technological University (M.V. Lomonosov Institute of Fine Chemical Technologies), Moscow 119571, Russia
[2]JSC "G.S. Petrov Institute of Plastics", Moscow 111024, Russia
[@]Corresponding author, e-mail: qsefdesx@gmail.com

In the course of this study, compositions and designed structures for the polysulfone (PSF) and short glass fibers systems were calculated. Additionally, disperse-filled polymer composite materials (DFPCM) based on PSF-190 were classified in accordance with their respective structures, and the optimal amount of glass fiber (13.5–18.5 vol %) was determined. This article describes the production of DFPCM using PSF and a short glass fiber with a twin-screw extruder (Labtech Engineering Company LTD, model Scientific FIC 20-40). Furthermore, optimal mixing parameters for the creation of composites wherein the glass fiber length exceeds the critical length (l_{cr}) were established. The critical length was calculated, and the curves for fiber size distribution of polysulfone composites were depicted, and a difference in fiber concentration between the dispenser and the extrusion head (up to ~10–15%) was found when the fiber content was at 18–25 vol %. For the first time, optimal parameters (which pertain to medium-filled dispersions) for the structure of DFPCM based on PSF and short glass fiber are able to be demonstrated.

Keywords: *polysulfone, composite materials, critical fiber length, short glass fibers.*

Структура, составы и получение литьевых композиционных материалов на основе стеклонаполненного полисульфона

А.Б. Баранов[1], Т.И. Андреева[2], И.Д. Симонов-Емельянов[1], О.Е. Пексимов[2]

[1]МИРЭА – Российский технологический университет (Институт тонких химических технологий имени М.В. Ломоносова), Москва 119571, Россия
[2]АО «Институт пластмасс им. Г.С. Петрова», Москва 111024, Россия
[@]Автор для переписки, e-mail: qsefdesx@gmail.com

Рассчитаны составы и спроектированы структуры для системы полисульфон (ПСФ) + короткие стеклянные волокна. Представлена классификация дисперсно-наполненных полимерных композиционных материалов (ДНПКМ) на основе ПСФ-190 по структурному

принципу, с учетом обобщенных параметров структуры и установлена оптимальная область содержания стеклянного волокна (13.5–18.5% об.). Описана технология получения ДНПКМ на основе ПСФ и короткого стеклянного волокна на двухшнековом экструдере фирмы Labtech Engineering Company LTD марки Scientific FIC 20-40 и определены оптимальные параметры смешения для создания композиций с длиной стекловолокна более $l_{кр}$. Рассчитана критическая длина ($l_{кр}$) и построены кривые распределения волокна по размерам в полимерных композиционных материалах на основе полисульфона. Впервые приведены данные по оптимальным параметрам структуры ДНПКМ на основе ПСФ и коротких стеклянных волокон, которые соответствуют средненаполненным дисперсным системам.

Ключевые слова: *полисульфон, композиционные материалы, критическая длина волокна, короткие стеклянные волокна, смешение.*

Introduction

In order to improve physicomechanical characteristics, heat-resistant engineering polymers belonging to the polysulfone (PSF) class may be modified by introducing fibrous fillers of different nature, thus making them more diverse and applicable in more situations.

The design of structures and compositions for disperse-filled polymer composite materials (DFPCM) should be performed according to the classification of the system by the structural principle [1].

This work demonstrates data on generation (by extrusion) of a PSF-based composite with varying content of short glass fiber.

The selection of glass fiber content was performed according to the classification of disperse systems by the structural principle: diluted systems (DS), low-filled systems (LFS), medium-filled systems (MFS) and high-filled systems (HFS), taking into account the generalized parameters of the structure for production of injection-molded DFPCM.

The publication [2] showed that, for diluted systems and low-filled systems, insignificant changes in physicomechanical characteristics were observed. The highest values were reached in the production of medium-filled systems below the yield point (MFS-1) and above it (MFS-2).

Materials and Methods

The Russian-made PSF-190 (JSC "G.S. Petrov Institute of Plastics") with the melt flow index (MFI) = 10 g/10 min (340 °C and 2.16 kgf) and the temperature interval of production at 295–305 °C [3], as well as glass roving EC17-1200 made by "Owens Corning", the diameter of its elementary thread is 13 μm and its linear density is 2180 tex [4], were chosen as subjects of research.

[1]Owens Corning catalog, OCV Reinforcements [electronic source]. URL: http://www.ocvreinforcements.com/pdf/products/SingleEndRovings_SE1200_ww_06_2008_Rev0.pdf

Polysulfone PSF-190 was dried at ~145 °C for 4 h in vacuum until the residual humidity was no more than 0.02%.

The mixing of the components and control of fiber content in PSF were performed during extrusion by measuring the PSF feed rate with a gravimetric feeder, at the constant rate of glass roving feed.

The mixing was performed on a twin-screw extruder Labtech Engineering Company LTD (model Scientific FIC 20-40). The scheme of the process, in which glass filled PSF is produced, is shown in Fig. 1.

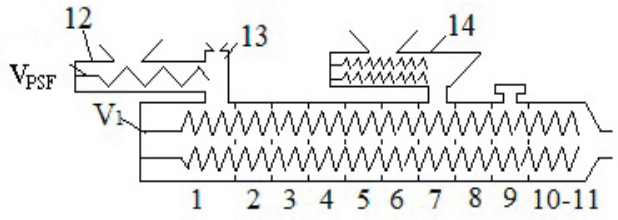

Fig. 1. The scheme of the process in which glass filled PSF is produced (*keys see following in the text*).

The laboratory extruder (Fig. 1), with the screw diameter D_s = 20 mm and L/D_s = 40, has 10 independently heated zones with the following temperatures: zone 1 with 260 °C, zones 2–9 with 310 °C, zones 10–11 with 295 °C. The extruder has a degassing zone (zone 9).

In the process of producing glass filled PSF, the torque was ~35–40 N×m. The rotational speed of the extruder's screws was constant, V_1 = 300 rpm.

The glass roving was introduced into the extruder by two different methods:

Method 1. The glass roving was introduced continuously through a loading spout (position 13) into zone 1 of the twin-screw extruder, at 260 °C, with linear speed of fiber feed V_f = 18 m/min, and the rotational speed of the extruder's screws V_1 = 300 rpm. The glass fiber feed rate was Q_f = 36 g/min.

Polysulfone was introduced by a gravimetric feeder (position 12) into the loading zone of the extruder (zone 1).

The feed speed for PSF (V_{PSF}) was varied between 3 and 10 rpm, and the feed rate Q_{PSF} was changing between 30 and 140 g/min.

Method 2. The glass roving was introduced through a side twin-screw loader (position 14) into the PSF melt, directly into zone 7 of the extrusion cylinder. The linear speed of fiber feed was constant, V_f = 1.3 m/min, and the feed rate was 36 g/min. The rotational speed of the extruder's screws was V_1 = 300 rpm. Polysulfone was introduced in the same way as in Method 1.

Glass fiber concentration in PSF was controlled by measuring the PSF-190 feed rate with a gravimetric feeder (position 12), while changing the rotational speed of the feeder's screw from 3 to 12 rpm, and with the constant glass fiber feed rate Q_f = 36 g/min.

Figure 2 shows the dependency of PSF-190 feed rate on the rotational speed of the feeder's screw (feeder in position 12).

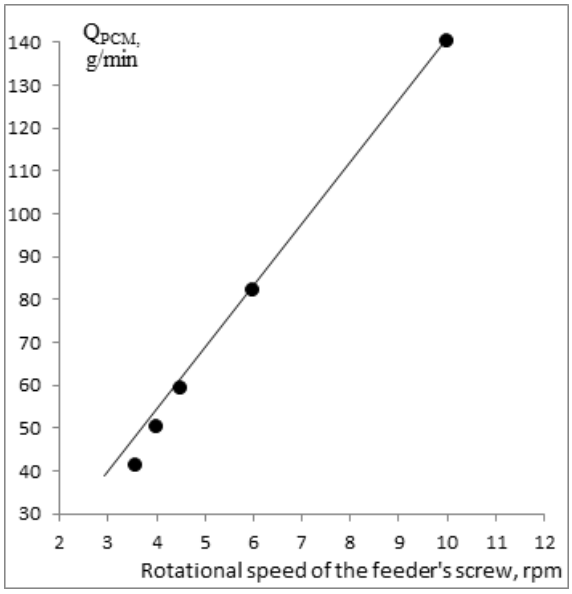

Fig. 2. Dependency of PSF-190 feed rate (Q_{PCM}) on the rotational speed of the feeder's screw (feeder in position 12).

According to Fig. 2, if the rotational speed of the feeder's screw (feeder in position 12) grows from 3 to 10 rpm, then the PSF-190 feed rate increases from 40 to 140 g/min. It may be characterized by a linear function: $Q_{PSF} = K(n - 4.2/K) = 14(n - 0.3)$, for the rotational speed interval between 3 and 10 rpm, n is the rotational speed of the feeder's screw (feeder in position 12), K is a proportionality factor.

The glass fiber content (φ_f) in polysulfone, at the constant glass roving feed rate Q_f = 36 g/min, was calculated as follows: $\varphi_f = Q_f/(Q_{PSF} + Q_f)$, where Q_{PSF} is PSF-190 feed rate, g/min; Q_f is glass fiber feed rate, g/min; φ_f is glass fiber content in PSF-190, mass fract.

In order to evaluate the influence of the structure on the properties of the glass filled PSF, mass fractions (φ) were re-calculated into volume fractions (φ_{vol}).

Results and Discussion

In order to produce DFPCM based on glass filled PSF with various structures and generalized parameters, compositions for the filler of choice (glass fiber) were calculated. For the short glass fiber, it was experimentally determined that the maximum content of glass fiber φ_{max} = 0.36 vol. fract. This was based on a known approach [4].

The following Table summarizes the compositions, generalized parameters of the structure for the disperse system polymer–glass fiber, and DFPCM classification by the structural principle.

The share of the polymer matrix in the boundary layer and the generalized parameter of the structure M for disperse systems with small specific surface area of the filler were not taken into account in our calculations.

When the DFPCM structure changes from one type to another, the change of the generalized parameter Θ leads to variation in technological characteristics and operational properties.

For example, increase in the coordination number of the lattice Z and packing density kpack; decrease in the amount of polymer interlayer between disperse particles (generalized parameter Θ); and increase in glass fiber content (φ_f) lead to an increase in viscosity; worse reprocessing; and a change in the mechanism of DFPCM fluidity.

During the use of HFS structures with generalized parameter Θ < 0.20 vol. fract. and glass fiber concentration higher than 0.27 vol. fract. in extrusion process, while producing a string, breaks in the latter have been observed, and extrusion became unstable.

To summarize, this granulation method has limitations in the structural parameters of DFPCM. To produce MFS-2 systems with Θ between 0.45 and 0.20 vol. fract., and HFS with Θ < 0.20 vol. fract., it is necessary to use the "granulation on the tip" method.

For further experiments, DFPCM based on glass filled PSF with the following parameters of the structure were produced:

– low-filled systems LFS:

Θ = 0.90 vol. fract. and φ_{vol} = 0.09 vol. fract.;

– medium-filled systems MFS-1:

Θ = 0.73 vol. fract. and φ_{vol} = 0.09 vol. fract.;

Θ = 0.60 vol. fract. and φ_{vol} = 0.135 vol. fract.;

– medium-filled systems MFS-2:

Θ = 0.45 vol. fract. and φ_{vol} = 0.185 vol. fract.;

Θ = 0.40 vol. fract. and φ_{vol} = 0.21 vol. fract.;

Θ = 0.27 vol. fract. and φ_{vol} = 0.25 vol. fract.;

– high-filled systems HFS:

Θ = 0.20 vol. fract. and φ_{vol} = 0.275 vol. fract.

Compositions and generalized parameters of the structure for the glass filled PSF (φ_{max} = 0.36 vol. fract., d =13 μm)

Glass fiber content		Generalized parameters of the structure of DFPCM
φ_{vol}, vol. fract.	φ, mass fract.	Θ, vol. fract.
Low-filled DFPCM with 0.9 > Θ ≥ 0.75 vol. fract.		
0.04	0.09	0.90
Medium-filled DFPCM with 0.75 > Θ > 0.2 vol. fract.		
MFS-1: **0.75** > Θ > 0.45 vol. fract. (DFPCM below the yield point)		
0.085	0.204	**0.75**
0.09	**0.215**	**0.73**
0.11	0.264	0.68
0.135	**0.32**	**0.6**
0.15	0.37	0.56
MFS-2: 0.45 > Θ > 0.2 vol. fract. (DFPCM above the yield point)		
0.183	**0.43**	**0.45**
0.21	**0.50**	**0.40**
0.25	**0.60**	**0.27**
High-filled DFPCM with 0.2 ≥ Θ ≥ 0.0 vol. fract.		
0.275	**0.66**	**0.2**
0.285	0.69	0.016
0.3	0.82	0.01
0.34	0.82	0.01
Ultrahigh-filled DFPCM with Θ < 0 vol. fract.		
0.37	0.864	–0.1

Figure 3 demonstrates the dependency of the short glass fiber concentration in DFPCM (*method 2*) on PSF-190 feed rate, in the feeder in position 12 (2) and in the exit from the extrusion head (1); with the constant fiber feed rate 36 g/min.

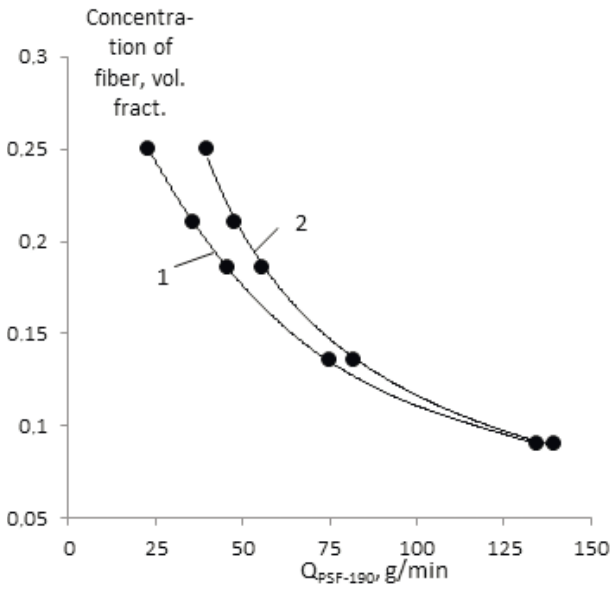

Fig. 3. Dependency of glass fiber concentration in DFPCM on PSF-190 feed rate, in the feeder 12 (2) and in the exit from the extrusion head (1).

Figure 3 shows that the feed rate data for the extrusion head and the gravimetric feeder are the same in the 75–150 g/min area; further decrease in the feed rate to 25 g/min leads to a difference of ~15%.

In the process of the introduction of continuous glass fiber and production of PSF-based DFPCM, grinding and shortening of the fiber occur in the extruder, which undoubtedly influences the physicomechanical characteristics of the glass-filled material.

The publication [4] shows that production of highly durable glass filled composites with short fibers, based on polymer matrices, requires that the following condition is satisfied: fiber length (l_f) should exceed the critical fiber length (l_{cr}).

The critical length (l_{cr}) for "Owens Corning" EC17-1200 glass fiber in PSF was calculated using the following formula:

$$l_{cr} = \frac{\sigma_f}{2\tau} \cdot d$$

If we assume that $\tau \approx \frac{\sigma_{flow}}{\sqrt{3}}$, then

$$l_{cr} \approx 0.866 \cdot \frac{\sigma_f}{\sigma_{flow}} \cdot d$$

where σ_f – tensile strength of glass fiber (2700 MPa); d – fiber diameter (13 μm); σ_{flow} – flow stress of PSF-190 (76 MPa); τ – shear stress on the fiber–polymer matrix boundary, MPa.

The calculated critical length for "Owens Corning" EC17-1200 glass fiber in PSF is ~220 μm.

To investigate the distribution of glass fiber in PSF by size, we used the Mikrofot type 5PO-1 device, made by "Moskinap", Russia. The samples of glass fiber for this experiment were obtained by two-step annealing of DFPCM in a muffle furnace, in accordance with GOST-15973-82.

Figure 4 shows distribution by length for glass fiber in PSF-based DFPCM, depending on the method of introduction (*method 1* – curve 5 and *method 2* – curves 1–4), with different fiber content.

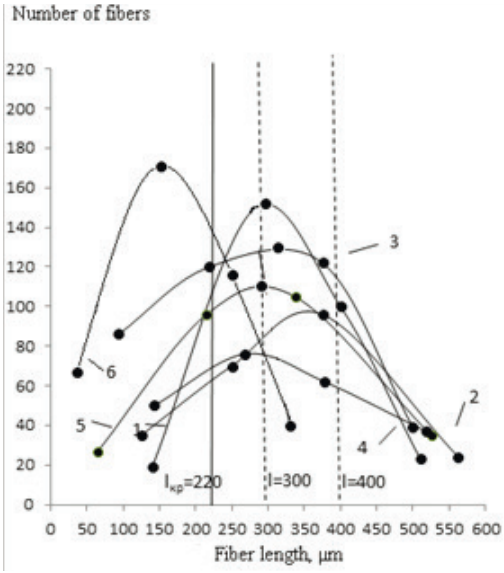

Fig. 4. Distribution of glass fiber by length in PSF-190. Introduction by *method 1* (curve 5) and *method 2* (curves 1–4). Fiber content: 13.5 vol % (1, 5), 18.5 vol % (2), 21 vol % (3), and 25 vol % (4).

Fig. 4 indicates that, when glass fiber is introduced into the loading zone of the extruder (*method 1*, curve 5), intensive grinding of glass fiber occurs, as a result of dry friction with granulated PSF, screws and the extrusion cylinder in the loading zone. In these conditions, fiber length in the composite material is less than l_{cr}, and the average length $l_{average} \approx 150$ μm.

The introduction of glass fiber directly into the PSF melt in zone 7 of the extrusion cylinder (curves 1–5) also results in fiber grinding (*method 2*). However, in this case, fiber length for the 13.5 vol % and 18.5 vol % situations is $l_{average} \approx 400$ μm, which is almost double of the critical length of fiber in PSF ($l_{cr} \approx 220$ μm). For composites with 25 vol % fiber content, the average length is ca. 300 μm, which is approximately 1.5 times higher than l_{cr}.

The tensile strength of the DFPCM based on PSF and glass fiber, with $l_{average} \approx 400$ μm and fiber content 13.5–18.5 vol %, reaches the maximal value of 120 MPa. This is 1.7 times higher than for the polymer matrix, and it is no worse than for foreign-made analogs.

When glass fiber is introduced by *method 1*, fiber length in the composite material is less than l_{cr} ($l_{average} \approx 150$ μm), and the tensile strength of the DFPCM does not exceed 75 MPa, which is almost the same as for PSF. In this case, glass fiber does not work as a reinforcing filler.

Conclusions

PSF formulations containing short glass fibers were designed based on the theory of lattices and packing. They were classified by the structural principle, and the optimal glass fiber content was determined to be 13.5–18.5 vol %.

The production technology of DFPCM based on PSF and short glass fiber (*method 2*) was described, and the optimal mixing parameters to create composites where glass fiber length exceeds l_{cr} were determined.

For the very first time, data on the optimal parameters of the structure for DFPCM based on PSF and short glass fiber was presented, which conform to the parameters of medium-filled disperse systems.

Acknowledgments

The authors are grateful to the staff of the Laboratory of Composite Materials Technology at JSC "G.S. Petrov Institute of Plastics" for assistance in the study.

The authors declare no conflicts of interest.

References:

1. Simonov-Emel'yanov I.D. Building structures in dispersion-filled polymers and properties of composite materials. *Plasticheskie massy* = Polymer Science and Technology. 2015;9(10):29-36 (in Russ.).

2. Mikhaylin Yu.A. Heat resistant polymers and polymeric materials. Saint Petersburg: Professiya Publ., 2006; 261-298 (in Russ.).

Список литературы:

1. Симонов-Емельянов И.Д. Построение структур в дисперсно-наполненных полимерах и свойства композиционных материалов // Пластические массы. 2015. № 9-10. С. 29–36.

2. Михайлин Ю.А. Термоустойчивые полимеры и полимерные материалы. СПб.: Профессия, 2006. 259 с.

3. Baranov A.B., Peksimov O.E., Prudskova T.N., Andreeva T.I., Simonov-Emel'yanov I.D., Shembel N.L. Study on technology characteristics materials based on polysulfone. *Tonkie khimicheskie tekhnologii = Fine Chemical Technologies*. 2016;11(5):87-90 (in Russ.). https://doi.org/10.32362/2410-6593-2016-11-5-87-90

4. Simonov-Emel'yanov I.D., Spembel' N.L., Prokopov N.I., Ushakova O.B., Surikov P.V., Markov A.V. Methods for determination of technological properties of fillers and polymer materials. Moscow: Publishing and Printing Center of MITHT, 2014;63-74 (in Russ.).

3. Баранов А.Б., Пексимов О.Е., Прудскова Т.Н., Андреева Т.И., Симонов-Емельянов И.Д., Шембель Н.Л. Исследование технологических характеристик материалов на основе полисульфона // Тонкие химические технологии. 2016. Т. 11. № 5. С. 87–90. https://doi.org/10.32362/2410-6593-2016-11-5-87-90

4. Симонов-Емельянов И.Д., Шембель Н.Л., Прокопов Н.И., Ушакова О.Б., Суриков П.В. Методы определения технологических свойств наполнителей и полимерных материалов. М.: ИПЦ МИТХТ, 2014. С. 63–74.

About the authors:

Artyom B. Baranov, Postgraduate Student of the Chair of Chemistry and Technology of Plastics and Polymer Composites, M.V. Lomonosov Institute of Fine Chemical Technologies, MIREA – Russian Technological University (86, Vernadskogo pr., Moscow, 119571, Russia). E-mail: qsefdesx@gmail.com. Scopus Author ID 57194107911

Tatyana I. Andreeva, Dr. of Sci. (Engineering), First Deputy General Director, JSC "G.S. Petrov Institute of Plastics" (35, Perovskii proezd, Moscow 111024, Russia). Scopus Author ID 7005954791

Igor D. Simonov-Emel'anov, Dr. of Sci. (Engineering), Professor, Head of the Chair of Chemistry and Technology of Plastics and Polymer Composites, M.V. Lomonosov Institute of Fine Chemical Technologies, MIREA – Russian Technological University (86, Vernadskogo pr., Moscow, 119571, Russia). Scopus Author ID 6603181099

Oleg E. Peksimov, Head of the Testing Laboratory, JSC "G.S. Petrov Institute of Plastics" (35, Perovskii proezd, Moscow 111024, Russia).

Об авторах:

Баранов Артем Борисович, аспирант кафедры химии и технологии переработки пластмасс и полимерных композитов Института тонких химических технологий имени М.В. Ломоносова ФГБОУ ВО «МИРЭА – Российский технологический университет» (Россия, 119571, Москва, пр. Вернадского, д. 86). E-mail: qsefdesx@gmail.com. Scopus Author ID 57194107911

Андреева Татьяна Ивановна, доктор технических наук, первый заместитель генерального директора АО «Институт пластмасс им. Г.С. Петрова» (Россия, 111024, Москва, Перовский проезд, д. 35). Scopus Author ID 7005954791

Симонов-Емельянов Игорь Дмитриевич, доктор технических наук, профессор, заведующий кафедрой химии и технологии переработки пластмасс и полимерных композитов Института тонких химических технологий имени М.В. Ломоносова ФГБОУ ВО «МИРЭА – Российский технологический университет» (Россия, 119571, Москва, пр. Вернадского, д. 86). Scopus Author ID 6603181099

Пексимов Олег Евгеньевич, начальник лаборатории испытаний АО «Институт пластмасс им. Г.С. Петрова» (Россия, 111024, Москва, Перовский проезд, д. 35).

For citation: Baranov A.B., Andreeva T.I., Simonov-Emel'yanov I.D., Peksimov O.E. The structure, composition and preparation of injection-molded composite materials based on glass-filled polysulfone. *Tonkie Khimicheskie Tekhnologii = Fine Chemical Technologies.* 2019;14(4):39-44 (in Russ.). https://doi.org/10.32362/2410-6593-2019-14-4-39-44

Для цитирования: Баранов А.Б., Андреева Т.И., Симонов-Емельянов И.Д., Пексимов О.Е. Структура, составы и получение литьевых композиционных материалов на основе стеклонаполненного полисульфона // Тонкие химические технологии. 2019. Т. 14. № 4. С. 39-44. https://doi.org/10.32362/2410-6593-2019-14-4-39-44

Translated by R. Trikin

Fine Chemical Technologies, 2019, Vol. 14, No. 4, pp. 45–58.
Original Russian Text © Ekaterina B. Yatsishina, Viktor M. Pozhidaev, Olga A. Vasilyeva, Olga P. Dyuzheva, Yana E. Sergeeva, Vasily M. Retivov, Elena Yu. Tereschenko, Irina S. Kulikova, Ekaterina S. Vaschenkova, Evgeniya I. Kozhukhova, published in Tonkie Khimicheskie Tekhnologii, 2019, Vol. 14, No. 4, pp. 45–58

ANALYTICAL METHODS IN CHEMISTRY AND CHEMICAL TECHNOLOGY

АНАЛИТИЧЕСКИЕ МЕТОДЫ В ХИМИИ И ХИМИЧЕСКОЙ ТЕХНОЛОГИИ

https://doi.org/10.32362/2410-6593-2019-14-4-45-58

UDC 543.8 (543.51+543.54) + 393.05

CC BY

The determination of the origin of natural bitumen in mummifying resins of Ancient Egyptian mummies from the collection of the Pushkin Museum of Fine Arts

Ekaterina B. Yatsishina[1], Viktor M. Pozhidaev[1,@], Olga A. Vasilyeva[2], Olga P. Dyuzheva[2], Yana E. Sergeeva[1], Vasily M. Retivov[3], Elena Yu. Tereschenko[1,4], Irina S. Kulikova[1], Ekaterina S. Vaschenkova[3], Evgeniya I. Kozhukhova[3]

[1]National Research Center "Kurchatov Institute", Moscow 123182, Russia
[2]The Pushkin State Museum of Fine Arts, Moscow 119019, Russia
[3]Institute of Chemical Reagents and High Purity Chemical Substances of National Research Center "Kurchatov Institute" (NRC "Kurchatov Institute" – IREA), Moscow 107076, Russia
[4]Shubnikov Institute of Crystallography FSRC "Crystallography and Photonics", Russian Academy of Sciences, Moscow 119333, Russia
[@]Corresponding author, e-mail: pojidaev2006@yandex.ru

This work presents the results of a study of the resins of seven Ancient Egyptian mummies from the collection of the Pushkin State Museum of Fine Arts using a complex of analytical methods: gas chromatography, atomic emission and mass spectrometry. Natural bitumen and beeswax were identified in the resins using the gas chromatography–mass spectrometry method. Based on the results of hydrocarbon distribution in the profiles of n-alkanes in the resin coatings of the mummies and naturally occurring bitumen, it was assumed that the Dead Sea bitumen was used. The gas chromatography–mass spectrometry studies of mummy resins in the selected ion mode (m/z 217 and 191) provided additional evidence of the bitumen's geographic origin. Atomic emission spectrometry with inductively coupled plasma was used as a means to determine the content of microelements. Vanadium, nickel and molybdenum were found in the tar of five mummies. The determined relative amounts of vanadium, nickel, and molybdenum in the resins of the studied mummies showed a good correlation with the available data on the content of these elements in the Dead Sea bitumen, as well as the Fayum mummy resin based on this bitumen. The advantages of using the method of identifying bitumen in mummy resins based on relative content of vanadium, nickel, and molybdenum were revealed.

Keywords: *Ancient Egyptian mummies, natural bitumen, gas chromatography, mass spectrometry, atomic emission spectrometry.*

Определение происхождения природного битума в мумифицирующих смолах древнеегипетских мумий из собрания ГМИИ им. А.С. Пушкина

Е.Б. Яцишина[1], В.М. Пожидаев[1,@], О.А. Васильева[2], О.П. Дюжева[2], Я.Э. Сергеева[1], В.М. Ретивов[3], Е.Ю. Терещенко[1,4], И.С. Куликова[1], Е.С. Ващенкова[3], Е.И. Кожухова[3]

[1]Национальный исследовательский центр «Курчатовский институт», Москва 123182, Россия
[2]Государственный музей изобразительных искусств имени А.С. Пушкина, Москва 119019, Россия
[3]Институт химических реактивов и особо чистых химических веществ Национального исследовательского центра «Курчатовский институт», Москва 107076, Россия
[4]Институт кристаллографии имени А.В. Шубникова ФНИЦ «Кристаллография и фотоника» РАН, Москва 119333, Россия
[@]Автор для переписки, e-mail: pojidaev2006@yandex.ru

В работе представлены результаты исследования составов смол семи древнеегипетских мумий из коллекции Государственного музея изобразительных искусств имени А.С. Пушкина с применением комплекса аналитических методов: газовой хроматографии (ГХ), атомно-эмиссионной и масс-спектрометрии (МС). Методом ГХ–МС в них идентифицированы природный битум и пчелиный воск. По результатам распределений углеводородов в профилях н-алканов в смоляных покрытиях мумий и природных битумов высказано предположение об использовании битума Мертвого моря. Дополнительные доказательства географического происхождения битума получены ГХ–МС-исследованием смол мумий в режиме мониторинга заданных ионов (m/z 217 и 191). Методом атомно-эмиссионной спектрометрии с индуктивно связанной плазмой определено содержание микроэлементов и показано, что в смолах пяти мумий присутствуют ванадий, никель и молибден. Полученные результаты свидетельствуют об удовлетворительной корреляции их с литературными данными по содержанию указанных элементов в битуме Мертвого моря и смоле Фаюмской мумии на основе этого битума. Выявлены преимущества использования метода идентификации битума в смолах мумий по относительному содержанию ванадия, никеля и молибдена.

Ключевые слова: *древнеегипетские мумии, природный битум, газовая хроматография, масс-спектрометрия, атомно-эмиссионная спектрометрия.*

Introduction

Mummification is an integral part of Ancient Egyptian culture. The origin of the practice can be traced back to the early period of Ancient Egyptian history – the Neolithic era, 5000–4000 BC [1–7]. The first evidence of the artificial preservation of bodies relates to the archaeological culture of Badari (about 4500–4100 BC): at that time, some parts of the body were tightly wrapped in linen bandages saturated with resinous substances. Ancient Egyptian sources describing mummification have not been preserved. The first detailed descriptions were made by the ancient authors who visited Egypt, Herodotus (5th century BC) and Diodorus of Sicily (1st century BC) [1–3].

Currently, comprehensive studies of mummies are carried out by specialists in various fields of science. Abroad, systematic studies of Egyptian mummies by natural-scientific methods have been carried out since the 1990s, for which an interdisciplinary approach is widely used [1, 4–6]. In Russia, a comprehensive interdisciplinary study of Ancient Egyptian mummies was first conducted at the National Research Center "Kurchatov Institute" [7].

A large number of organic substances, including beeswax, natural bitumen, tar, resins of coniferous trees, animal fats, vegetable oils, as well as aromatic oils of some plants, were used for mummification in different periods in the history of Ancient Egypt [20]. Research of the resins for mummification was mainly related to the determination of the nature of the substances included in their composition. The quantitative composition of the components of the resins for mummification has not been extensively studied [9, 19, 20]. The most complete quantitative study of the composition of resins in eight Ancient Egyptian mummies from Mostageddah

(Badari culture, Upper Egypt) by a method of gas chromatography combined with mass spectrometry (GC–MS) was presented in a research by J. Jones et al. [19], where identified the following in the composition of the resins: vegetable oils and animal fat (34–95%), aromatic plant extracts (2.4–54%), pine resins (0.3–11%), bitumen (0.2–19%), vegetable and beeswax (0.2–7%).

One of the key points in the studying the resin coatings of Ancient Egyptian mummies is the development of methods for proving the use of bitumen in compositions for mummification and the determination of its geographical origin. The earliest occurrences of using the word "mummy" date around 1000 BC. According to the descriptions of Herodotus, Plutarch and Diodorus, natural bitumen was widely used in Egypt in preserving the bodies of the dead. Diodorus, Strabo, Pliny, Flavius, and Tacitus described the use of bitumen found in the Dead Sea [1–7] for these purposes.

A significant number of works in contemporary scientific literature has been devoted to the study of the use of bitumen in mummification. The primary areas of research are the reliable confirmation of the presence of bitumen in resin coatings of mummies and the determination of its origin. One of the first works on bitumen identification was the work of Benson et al. [21]: using gas chromatography, the authors studied the resin of the Egyptian mummy No. 1770 from the Historical Museum of Manchester. The profiles of *n*-alkanes in the mummy resin and bitumen from the Dead Sea were compared, and it was discovered that the Dead Sea bitumen has a characteristic alkane profile and is identical to the hydrocarbon profile of the mummy resin. Proefke and Rinehart conducted a study of an Egyptian mummy found in Fayoum oasis of Egypt [22] with the GC–MS method. *n*-Alkanes with a chain length of 19 to 33 carbon atoms were found in the mummy's resin. Distribution of saturated hydrocarbons in the resin coincided with the hydrocarbon profile of natural bitumen [23]. Normal paraffins with a chain length of 22 to 32 carbon atoms in the sample of mummy resin were discovered by Beck and Borromeo [24] and the bitumen was identified by their distribution. Hydrocarbon fractions of resins of four Egyptian mummies of a wide range of ages from the British Museum collection were studied by J. Rullkötter and A. Nissenbaum [25]: share of saturated alkanes in the hydrocarbon fractions of resins was at roughly 3%, close to the composition of the Dead Sea bitumen.

The GC analysis of the resins' hydrocarbon fraction of the Egyptian mummies dating to the 4th century BC from the Dakhleh oasis showed the presence of the long-chain *n*-alkanes with a predominance of hydrocarbons with an odd number of carbon atoms (C_{25}–C_{33}) [11], in addition to the Dead Sea bitumen. This, according to the authors, indicated the presence of terrestrial plant waxes. The distribution of *n*-alkanes, typical of the Dead Sea bitumen, was found only in one sample, while isoprenoid hydrocarbons, as well as marina and phytane, were completely absent.

Natural bitumen contains compounds known as "biomarkers", which have distinctive chemical structures closely related to their biological precursors: plants, bacteria and algae. Steranes and pentacyclic triterpenes (aromatic steroid hydrocarbons), which are widely used in organic geochemical correlation studies, are recognized as such biomarkers [26]. The distribution of these hydrocarbons varies across different deposits and is dependent on the geographical origin of bitumen [26–30]. Low chemical reactivity of the biomarkers and their resistance to photochemical and microbial degradation made it possible to use them to identify biodegraded crude oils [31–34], as well as naturally weathered bitumen [35, 36].

The distribution of steranes and triterpenes in the Dead Sea bitumen [37] was studied with the GC–MS method in the mode of monitoring specified characteristic ions (*m/z* 217 and 191). The presence of bitumen in the balms of 39 Egyptian mummies was analyzed with the same method and it was concluded [9, 14] that the black color of the mummy resin is not related to the content of bitumen, as was previously assumed. A number of mummies with an intense black resin coating did not contain bitumen; the black color of the resin was caused by the aging of animal or vegetable fats and beeswax esters. An additional confirmation of this conclusion was obtained via artificial replication of mummifying balms and their long-term heat treatment. Comparison of the distribution of steranes in the resins of the four mummies of the Roman period (4th century AD) from the Dakhleh oasis (Western Egypt) and the bitumen of the Dead Sea showed that they are close or practically coincided [11]. It should be noted, that the Dead Sea bitumen was identified in almost all studies of the compositions of mummifying resins in Ancient Egyptian mummies [11, 25, 31–33, 38, 39]. The bitumen of the Gebel El Zeit deposits was identified by studying the molecular distribution of steranes and terpenes by the GC–MS method in the bitumen of the Abu Durba and Gebel El Zeit deposits, (Gebel El Zeit, Suez Canal) and the scanning at *m/z* 191 and 217 in the resins of two Egyptian mummies [40, 41].

Thus, fossil hydrocarbons, such as profiles of *n*-alkanes (C_{19}–C_{35}), pristane, phytane, hopane derivatives and isomeric terpenes, may serve as the biomarkers of the presence and origin of bitumen in the embalming resins of Egyptian mummies.

Obstacles to the application of this identification method may be either the impossibility (in some cases) to detect pristane, phytane, hopanes and terpenes or their presence in trace amounts, that is, the lack of guarantees for their reliable identification in the mummifying compositions [12, 15]. At the same time, the presence of a well-defined profile of *n*-alkanes (C_{19}–C_{35}) makes it possible to reliably identify the presence of the products of oil origin in the mummies' resins [1, 12]. However, the lack of experimental data on the correspondence of the *n*-alkane profile to a specific field does not yet allow for determining the geographical origin of bitumen.

Most oils are characterized by the content of vanadium and nickel [42]. In the oils of some Volga-Ural deposits, the content of vanadium reaches 200–500 g/t. Approximately the same levels of vanadium and nickel are typical for the oils and bitumen in the West Canadian basin and the Orinoca basin in Venezuela [42–46]. The contents of vanadium and nickel are 4–6 and 0.3–0.5 kg/t respectively in the asphaltenes of carbonic oils of the Tatarstan Republic and Samara oblast. In the bitumen of oil fields in Syria, the share of these elements is 10–20 times lower [44–46]. These elements concentrate in bitumen and their ratio does not change in the course of oil refining or natural conversion processes. Therefore, the content and ratio of vanadium and nickel in natural bitumen can also serve as a biomarker of geographical origin.

Spielman was one of the first to detect the presence of vanadium, molybdenum, and nickel in the resins of Egyptian mummies [47]. He proved that the presence of these elements is a characteristic feature of the Dead Sea bitumen. Zaki and Iskander also identified vanadium, molybdenum and nickel [48] in the Persian mummy resin by spectrographic analysis and confirmed that the presence of these elements is an attribute of the Dead Sea bitumen. Also, 11.0 *ppm* vanadium and 93.8 *ppm* molybdenum[1] were detected in the resin of mummy No. 1770 by an atomic absorption spectroscopy [21]. The detection of 65 *ppm* vanadium, 33.4 *ppm* nickel and 17.4 *ppm* molybdenum [10] in the resin of the mummy from the Fayoum oasis confirmed Spielman's assumption [47] about the presence of the characteristic metals in the petroleum bitumen. Marshner and Wright [49] found Ni 10–200 *ppm* and V 30–300 *ppm* in several natural bitumen deposits of Mesopotamia.

Thus, the detection of vanadium, nickel and molybdenum in the resins of the mummies may be used to identify the presence of bitumen in mummification compositions. Furthermore, the quantitative ratios of these elements may be useful for determining the geographical origin of bitumen.

The purpose of this study is to identify and determine the origin of natural bitumen in the resins of seven Ancient Egyptian mummies from the Pushkin State Museum of Fine Arts collection using a set of analytical methods: gas chromatography, combined gas chromatography with mass spectrometry, and atomic emission spectroscopy.

Materials and Methods

Raw materials and reagents. The description of the exhibits from the Pushkin State Museum of Fine Arts collection submitted for the study is given in Table 1. The approximate dating of the mummies is 1000 years BC.

Table 1. The description of the studied exhibits from the Pushkin State Museum of Fine Arts collection

Mummy No.	Description, inventory No. of the Pushkin State Museum of Fine Arts
1	I – 1a 7150 Human mummy head in tarred shrouds. Length – 20 sm
2	I – 1a 6932 Mummy head. Height – 22 sm; girth – 53 sm
3	I – 1a 6505 Male mummy head. Height – 28 sm; girth – 54 sm
4	I – 1a 6506 Female mummy head. Height – 25 sm; girth – 53.5 sm
5	I – 1a 1241 Headless mummy, swaddled in a large number of bandages
6	I – 1a 5934 Female mummy head. Height – 24 sm, girth – 52 sm
7	I – 1a 1239 Mummy of Ipanha in a cardboard case

Test pieces of resinous substance were taken from the surface of the mummified bodies in the form of a naturally separated piece of resinous material of practically black color and odorless.

All solvents and reagents used in the work were qualified as "CP" (chemically pure) or "for HPLC" (for the high-performance liquid chromatography).

Sample preparation for the study and the identification of substances in the composition of the mummy resin. About 100 mg of the resin sample was ground, and 5 ml of *n*-hexane was added. Extraction was carried out in an ultrasonic bath for 60 min at 50 °C.

[1]For comparison: the Dead Sea natural bitumen contains V – 463 *ppm*, Ni – 251 *ppm*, Mo – 219 *ppm*.

The resulting suspension was centrifuged for 10 min at 5000 rpm. The supernatant was transferred to a mixing funnel, treated with an aqueous KOH solution (5%, 2×5 ml) and washed with water (2×5 ml). The organic layer was filtered through a paper filter with a small amount of anhydrous sodium sulfate, transferred to an evaporation cup, and the solvent was removed at room temperature. The residue was dissolved in 50 µl of hexane. Five milliliters of chloroform were added to the dry residue after extraction with hexane, and then extraction was carried out on an ultrasonic bath for 60 min at 50 °C, the resulting suspension was centrifuged (5000 rpm, 10 min). The supernatant was transferred to a mixing funnel, treated with an aqueous KOH solution (5%, 2×5 ml) and washed with water (2×5 ml). The organic layer was filtered through a paper filter with a small amount of anhydrous sodium sulfate and transferred to an evaporation cup. The solvent was removed at room temperature. The residue was dissolved in 50 µl of chloroform.

Fatty acid methyl esters (FAME) were obtained to confirm the presence of beeswax. For this purpose, the aqueous KOH solution after treatment with the hexane extract was acidified with a 20% aqueous solution of sulfuric acid and extracted with diethyl ether (2×5 ml). The ether layer was separated, filtered through a paper filter with a small amount of anhydrous sodium sulfate, transferred to an evaporation cup, after which the solvent was removed at room temperature. The residue was dissolved in 100 µl of chloroform and treated with methanol in presence of acetyl chloride according to the procedure described previously [50].

Hardware and auxiliary equipment

Chromatographic system 1. Gas chromatograph HP 6890 with mass spectrometric detector MSD 5975 (Agilent Technologies).

Chromatography conditions: the capillary column DB–5 ms, length is 30 m, inner diameter is 0.25 mm, stationary phase film thickness is 0.25 µm. The initial temperature of the column is 100 °C; temperature programming from 100 to 280 °C at a speed of 15 deg/min. Endurance at the final temperature is 10 min. The flow rate of the carrier gas (helium) is 1 ml/min; flow division 1:10. The temperature of the evaporator is 280 °C, the detector interface is 280 °C. The sample volume is 1 µl.

The analysis of the hexane extract was carried out in the scanning mode for the total ion current. Compounds were identified by mass spectra and retention indices of the NIST 14 2014/EPA/NIH database. The analysis of the chloroform extract was carried out in the mode of monitoring the specified ions (*m/z* 217 and 191).

Chromatographic system 2. Bruker 430 GC gas chromatograph with flame ionization detector.

Chromatography conditions: Capillary column Select™ Biodiselfor FAME, its length is 30 m, inner diameter is 0.32 mm, stationary phase film thickness is 0.25 µm. Temperature program of the column: initial temperature is 140 °C, held for 4 minutes. The temperature is risen to 260°C at the speed of 4 deg/min and held in isothermal mode for 10 minutes at 260 °C. Injector temperature is 260 °C, detector temperature is 260 °C. The flow rate of the carrier gas (nitrogen) is 2 ml/min, the division of the flow is 1:20. Sample volume is 2 µl.

Fatty acid methyl esters were identified using a FAME standard mixture (Supelco 37 Component $FAME_{Mix}$) and a comparison of the compounds retention parameters with the published data [12,13].

The determination of the micro-element content in mummy resins was carried out using inductively coupled plasma atomic emission spectroscopy (ICP) with iCAP 6300duo Thermo Scientific (USA) and the Thermo iTEVA (v. 2.5.0.84) software.

Standard 1 is the multielement calibration standard for ICP-spectroscopy ICP-MS-68B-100 Solution A (ICP-MS-68B-A-100) (5% HNO_3); standard 2 is the multielement calibration standard for ICP-spectroscopy ICP-MS-68B-100 Solution B (ICP-MS-68B-B-100) (5% HNO_3); standard 3 is the multielement calibration standard for ICP-spectroscopy MS-3 (5% HNO_3).

Sample preparation. About 10 mg of a sample of a mummy resin was weighed with an accuracy of up to 0.000001 g, then placed into an autoclave from PFA with a volume of 50 ml and dissolved in a mixture of nitric (4.5 ml) and hydrochloric acid (0.5 ml) in the unit for microwave decomposition of samples SINEO MDS10 (205 °C, 30 min). The solution was quantitatively transferred to an inert crucible, evaporated to a volume of 0.5 ml, transferred to a polymeric tube. The volume was adjusted to 10 ml with a 2% nitric acid solution.

Results and Discussion

In order to determine the composition of organic compounds present in the test resin taken from the surface of the body of the mummy, the sample was subjected to sequential extraction with various solvents. Identification of compounds in the extracts of embalming resins was carried out with GC–MS.

The chromatograms of the extracts of resins of two mummies in *n*-hexane are presented in Fig.1.

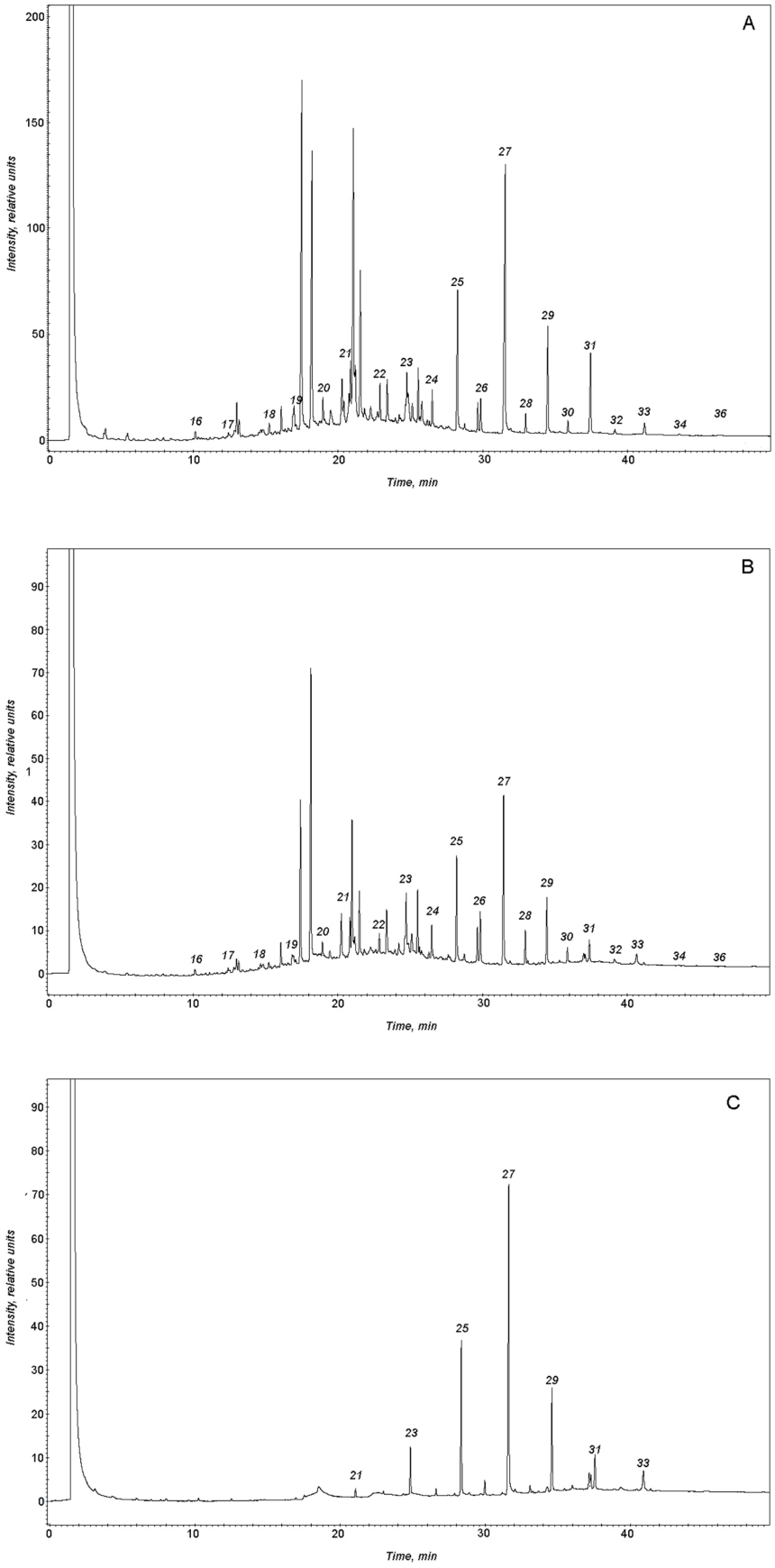

Fig. 1. Chromatograms of hydrocarbons in hexane extracts of the resins of two mummies (A, B) and beeswax (C).

The *n*-alkanes with a chain length of 16 to 35 carbon atoms were identified on the chromatograms of hexane extracts. There were three possible sources of normal saturated hydrocarbons (*n*-alkanes) with such a chain length: natural bitumen, bee and plant waxes in ancient Egypt. The predominance of *n*-alkanes C_{27}, C_{29}, C_{31} and C_{33} is typical for beeswax. A chromatogram of a solution of modern beeswax in *n*-hexane was recorded to identify wax in the resin.

The chromatogram of beeswax is also shown in Fig. 1. The predominance of C_{25}–C_{33} hydrocarbons in chromatograms of hexane resin extracts, typical for beeswax, leads to the assumption of its use in the embalming composition for the mummies.

To confirm the presence of beeswax fatty acids in the composition of mummies, alkaline solutions obtained after hexane extract treatment were studied. For what these solutions were acidified, extracted with diethyl ether, and then fatty acid methyl esters were obtained. Chromatographic separation was performed on a Select^{TM} Biodisel for FAME capillary column. The chromatograms of the FAME extract of one of the mummies resin and the beeswax are shown in Fig. 2.

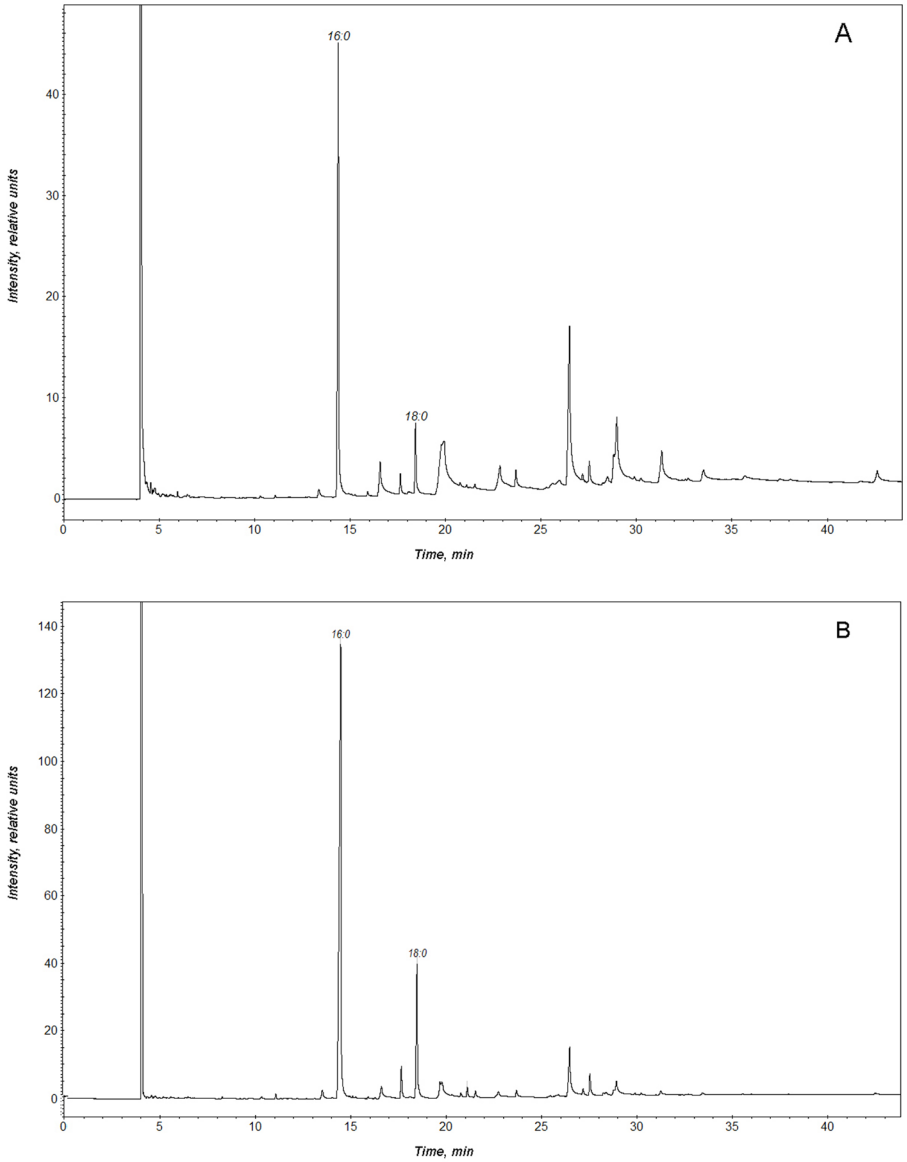

Fig. 2. Chromatograms of the FAME extract of one of the mummies (A) and the beeswax (B).

The chromatograms identified methyl esters of palmitic and stearic acids (Fig. 2). The relative content of these acids in resin samples of different mummies is 4.7–6.9 (for comparison: this ratio in the beeswax sample is about 5.2). A comparison of the obtained chromatograms confirms the beeswax using in the balsamic compositions of the studied mummies.

The *n*-alkanes with an even number of carbon atoms and a chain length of less than 23 atoms are absent at the beeswax chromatogram (Fig. 1B). These hydrocarbons were found in hexane extracts of resins of five mummies (Nos. 1, 3, 4, 6, 7), which allows

for the assumption of the presence of natural bitumen in the composition of the resins of these mummies. The examples of the presence of beeswax and natural bitumen in the resins of the mummies are described earlier [11, 19, 20, 51–53].

In order to establish the geographical origin of bitumen, histograms of the distribution of *n*-alkanes in the hydrocarbon profile of mummies were constructed. In order to exclude the influence of beeswax, the distribution profiles of *n*-alkanes were constructed by hydrocarbons with an even number of carbon atoms. The resulting histograms of hydrocarbon profiles are presented in Fig. 3. They show an approximately similar distribution of bitumen hydrocarbons in the resins of the studied mummies. The maximum hydrocarbon content is corresponded to the *n*-alkanes with the number of carbon atoms 22–26. The distribution of hydrocarbons in the resins of the mummies, in which bitumen from the Dead Sea basin was identified but beeswax was absent, was established in [19, 20]. The maximum distribution of hydrocarbons was observed in the region of 20–25 carbon atoms.

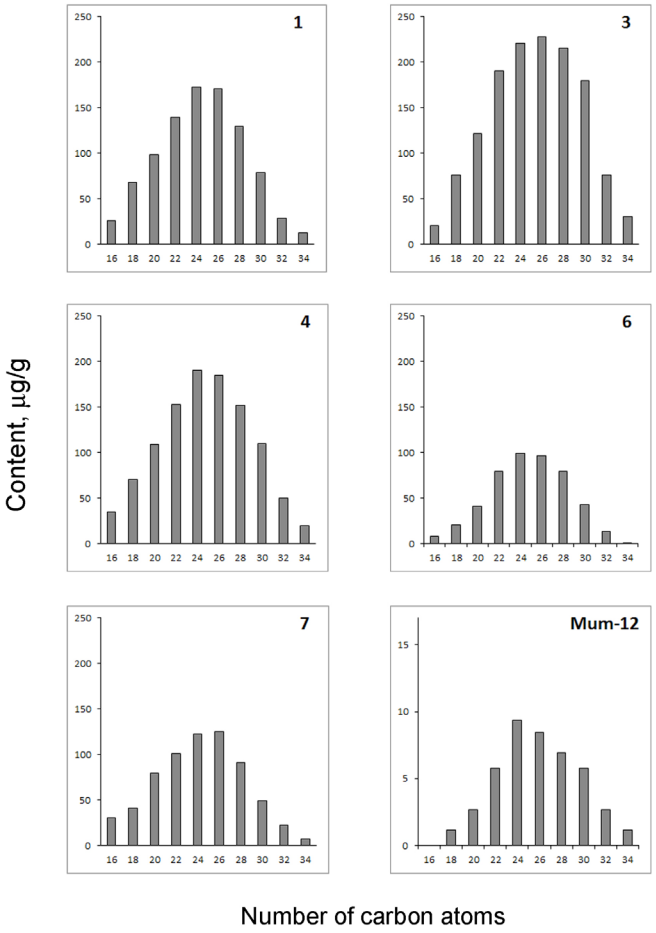

Fig. 3. Histograms of distribution of *n*-alkanes in the hydrocarbon profile of the resins of the studied mummies (Nos. 1, 3, 4, 6, 7) and the resin of Mum-12 mummy from Dakhleh oasis [8].

Based on the study of the distribution of *n*-alkanes in present-day bitumen from the Dead Sea and the resins of the Egyptian mummies from the Dakhleh oasis, it was shown [11] that the maximum in the Dead Sea bitumen profile was in the region of 19–22 carbon atoms. The maximum distribution of bitumen hydrocarbons in mummy resins (excluding beeswax hydrocarbons) was in the area of 20–26 carbon atoms. Despite a significant difference in the position of the maxima in the hydrocarbon profiles of bitumen resins of mummies and modern bitumen of the Dead Sea, the authors of [11] nevertheless made a conclusion about the use of bitumen from tar deposits of the Dead Sea basin in the composition of the mummy resins. It was confirmed by studies of the profiles of steranes in natural bitumen and mummies resins using the GC–MS method in the regime of monitoring the set ions (*m/z* 217).

The comparison of the distributions of hydrocarbons in resins that were obtained with the published data [11, 19, 20] allows for the assumption that the bitumen from the Dead Sea basin deposits was used in the resins of the studied mummies. We studied the chloroform extracts of mummy resins by GC–MS via scanning in the mode of monitoring the set ions (*m/z* 217 and 191) to confirm this assumption. The histograms of the content of some steranes in the extracts of mummy resins are presented in Figs. 4 and 5.

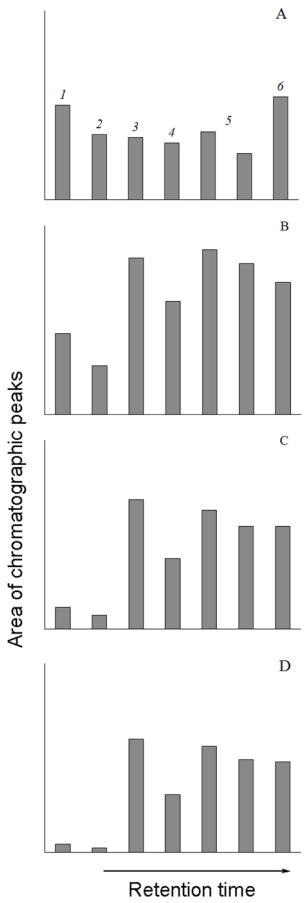

Fig. 4. Histograms of the content of steranes and hopanes (*m/z* 217) in the bitumen deposits of Gebel El Zeit (A); Abu Durba (B); Dead Sea (C) and in the resin of the mummy No. 7 (D):
1 – 13β,17α-diacholestane 20S (diasterane);
2 – 13β,17α-diacholestane 20R (diasterane);
3 – 5α,14β,17β-cholestane 20S;
4 – 5α,14α,17α-stigmastane 20S;
5a – 5α,14β,17β-stigmastane 20R;
5b – 5α,14β,17β-stigmastane 20S;
6 – 5α,14α,17α-stigmastane 20R.

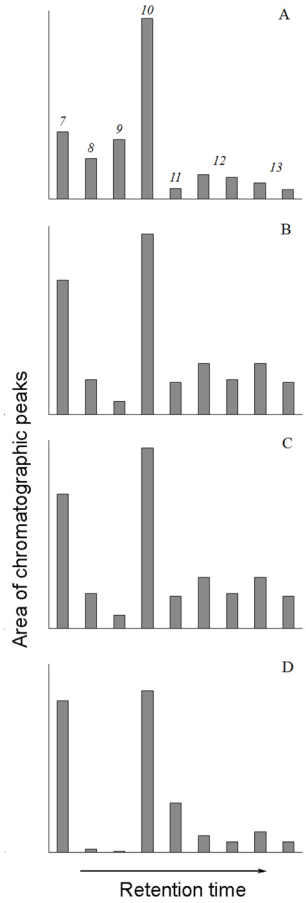

Fig. 5. Histograms of the content of steranes and hopanes (*m/z*191) in the bitumen deposits of Gebel El Zeit (A); Abu Durba (B); Dead Sea (C) and in the resin of the mummy No. 7 (D):
7 – 17α,1β(H)-30-norhopane;
8 – 18α(H)-30-neonorhopane; 9 – oleanane;
10 – 17α,21β(H)-30-hopane; 11 – gammacerane;
12a – 17α,21β(H)-29-tris-homohopane 22S;
12b – 17α,21β (H)-29-tris-homohopane 22R;
13a – 17α,21β(H)-29-pentakis-homohopane 22S;
13b – 17α,21β(H)-29-pentakis-homohopane 22R.

The obtained data were compared with the experimental data on the distributions of steranes and pentacyclic terpenes in the modern bitumens of three deposits in the basins of the Suez Canal and the Dead Sea, published in [41]. The phytane and prystane were not detected in the resins of the studied mummies. In resins of mummies No. 2 and No. 5, steranes and terpenes were also absent. In the resins of these two mummies, there were no *n*-alkanes with an even number of carbon atoms and a chain length of less than 23 atoms. The obtained results led to the assumption that there is no bitumen in the embalming compositions for mummies Nos. 2, 5.

There were practically no neonorhopane (18α(H)-30-neonorhopane) and oleanane on the chromatograms of chloroform extracts of the resins of mummies Nos. 1, 3, 4, 6, 7 under ion monitoring conditions at *m/z* 191. According to [41], these compounds are present in the bitumen of the Suez Canal deposits. In the bitumen of the Gebel El Zeit deposit, hydrocarbons are contained in rather large quantities, and in somewhat smaller quantities in the bitumen of the Abu Durba deposit. In the composition of the Dead Sea bitumen, only trace amounts of neonorhopane and oleanane are present [41].

The chromatograms of the resins of the studied mummies under ion monitoring at *m/z* 191 show a peak of gammacerane, which is typical for Dead Sea bitumen. In the bitumen deposits of the Suez Canal, only trace amounts of gammacerane are present [41].

The GC–MS analysis of chloroform extracts of the resins of mummies Nos. 1, 3, 4, 6, 7 at *m/z* 217 showed an almost complete absence of diasteranes, which is typical

for the Dead Sea bitumen. Diasteranes are present in the bitumen deposits of the Suez Canal basin [41].

Thus, the results of the study of the resins via the GC–MS method in the monitoring mode of the specified ions (*m/z* 217 and 191) confirmed the hypothesis about the use of natural bitumen from the Dead Sea basin deposits in the compositions of the resins of mummies Nos. 1, 3, 4, 6, 7.

As noted above, the ratio of the content of vanadium and nickel in the mummy resin may serve as a biomarker of their geographical origin [42]. For this purpose, the content of certain trace elements in the resins of the studied mummies was determined with the method of an atomic emission spectroscopy with inductively coupled plasma. The results of elemental analysis are given in Table 2.

Table 2. Quantitative content of the elements in the mummy resins

Element/ λ, Å	Content of elements, *ppm*						
	Mummy No.						
	1	2	3	4	5	6	7
Al_{3961}	6925.6	118.9	307.8	5382.6	≤0.1	183.4	706.6
Ba_{4554}	19.6	1.6	24.9	32.2	≤0.1	5.307	12.427
Cd_{2288}	0.6	0.3	0.1	1.0	0.2	0.2	0.4
Co_{2286}	5.5	0.6	0.7	7.1	0.7	0.3	1.4
Cr_{2677}	9.3	6.3	0.8	7.0	≤0.1	2.6	4.5
Cu_{3247}	174.1	13.5	14.6	103.7	3.1	43.7	80.1
Fe_{2599}	6462.4	571.9	485.3	7387.0	85.8	299.5	1051.1
K_{7664}	2070.5	10310.4	1617.2	5943.4	5180.6	551.3	412.4
Li_{6707}	3.9	0.3	0.1	2.0	0.2	0.1	0.7
Mg_{2795}	2105.8	644.6	835.3	2448.1	1485.4	111.5	876.4
Mn_{2576}	74.1	10.7	20.8	132.9	0.2	7.1	34.5
Mo_{2020}	26.2	0.6	6.2	6.0	0.2	6.2	20.7
Na_{5895}	1176.9	21237.1	3399.6	4611.1	20401.1	1095.1	624.4
Nb_{3094}	8.8	0.3	2.2	6.0	0.2	2.6	8.3
Ni_{2316}	44.7	0.3	6.6	17.1	≤0.1	11.7	39.6
P_{2136}	229.2	8881.4	284.3	1281.9	3814.7	58.2	91.1
Pb_{2203}	16.7	≤0.1	1.5	424.9	≤0.1	33.4	≤0.1
Sb_{2068}	0.6	4.4	0.2	7.0	0.4	1.1	1.7
Se_{1960}	1.1	5.7	2.5	7.1	2.2	3.6	≤0.1
Si_{2516}	703.8	≤0.1	532.2	1027.2	338.6	523.9	103.9
Sr_{4215}	46.5	5.0	43.2	64.4	6.7	3.4	35.5
Ti_{3361}	665.9	≤0.1	36.7	610.3	≤0.1	25.6	59.3
V_{2924}	87.3	≤0.1	20.6	42.3	≤0.1	22.9	77.6
Zn_{2138}	21.3	78.2	7.4	35.2	25.0	8.4	2.1
Σ(Mo, Ni, V), *ppm*	**158.4**	**-**	**33.6**	**65.5**	**-**	**41.0**	**138.1**
V, %	**55.1**	**-**	**61.3**	**64.6**	**-**	**55.9**	**56.2**
Mo, %	**16.5**	**-**	**18.4**	**17.3**	**-**	**15.4**	**15.0**

It should be noted from the data in Table 2 that vanadium and nickel are found in all the examined resins, with the exception of mummies Nos. 2 and 5. This confirms the conclusion about the absence of natural bitumen in the resins of these mummies. It is also interesting to note the absence of lead, niobium, and titanium in the resin compositions of mummies Nos. 2 and 5. It is possible that the presence of these elements is also a feature of natural bitumen, but data on this are not yet available in publications.

Molybdenum was found in the resins of mummies Nos. 1, 3, 4, 6, 7, in addition to vanadium and nickel. According to the results of the research of a number of authors [10, 21, 47, 48], molybdenum was found only in the bitumen of the Dead Sea. According to [21], the shares of vanadium and molybdenum in the natural Dead Sea bitumen from the sum of the three elements were about 50 and 24%, respectively. The shares of these elements in the embalming composition of the mummy based on the Dead Sea bitumen found in the Fayoum Oasis of Egypt [10] amounted to 56.3 and 15.1%, respectively.

The share of vanadium in the resins of the studied mummies was 55.1–64.6%; molybdenum was

at 15.0–18.4%. The results correlate with the published data on the content of vanadium, nickel and molybdenum in the bitumen of the Dead Sea and in the resin of the Fayoum mummy based on this bitumen. Consequently, natural bitumen from deposits of the Dead Sea basin was used in the resins of mummies Nos. 1, 3, 4, 6, 7.

Using the method of identification of the bitumen in mummy resins for determining the contents of vanadium, nickel and molybdenum has several significant advantages:

– instruments used for this method allow for the detection of these elements at the level of 0.05 *ppm*;

– the method has high selectivity, which allows one to determine the elements in the presence of any organic compounds, regardless of their quantity;

– the analyzed elements were not subjected to physical, chemical or biological influences in the process of a long-term immurement;

– vanadium, nickel and molybdenum are concentrated as a result of natural bitumen formation, and their relative content remains constant.

Thus, the detection of the relative content of vanadium, nickel and molybdenum in mummy resins can provide a reliable identification for the geographic origin of natural bitumen in mummification balms.

Conclusions

A GC–MS study of the resins of seven Ancient Egyptian mummies from the collection of the Pushkin State Museum of Fine Arts was carried out, its objective being of determining the presence and origin of natural bitumen. *n*-Alkanes with a chain length of 16 to 35 carbon atoms have been identified in the resins. The dominance of C_{25}–C_{33} hydrocarbons, typical of beeswax, led to the assumption of its use in mummies' resins, which was confirmed by the GC analysis of FAME. In the resins of five mummies, *n*-alkanes with the number of carbon atoms less than 23 atoms were found, which points to the presence of natural bitumen. The bitumen from the Dead Sea basin was identified by comparing the distributions of hydrocarbons with the profiles of *n*-alkanes of mummy resins from the published sources. Evidence of the geographical origin of the bitumen was obtained by studying the mummy resins with the GC–MS method in the mode of ion monitoring (*m/z* 217 and 191).

The content of trace elements in the samples taken for the study was determined using the method of atomic emission spectroscopy with inductively coupled plasma. Vanadium, nickel and molybdenum were found in the resins of five mummies. The absence of these elements in two of the seven studied mummies confirmed the conclusion about the absence of natural bitumen in the composition of their resins. The results of determining the relative quantities of vanadium, nickel and molybdenum in the resins of the studied mummies showed a good correlation with the published data on the content of elements in the Dead Sea bitumen and in the resin of the Fayum mummy.

The advantages of identifying bitumen in mummy resins by the relative contents of vanadium, nickel and molybdenum are shown.

Acknowledgments

The research was carried out in the Kurchatov complex of Nano-, Bio-, Info-, Cognitive and Socio-humanitarian Sciences and Technologies of the National Research Center "Kurchatov Institute". The work was supported by the Russian Foundation for Basic Research, grants Nos. ofi-m 17-29-04144, 17-29-04100.

The authors declare no conflict of interest.

References:

1. Taylor J.H., Antoine D. Ancient Lives. New Discoveries: Eight Mummies, Eight Stories. London: British Museum Press, 2014. 192 p.

2. Egyptian Mummies and Modern Science. Ed. Rosalie David A. Cambridge and New York: Cambridge University Press, 2008. 304 p. https://doi.org/10.1017/CBO9780511499654

3. David A.R. Ancient Egyptian Materials and Technology. Ed. P.T. Nicholson, I. Shaw. Cambridge: Cambridge University Press, 2000. 372 p. ISBN 0521-45257-0

4. Monuments and people. Sci. ed. K.K. Iskoldskaya. Moscow: Vostochnaya literature Publ., 2003. 454 p. (in Russ.). ISBN 5-02-018341-5

5. Regarding the Dead: Human Remains in the British Museum. Eds. A. Fletcher, D. Antoine, J.D. Hill. London: British Museum Press, 2014. 142 p. ISBN 978-086159-197-8

6. Aufderheide A. The Scientific Study of Mummies. London: Cambridge University Press, 2003. 590 p. ISBN 978-0-521-17735-1

7. Yatsishina E.B., Kovalchuk M.V., Loshak M.D., Vasilyev S.V.,Vasilieva O.A., Dyuzheva O.P., Pozhidaev V.M., Ushakov V.L. Interdisciplinary study of Egyptian mummies from the Pushkin State Museum of Fine Arts collection at the National Research Centre "Kurchatov Institute". *Crystallography Rep.* 2018;63(3):500-511. https://doi.org/10.1134/S1063774518030343

8. Menager M., Azémard C., Vieillescazes C. Study of Egyptian mummification balms by FT-IR spectroscopy and GC–MS. *Microchemical J.* 2014;114:32-41. https://doi.org/10.1016/j.microc.2013.11.018

9. Buckley S.A., Evershed R.P. Organic chemistry of embalming agents in Pharaonic and Graeco-Roman mummies. *Nature.* 2001;413:837-841. https://doi.org/10.1038/35101588

10. Proefke M.L., Rinehart K.L. Analysis of an Egyptian Mummy resin by mass spectrometry. *J. Am. Soc. Mass Spectrom.* 1992;3(5):582-589. https://doi.org/10.1016/1044-0305(92)85036-J

11. Maurer J., Mohring Th., Rullkotter J. Plant lipids and fossil hydrocarbons in embalming material of Roman period mummies from the Dakhleh Oasis, Western Desert, Egypt. *J. Arch. Sci.* 2002;29(7):751-762. https://doi.org/10.1006/jasc.2001.0773

12. Brettell R., Martin W., Atherton-Woolham S., Stern B., McKnight L. Organic residue analysis of Egyptian votive mummies and their research potential. *Studies in Conservation.* 2017;62(2):68-82. https://doi.org/10.1179/2047058415Y.0000000027

13. Colombini M.P., Modugno C., Silvano F., Onor M. Characterization of the balm of an Egyptian mummy from the seventh century B.C. *Studies in Conservation.* 2000; 45(1): 19-29.https://doi.org/10.1179/sic.2000.45.1.19

14. Buckley S.A., Clark K.A., Evershed R.P. Complex organic chemical balms of Pharaonic animal mummies. *Nature.* 2004;431:294-299. https://doi.org/10.1038/nature02849

15. Łucejko J., Connan J., Orsini S., Ribechini E., Modugno F. Chemical analyses of Egyptian mummification balms and organic residues from storage jars dated from the Old Kingdom to the Copto-Byzantine period. *J. Arch. Sci.* 2017;85:1-12. https://doi.org/10.1016/j.jas.2017.06.015

16. Łucejko J., Lluveras-Tenorio A., Modugno F., Ribechini E., Colombini M. An analytical approach based on X-ray diffraction, Fourier transform infrared spectroscopy and gas chromatography/mass spectrometry to characterize Egyptian embalming materials. *Microchem. J.* 2012;103:110-118. http://dx.doi.org/10.1016/j.microc.2012.01.014

17. Sarret M., Adam P., Schaeffer P., Ebert Q., Perthuison J., Pierrat-Bonnefois G. Organic substances from Egyptian jars of the Early Dynastic period (3100–2700 BCE): Mode of preparation, alteration processes and botanical (re)assessment of "cedrium". *J. Arch. Sci.: Reports.* 2017;14:420-431.http://dx.doi.org/10.1016/j.jasrep.2017.06.021

18. Degano I., Colombini M.P. Multi-analytical techniques for the study of pre-Columbian mummies and related funerary materials. *J. Arch. Sci.* 2009;36(8):1783-1790. https://doi.org/10.1016/j.jas.2009.04.015

19. Jones J., Higham Th.F.G., Chivall D., Bianucci R., Kay G.L., Pallen M.J., Oldfield R., Ugliano F., Buckley S.A. A prehistoric Egyptian mummy: Evidence for an 'embalming recipe' and the evolution of early formative funerary treatments. *J. Arch. Sci.* 2018;100:191-200. https://doi.org/10.1016/j.jas.2018.07.011

20. Jones J., Higham Th.F.G., Oldfield R., O'Connor T.P., Buckley S.A. Evidence for prehistoric origins of Egyptian mummification in Late Neolithic Burials. *PLoS One.* 2014. Aug 13;9(8):e103608. https://doi.org 10.1371/journal.pone.0103608

21. Benson G.G., Hemingway S.R., Leach F.N. The analysis of the wrappings of mummy 1770. In: The Manchester Museum mummy project: multidisciplinary research on ancient Egyptian mummified remains. Ed. by A.R. David. Manchester: Manchester University Press, 1979. P. 119-132. ISBN 0-7190-1293-7

22. Proefke M.L., Rinehart K.L., Raheel M., Ambrose S.H., Wisseman S.U. Probing the mysteries of ancient Egypt: chemical analysis of a Roman period Egyptian mummy. *Anal. Chem.* 1992;64(2):105A-111A. https://doi.org/10.1021/ac00026a002

23. Lucas A., Harris J.R. Ancient Egyptian Materials and Industries, 4th ed. London: Historiesand Mysteries of Man, 1989. P. 303-308. ISBN-10: 1854170465; ISBN-13: 978-1854170460

24. Beck C.W., Borromeo C. Ancient pine pitch: technological perspectives from a Hellenistic shipwreck. *MASCA Res. Pap. Sci. Archaeol.* 1990;7:51-58.

25. Rullkotter J., Nissenbaum A. Dead Sea asphalt in Egyptian mummies: molecular evidence. *Naturwissenschaften.* 1988;75(12):618-621. https://doi.org/10.1007/BF00366476

26. Petrov A.A. Oil Hydrocarbons. Moscow: Nauka Publ., 1984. 264 p. (in Russ.).

27. Kim N.S., Rodchenko A.P. Hopane hydrocarbons in bitumens of Mesozoic deposits of the western Enisey-Khatanga regional trough. *Geologiya i geofizika = Russian Geology and Geophysics.* 2016;57(4):597-607. https://doi.org/10.1016/j.rgg.2015.06.011

28. Harrell J.A., Lewan M.D. Sources of mummy bitumen in ancient Egypt and Palestine. *Archaeometry.* 2002;44(2):285-293. http://dx.doi.org/10.1111/1475-4754.t01-1-00060

29. Wendt C.J., Lu Shan-Tan. Sourcing archaeological bitumen in the Olmec region. *J. Arch. Sci.* 2006;33(1):89-97. https://doi.org/10.1016/j.jas.2005.06.012

30. Mackenzie A.S. Applications of biological markers in petroleum geochemistry. In: Advances in petroleum geochemistry. Ed. J. Brooks and D. Welte. London: Academic Press Publisher. 1984;1:115-214. https://doi.org/10.1016/B978-0-12-032001-1.50008-0

31. Connan J. Biodegradation of crude oils in reservoirs. In: Advances in petroleum geochemistry. Ed. J. Brooks and D. Welte. London: Academic Press Publisher. 1984;1:299-335. https://doi.org/10.1016/B978-0-12-032001-1.50011-0

32. Connan J., Dessort D. Du bitumen de la Mer Morte dans les baumes d'une momie Égyptienne: Identification par critères moléculaires. *Comptes Rendus de l'Académie des Sciences de Paris Série II.* 1989;309:1665-1672 (in French).

33. Connan J., Nissenbaum A., Dessort D. Molecular archeology: Export of Dead Sea asphalt to Canaan and Egypt in the Chalcolithic-Early Bronze Age (4th – 3rd millennium B.C.). *Geochim. Cosmochim. Acta.* 1992;56(7):2743-2759. https://doi.org/10.1016/0016-7037(92)90357-O

34. Seifert W.K., Moldowan J.M., Demaison G.J. Source correlation of biodegraded oils. *Organic Geochemistry.* 1984;6:633-643. https://doi.org/10.1016/0146-6380(84)90085-8

35. Boehm P.D., Douglas G.S., Burns W.A., Mankiewicz P.J., Page D.S., Bence E. Application of petroleum hydrocarbon chemical fingerprinting and allocation techniques after the Exxon Valdez oil spill. *Marine Pollut. Bull.* 1997;34:599-613. http://dx.doi.org/10.1016/S0025-326X(97)00051-9

36. Barakat A.O., Qian Y., Kim M., Kennicutt M.C. Chemical characterization of naturally weathered oil residues in arid terrestrial environment in Al-Alamein, Egypt. *Environment Int.* 2001;27(4):291-310. https://doi.org/10.1016/S0160-4120(01)00060-5

37. Rullkotter J., Spiro B., Nissenbaum A. Biological marker characteristics of oils and asphalts from carbonate source rocks in a rapidly subsiding graben, Dead Sea, Israel. *Geochim. Cosmochim. Acta.* 1985;49(6):1357-1370. https://doi.org/10.1016/0016-7037(85)90286-8

38. Nissenbaum A. Molecular archaeology: Organic geochemistry of Egyptian mummies. *J. Arch. Sci.* 1992;19(1):1-6. https://doi.org/10.1016/0305-4403(92)90002-K

39. Nissenbaum A., Aizenshtat Z., Goldberg M. The floating asphalt blocks of the Dead Sea. *Physics and Chemistry of the Earth.* 1980;12:157-161. https://doi.org/10.1016/0079-1946(79)90098-3

40. Barakat A.O., Mostafa A., Qian Y., Kim M., Kennicutt M.C. Organic geochemistry indicates Gebel El Zeit, Gulf of Suez, is a source of bitumen used in some Egyptian mummies. *Geoarchaeology: Int. J.* 2005:20(3):211-228. https://doi.org/10.1002/gea.20044

41. Harrell J.A., Lewan M.D. Sources of mummy bitumen in ancient Egypt and Palestine. *Archaeometry.* 2002;44:285-293. https://doi.org/10.1111/1475-4754.t01-1-00060

42. Dechaine G.P., Gray M.R. Chemistry and association of vanadium compounds in heavy oil and bitumen, and implications for their selective removal. *Energy & Fuels.* 2010;24(5):2795-2808. https://doi.org/10.1021/ef100173j

43. Marcano F., Flores R., Chirinos J., Ranaudo M.A. Distribution of Ni and V in A1 and A2 asphaltene fractions in stable and unstable Venezuelan crude oils. *Energy&Fuels.* 2011;25(5):2137-2141. https://doi.org/10.1021/ef200189m

44. Galimov R.A., Krivonozhkina L.B., Romanov G.V., Petrova L.M. Patterns of the distribution of vanadium, nickel and their porphyrin complexes in oil components. *Neftekhimiya* = Petroleum Chemistry. 1990;9:12-13 (in Russ.).

45. Aleshin G.N., Altukhova Z.P., Antipenko V.R., Marchenko S.P., Kamyanov V.F. Distribution of vanadium and vanadylporphyrins by oil fractions of various chemical types. *Neftekhimiya* = Petroleum Chemistry. 1984;24(6):729-732 (in Russ.).

46. Nadirov N.K., Kotova A.V., Kamyanov V.F., Titov V.I., Aleshin G.N., Solodukhin V.P., Bakirova S.F., Glukhov G.G., Koryabin N.M. New oils of Kazakhstan and their using: Metals in oils. Alma-Ata: Nauka Publ., 448 p. (in Russ.).

47. Spielman P.E.To what extent did the Ancient Egyptians employ bitumen for embalming? *J. Egyptian Archaeology.* 1932;18(3/4):177-180. https://doi.org/10.2307/3854980

48. Zaki A., Iskander Z. Materials and methods used for mummifying the body of Amentefnekht, Saqqara 1941. *Ann. Serv. Antiquites Egypte.*1943;XLII:223-250.

49. Marschner R.F., Wright H.T. Asphalts from Middle Eastern Archaeological Sites. In: Archaeological Chemistry – II, ACD Advances in Chemistry series (ed. G.H. Carter). Washington DC, 1978. (171):150-171. https://doi.org/10.1021/ba-1978-0171.ch010

50. Pozhidaev V.M., Sergeeva Ya.E., Kamayev A.V. Study of archeological abstract by chromatography-mass spectrometry. *Zhurnal analiticheskoj khimii = J. Analit. Chem.* 2017;72(6):699-702. https://doi.org/10.7868/S0044450217060135

51. Mills J.S., White R.The Organic Chemistry of Museum Objects. 2nd ed. Oxford. Butterworth–Heinemann, Boston., 1994.206 p. eBook ISBN 9780080513355 https://doi.org/10.4324/9780080513355

52. Serpico M., White R. Resin, pitch and bitumen. In: Ancient Egyptian Materials and Technology. Eds. P. Nicholson, I. Shaw. Cambridge: Cambridge University Press, 2000. P. 430-474

53. Buckley S.A., Stot, A.W., Evershed R.P. Studies of organic residues from ancient Egyptian mummies using high temperature – gas chromatography – mass spectrometry and sequential thermal desorption – gas chromatography – mass spectrometry and pyrolysis – gas chromatography – mass spectrometry. *Analyst.* 1999;124:443-452. https://doi.org/10.1039/A809022J

About the authors:

Ekaterina B. Yatsishina, Cand. of Sci. (Philosophy), Deputy Director for Research, National Research Center "Kurchatov Institute" (1, Akademika Kurchatova pl., Moscow 123182, Russia). Scopus Author ID 55062074900. E-mail: Yatsishina_EB@nrcki.ru

Viktor M. Pozhidaev, Cand. of Sci. (Chemistry), Senior Researcher, Department of Biotechnology and Bioenergy of the National Research Center "Kurchatov Institute" (1, Akademika Kurchatova pl., Moscow 123182, Russia). https://orcid.org/0000-0001-5916-4374, Scopus Author ID 7004257999. E-mail: pojidaev2006@yandex.ru

Olga A. Vasilyeva, Cand. of Sci. (History),Head of Department, the Pushkin State Museum of Fine Arts (12, Volkhonka ul., Moscow, 119019, Russia). https://orcid.org/0000-0002-1946-8346. E-mail: vassilievagmii@gmail.com

Olga P. Dyuzheva, Cand. of Sci. (Art History), Senior Researcher, the Pushkin State Museum of Fine Arts (12, Volkhonka ul., Moscow, 119019, Russia).https://orcid.org/0000-0002-2084-1881. E-mail: olga.dyuzheva@arts-museum.ru

Yana E. Sergeeva, Cand. of Sci. (Chemistry), Senior Researcher, Department of Biotechnology and Bioenergy, National Research Center "Kurchatov Institute" (1, Akademika Kurchatova pl., Moscow 123182, Russia). http://orcid.org/0000-0002-6190-8800, ResearcherID M-2766-2014, Scopus Author ID: 12784841000. E-mail: yanaes2005@gmail.com

Vasily M. Retivov, Cand. of Sci. (Chemistry),Chief Chemist, Head of Analytical Testing Center,Head of the National Research Center "Kurchatov Institute" (NRC "Kurchatov Institute" – IREA) (3, Bogorodskii Val, Moscow, 107076, Russia). SPIN-code 5544-5600, Scopus Author ID 26029517500, ResearcherID A-6077-2014. E-mail: retivov_vm@irea.org.ru

Elena Yu. Tereschenko, Cand. of Sci. (Phys.-Math.), Deputy Head, Laboratory of Natural-Scientific Methods in the Humanities of the National Research Center "Kurchatov Institute" (1, Akademika Kurchatova pl., Moscow 123182, Russia); Senior Researcher of the Laboratory of X-ray Analysis Methods and Synchrotron Radiation, Shubnikov Institute of Crystallography FSRC "Crystallography and Photonics", Russian Academy of Sciences (59, Leninskii pr., Moscow 119333, Russia). Scopus Author ID 7801407652 , ResearcherID A-8731-2014. E-mail: helena.tereschenko@gmail.com

Irina S. Kulikova, Engineer, Resource Center of the National Research Center "Kurchatov Institute" (1, Akademika Kurchatova pl., Moscow 123182, Russia). http://orcid.org/0000-0001-6734-6047. E-mail: kef-irka08@mail.ru

Ekaterina S. Vaschenkova, Deputy Head of the Analytical Testing Center of the National Research Center "Kurchatov Institute" (NRC "Kurchatov Institute" – IREA) (3, Bogorodskii Val, Moscow, 107076, Russia). https://orcid.org/0000-0002-9921-4142. E-mail: e_katerina2708@mail.ru

Evgeniya I. Kozhukhova, Junior Researcher, Analytical Testing Center of the National Research Center "Kurchatov Institute" (NRC "Kurchatov Institute" – IREA) (3, Bogorodskii Val, Moscow, 107076, Russia). http://orcid.org/0000-0001-7128-6286. E-mail: evgeshapanarina@gmail.com

Об авторах:

Яцишина Екатерина Борисовна, кандидат философских наук, заместитель директора по научной работе НИЦ «Курчатовский институт» (123182, Россия, Москва, пл. Академика Курчатова, д.1). Scopus Author ID 55062074900. E-mail: Yatsishina_EB@nrcki.ru

Пожидаев Виктор Михайлович, кандидат химических наук, старший научный сотрудник отдела Биотехнологии и Биоэнергетики НИЦ «Курчатовский институт» (123182, Россия, Москва, пл. Академика Курчатова, д.1). https://orcid.org/0000-0001-5916-4374, Scopus Author ID 7004257999. E-mail: pojidaev2006@yandex.ru

Васильева Ольга Александровна, кандидат исторических наук, начальник отдела ГМИИ им. А.С. Пушкина (119019, Москва, ул. Волхонка, д. 12). https://orcid.org/0000-0002-1946-8346. E-mail:vassilievagmii@gmail.com

Дюжева Ольга Павловна, кандидат искусствоведения, старший научный сотрудник ГМИИ им. А.С. Пушкина (119019, Москва, ул. Волхонка, д. 12). https://orcid.org/0000-0002-2084-1881. E-mail: olga.dyuzheva@arts-museum.ru

Сергеева Яна Эдуардовна, кандидат химических наук, старший научный сотрудник отдела Биотехнологии и Биоэнергетики НИЦ «Курчатовский институт» (123182, Россия, Москва, пл. Академика Курчатова, д. 1). http://orcid.org/0000-0002-6190-8800, ResearcherID M-2766-2014, Scopus Author ID: 12784841000. E-mail: yanaes2005@gmail.com

Ретивов Василий Михайлович, кандидат химических наук, главный химик, заведующий аналитическим испытательным центром, руководитель ЦКП «Исследовательский научно аналитический центр НИЦ «Курчатовский институт – ИРЕА» (107076, Россия, Москва, Богородский Вал, д. 3). SPIN-код 5544-5600, Scopus Author ID 26029517500, ResearcherID A-6077-2014. E-mail: retivov_vm@irea.org.ru

Терещенко Елена Юрьевна, кандидат физико-математических наук, заместитель начальника лаборатории Естественно-научных методов в гуманитарных науках НИЦ «Курчатовский институт» (123182, Россия, Москва, пл. Академика Курчатова, д. 1); старший научный сотрудник лаборатории рентгеновских методов анализа и синхротронного излучения, Институт кристаллографии имени А.В. Шубникова ФНИЦ «Кристаллография и фотоника» РАН (119333, Россия, Москва, Ленинский пр., д. 59). Scopus Author ID 7801407652, ResearcherID A-8731-2014. E-mail: helena.tereschenko@gmail.com

Куликова Ирина Сергеевна, инженер ресурсного центра НИЦ «Курчатовский Институт» (123182, Россия, Москва, пл. Академика Курчатова, д. 1). http://orcid.org/0000-0001-6734-6047. E-mail: kef-irka08@mail.ru

Ващенкова Екатерина Сергеевна, заместитель заведующего аналитическим испытательным центром НИЦ «Курчатовский институт – ИРЕА» (107076, Россия, Москва, Богородский Вал, д. 3). https://orcid.org/0000-0002-9921-4142. E-mail: e_katerina2708@mail.ru

Кожухова Евгения Игоревна, младший научный сотрудник аналитического испытательного центра НИЦ «Курчатовский институт – ИРЕА» (107076, Россия, Москва, Богородский Вал, д. 3). http://orcid.org/0000-0001-7128-6286. E-mail: evgeshapanarina@gmail.com

For citation: Yatsishina E.B., Pozhidaev V.M., Vasilyeva O.A., Dyuzheva O.P., Sergeeva Ya.E., Retivov V.M., Tereschenko E.Yu., Kulikova I.S., Vaschenkova E.S., Kozhukhova E.I. The determination of the origin of natural bitumen in mummifying resins of Ancient Egyptian mummies from the collection of the Pushkin Museum of Fine Arts. *Tonkie Khimicheskie Tekhnologii = Fine Chemical Technologies.* 2019;14(4):45-58 (in Russ.). https://doi.org/10.32362/2410-6593-2019-14-4-45-58

Для цитирования: Яцишина Е.Б., Пожидаев В.М., Васильева О.А., Дюжева О.П., Сергеева Я.Э., Ретивов В.М., Терещенко Е.Ю., Куликова И.С., Ващенкова Е.С., Кожухова Е.И. Определение происхождения природного битума в мумифицирующих смолах древнеегипетских мумий из собрания ГМИИ им. А.С. Пушкина // Тонкие химические технологии. 2019. Т. 14. № 4. С. 45–58 https://doi.org/10.32362/2410-6593-2019-14-4-45-58

Translated by V. Gusar

Fine Chemical Technologies, 2019, Vol. 14, No. 4, pp. 59–68.
Original Russian Text © Vladimir V. Bannikov, Tatyana V. Savitskaya, published in Tonkie Khimicheskie Tekhnologii, 2019, Vol. 14, No. 4, pp. 59–68

MATHEMATICS METHODS AND INFORMATION SYSTEMS IN CHEMICAL TECHNOLOGY
МАТЕМАТИЧЕСКИЕ МЕТОДЫ И ИНФОРМАЦИОННЫЕ СИСТЕМЫ В ХИМИЧЕСКОЙ ТЕХНОЛОГИИ

https://doi.org/10.32362/2410-6593-2019-14-4-59-68

UDC 004.4

CC BY

The development of a decision support information-modeling system for safety in the chemical industry

Vladimir V. Bannikov[@], Tatyana V. Savitskaya

D. Mendeleyev University of Chemical Technology of Russia, Moscow 125047, Russia
[@] Corresponding author, e-mail: tiron2007@rambler.ru

The analysis of the urgency of developing a decision and support information-modeling system for safety in the chemical industry is carried out. The article also covers the main elements of this information-modeling system. Key normative documents backing up the knowledge base of such an information-modeling system are listed below. The algorithm of the safety decision supporting information-modeling system is proposed. A database model of the safety decision supporting information-modeling system is elaborated below. A production rule system is set forth to manage issuing recommendations on the robust decision support information-modeling system in the chemical industry based on a methodological document. An implementation plan is laid out for the robust decision support information-modeling system in chemical industry. It is a ready-made software package based on two-level (client–server) architecture of information systems. This article also contains recommendations based on a test case of a tank equipment total destruction. Results of the computational experiments' simulation in the TOXI^{+Risk} software corresponding to the test selected values are available.

Keywords: *information-modeling system, industrial safety, database, client–server architecture, production model, software.*

Разработка информационно-моделирующей системы поддержки и принятия решений по управлению безопасностью химических производств

В.В. Банников[@], Т.В. Савицкая

Российский химико-технологический университет имени Д.И. Менделеева, Москва 125047, Россия
[@] Автор для переписки, e-mail: tiron2007@rambler.ru

Проведен анализ актуальности разработки информационно-моделирующей системы (ИМС) поддержки и принятия решений по управлению безопасностью химических производств. Приведены основные подсистемы структуры данной ИМС. Перечислены основные нормативные документы для заполнения базы знаний ИМС; предложен алгоритм работы и разработана модель базы данных ИМС. Разработана система продукционных правил для управления выдачи рекомендаций ИМС на основе методического документа. Приведена программная реализация ИМС, представляющая собой готовый комплекс программного обеспечения на основе двухуровневой (клиент–серверной) архитектуры информационных систем. Приведен вывод рекомендаций, полученных для тестового примера аварии полного разрушения резервуарного оборудования. Приведены результаты моделирования вычислительных экспериментов в программном комплексе ТОКСИ$^{+Risk}$ для заполнения тестовой выборки.

Ключевые слова: *информационно-моделирующая система, промышленная безопасность, база данных, клиент–серверная архитектура, продукционная модель, программное средство.*

Introduction

Today, many chemical, petrochemical and oil and gas production facilities are located near residential or socially significant accommodations and public transport facilities. Because of this, the potential number of victims in possible accidents at these facilities increases.

One of the important research methods is emergency forecasting. Therefore, it is most effective to model accidents at a given facility of a chemical, petrochemical or oil and gas industry.

Currently, information and computer technologies have been widely used in the field of chemical process control, the environmental monitoring of chemical enterprises and industrial safety, both in Russia [1–5] and abroad [6–8]. There is a number of software systems for modeling and/or forecasting emergencies at hazardous production facilities (HPF), and a practical experience has been accumulated in using them in the chemical and petrochemical industries [9, 10].

However, in a real accident, it is impossible to model the unfolding situation in real time. Therefore, it is necessary to enact a procedure for modeling possible emergencies for the standard equipment and initial parameters for storing hazardous substances in advance. Upon obtaining the modeling results, the decision maker (DM) should immediately analyze the gathered data and make a management decision regarding enterprise personnel rescue and the mitigation of the severity of the consequences. However, this procedure takes up considerable time in the real situation.

To solve these problems, it is proposed to implement an information-modeling system (IMS) for the support and decision making in managing the safety of chemical plants based on production models. This system will allow one to select a pre-modeled accident scenario, most likely in the given situation, obtain information on the damage zones associated with various types of fires, explosions, hazardous matters dispersion, and then give recommendations on improving the safety of the recipients in the zone of damage.

Developing a safety decision support IMS in the chemical industry

When creating an IMS, the two-level architecture of an information system was used. It is a client-server architecture, which uses only a server containing a database and a database management system (DBMS), and a client holding the level of data representation.

1. *Data presentation level.* At this level, the interaction of the system with the user is formed. It is executed in the form of a program for working with the user, containing the procedure and conditions for the reactions of the information system to user actions based on clear functions.

2. *Level of access to the data* (server). It provides for the functions of storage, deletion, modification, processing and selection of data in the database.

Structural element of IMS includes five subsystems (Fig. 1):

• *The subsystem of interaction with the user (User Interface)*. This subsystem is meant for the intuitive interaction of the user with the system.

• *Input data selection subsystem.* The selection of substances in the database (DB) by their properties (toxicity, inflammability), the selection of accident properties and screening equipment to set the input data for the calculation.

• *Data storage subsystem.* This subsystem consists of the following databases: the DB of hazardous substances and their properties; the DB of HPF standard equipment; the DB of computational experiments (CE DB).

• *Decision making support subsystem.* It is a knowledge base of recommendations which is

composed of normative, normative-methodological and normative-technical documents, algorithms, methods, decision making models. An important part is also the unit of analysis and comparison of the obtained results. Production models of knowledge presentation are the basis of recommendations aimed at the reduction of the severity of the accident's consequences for personnel. The condition criterion is minimizing the number of victims and the injured at HPF.

• *The subsystem for issuing recommendations and visualizing the results.* The results are presented in the program's user interface [11].

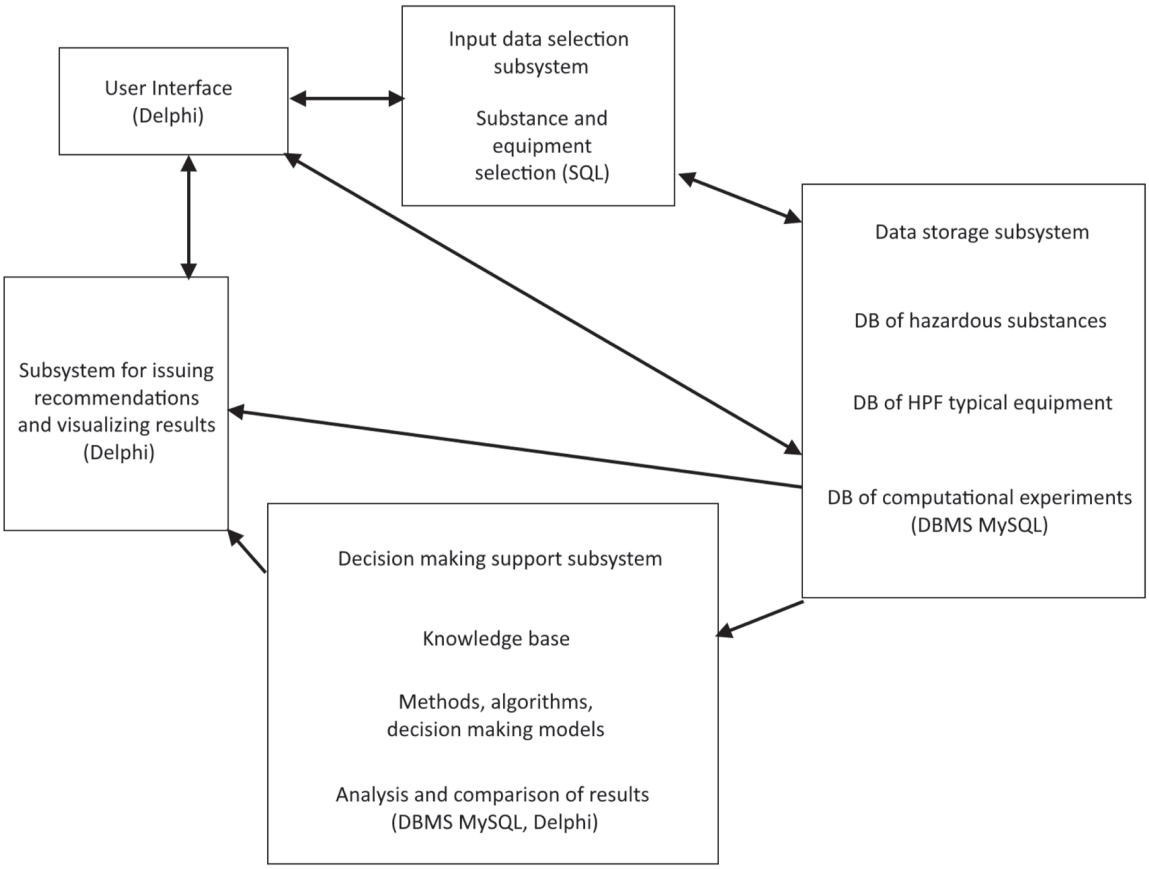

Fig. 1. IMS functional diagram.

Relevant information from normative documents in the knowledge base of recommendations is a guarantee of the effective use of the IMS. Below is a list of such documents (safety guides):

the methodological guideline for modeling the accidental releases[1]; the methodological guide for accident risk assessment at the oil and gas industry HPF[2]; the guide for assessing the consequences of accidents at explosive and fire hazardous chemical plants[3]; the methodological guideline for conducting hazard analysis and risk assessment for the accidents at hazardous production facilities[4]. These guides are based on the Federal Law[5] and federal norms and rules in the field of industrial safety[6].

For the above system, an algorithm is developed, as shown in Fig. 2. The first two steps allow one to enter the input data into the developed system. The next step is the search for the selected data in the CE

[1] Safety guide "Methodological guideline for modeling the accidental releases of hazardous substances" (Ratified in the Rostechnadzor order dated April 20, 2015, no. 158).
[2]Safety guide "Methodological guideline for assessing the risk of accidents at hazardous production facilities of the oil and gas processing, and oil and gas chemical industries" (Ratified in the Rostechnadzor order dated June 29, 2016, no. 272).
[3]Safety guide "Methodological guideline for assessing the consequences of accidents at the explosive and fire hazardous chemical plants" (Ratified in the Rostechnadzor order dated April 20, 2015, no. 160).
[4]Safety guide "Methodological guideline for the hazards analysis and risk assessment for the accidents at hazardous production facilities" (Ratified in the Rostechnadzor order dated April 11, 2016, no. 144).
[5]Federal law dated July 21, 1997, no. 116-FZ (edition dated March 07, 2017) "On industrial safety of hazardous production facilities"(with additions and ammendments effective of March 25, 2017).
[6]Federal rules and regulations in the sphere of industrial safety "General requirements to justification of safety of hazardous production facility" (Ratified in the Rostechnadzor order dated July 15, 2013, no. 306).

database and the selection of the appropriate scenario. The processing of large amounts of data obtained as a result of modeling using specialized software is required in order to implement the request. If the input parameters and the CE database data are equal, the corresponding emergency modeling results are issued. Then the CE database results are compared with the criteria values in the normative documents, a list of recommendations aimed at localizing the consequences of the accident is elaborated and issued to the user.

It was decided to use a free relational database management system MySQL[7] to develop the IMS database.

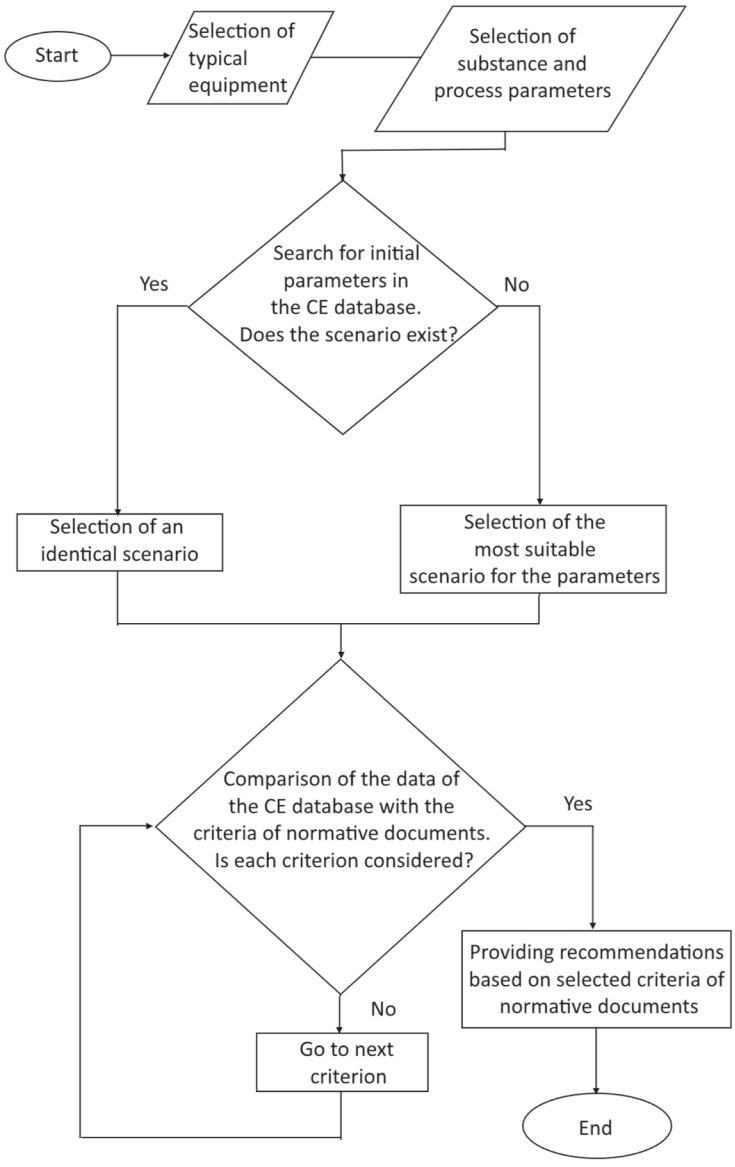

Fig. 2. The block diagram of the IMS algorithm.

The physical model of the database is presented on Fig. 3. A total of 10 tables were used in the current database. Each table has a primary key which characterizes a unique record number; for the table of substances, this is an identifier of a substance, for the table of stratifications—an identifier of stratifications, etc. The presence of external keys is clearly shown in the tables of input and experimental data. With their help, the tables of substances, stratifications and clutters are connected with the table of input data, and an outcome table (spill fire, fuel-air mix explosion, blowup fire, and dispersion), equipment and input data are connected with the table of computational experiments data.

Several types of data were used during the model creation. Each identifier field has a whole number format —an integer. Text data are presented as a varchar (30) type, which allows for input of 30 characters per line. All variable values which are used in recording the rest

[7]Free relational database management system "MySQL", 2018. URL: https://www.mysql.com/ (accessed March 22, 2018).

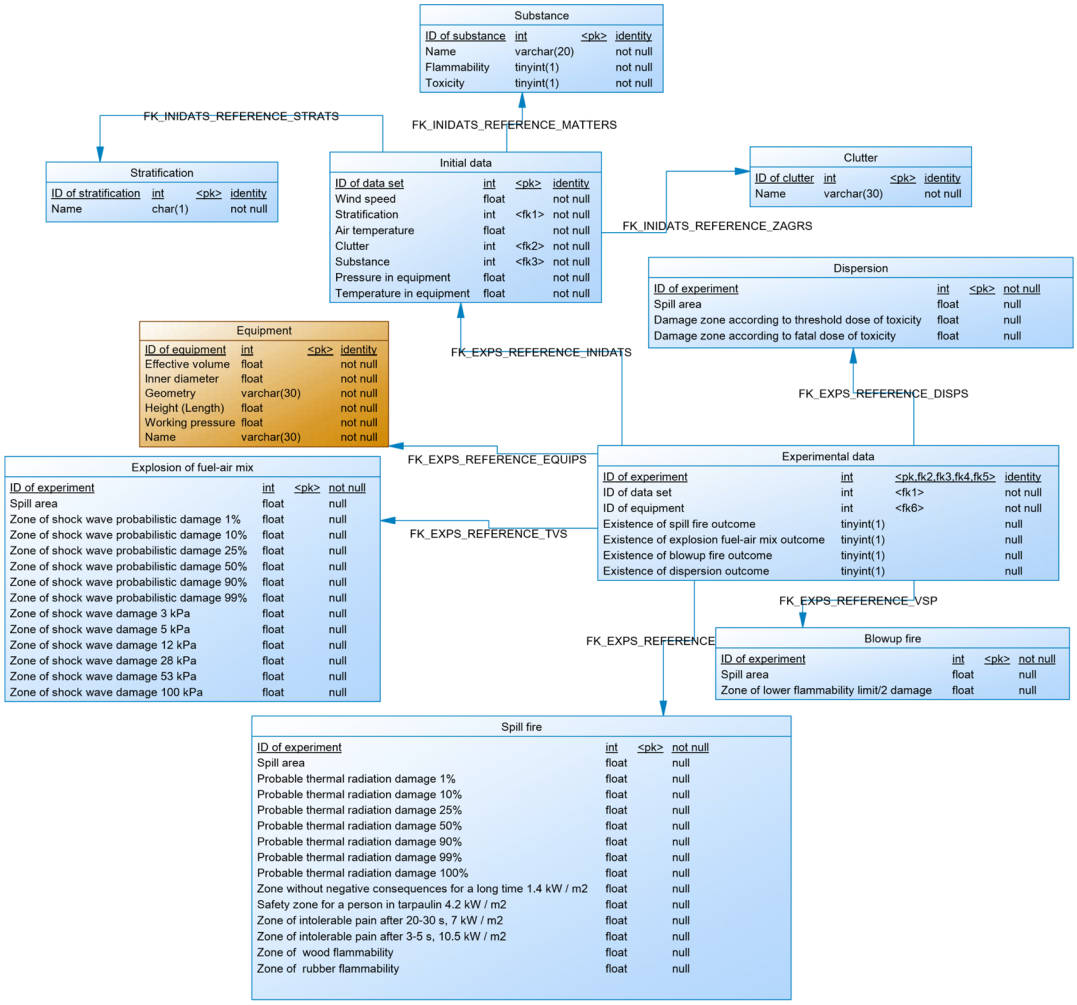

Fig. 3. The physical model of the database.

of the data have the format of floating numbers—float. It should be noted that, in the stratification table, there is a unique column which contains a record of the names of stratifications consisting of one letter, and it has a char (1) format. Another unique type is a tinyint (1), which is used to mark the presence of a certain outcome in a given computational experiment in the table of computational experiments, called a "flag".

Since the parameters are entered by the user to search for scenarios, for the sake of correctness they cannot have gaps. Therefore, the fields of the source data tables should not have NULL values (gaps) in their cells. At the same time, there is no such requirement for the tables which contain the data of computational experiments (except identifiers), so they do not need the Mandatory (not NULL) property.

The tables for the input of initial data allowing for the assessment of the scale of an accident are the two main tables with initial parameters.

The data table "Input data" contains data on the substance and its storage parameters, meteorological conditions. It is also connected with the tables "Substance", "Stratification", and "Clutter", which are filled with the values used in combining input data. The "Substance" table has 25 records of various substances, the "Stratification" table – only 6 records, and the "Clutter" table – 4. The data table "Equipment" is filled with the data on standard pieces of equipment and their properties.

The CE database contains the data obtained during modeling in TOXI^{+Risk} [1]. The scenarios of hazardous outcomes may group the accident data. In this paper, the accidents occurring on stand-alone units of equipment (tanks) are considered. Groups of criteria collected into each outcome are divided into deterministic and probabilistic.

The client part was created using the Borland Delphi[8] 7 programming environment based on a structured Delphi object-oriented programming language.

Edit type fields, which allow one to input parameters, are used to input numerical data. Other values are entered into the Combobox drop-down boxes.

[8]Software tool «Delphi». Company Embarcadero, 2018. URL: https://www.embarcadero.com/ru/products/delphi (accessed March 22, 2018).

When one clicks the "Select Scenario" button, a similar scenario is searched for in the database of computational experiments. The selected scenario will be displayed in the Memo field ("white square" on Fig. 4). If such a scenario does not exist, the program will select the scenario with the most matching parameters.

When one clicks on the "Damage zones" button, the values of the damaged zones of the hazardous outcomes are displayed.

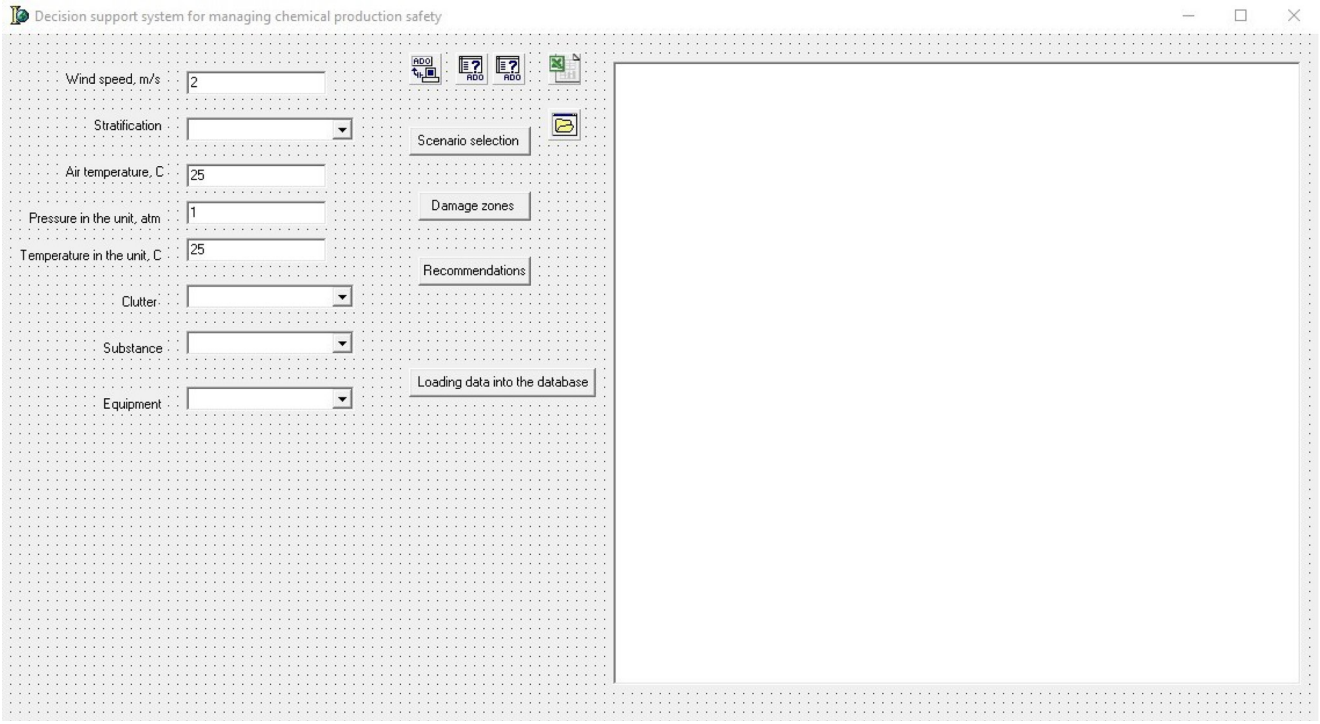

Fig. 4. The screen form of the interface of the decision support system.

On Fig. 5 the scenario is displayed under the unique identifier 23. It has labels of different outcomes. In the presence or absence of this outcome, the value varies from 1 to 0 respectively. In this example, the substance "Butane" is located in standard equipment "LPG tank 15-1200-02" (EQUIP_ID=15) at the pressure of 20 atm. The results of a computational experiment were obtained for the scenario including a wind speed of 1 m/s, stratification F, temperature in the apparatus equals to the ambient temperature – 25 °C, the location is heavily cluttered (all of the above data on the process parameters are included in the initial data set INIDAT_ID = 15). Toxic damage is absent, EXP_RAS (Dispersion) label is 0.

SELECT * FROM disserdb.exps WHERE EXP_ID=23 | Enter a SQL expression to filter results (use Ctrl+Space)

	EXP_ID	INIDAT_ID	EQUIP_ID	EXP_PROLIV	EXP_TVS	EXP_VSP	EXP_RAS
1	23	15	15	1	1	1	0

Fig. 5. Scenario No. 23.

Having identified the presence of certain outcome marks, the software starts to display the values of the recorded criteria from the database for the user (Fig. 6). As one can see, the scenario of toxic damage from the "Butane" substance is absent.

Having received these values of the damage zones, the user must be given recommendations on the actions in case of an accident. After analyzing a number of safety guides, it was decided to use the guide "Methodological guideline for the hazard analysis and risk assessment for the accidents at hazardous production facilities" (see Footnote 4 on page 61), as it clearly indicates the criteria for safe locations and fatal injury. On Fig. 7, recommendations for the above butane scenario are presented. The recommendations are derived based on production rules. The criteria described in the manual mentioned above are checked. If a specific criterion in the CE database exists, the user will be presented with its description in the form of a recommendation based on the text of the document. For the user's convenience, recommendations are presented in the form of a system of production rules, the main components of which are shown in the table.

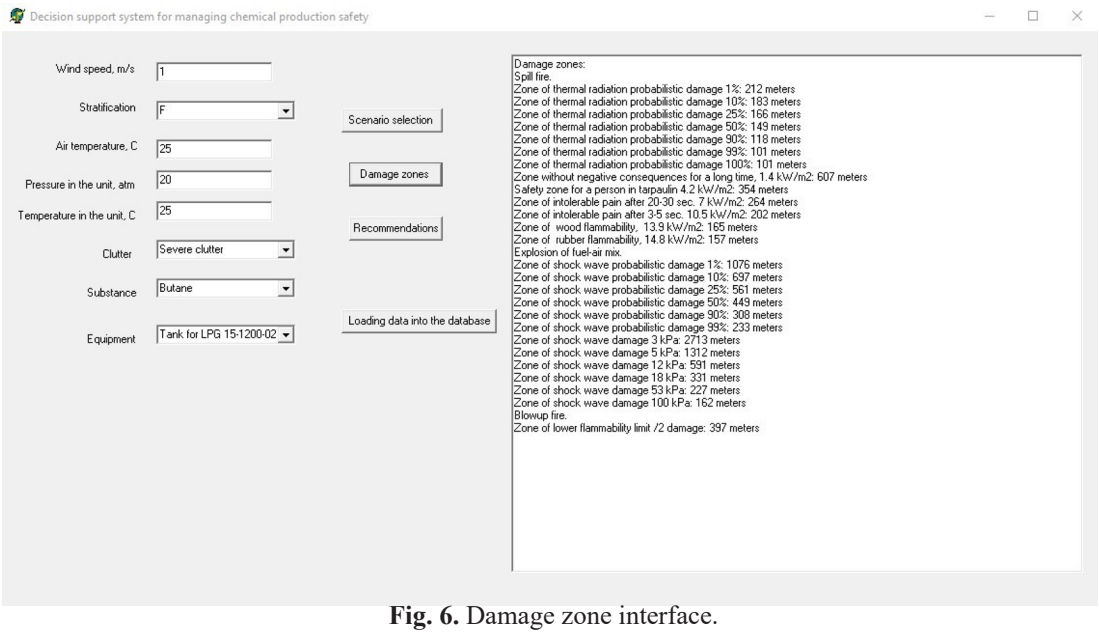

Fig. 6. Damage zone interface.

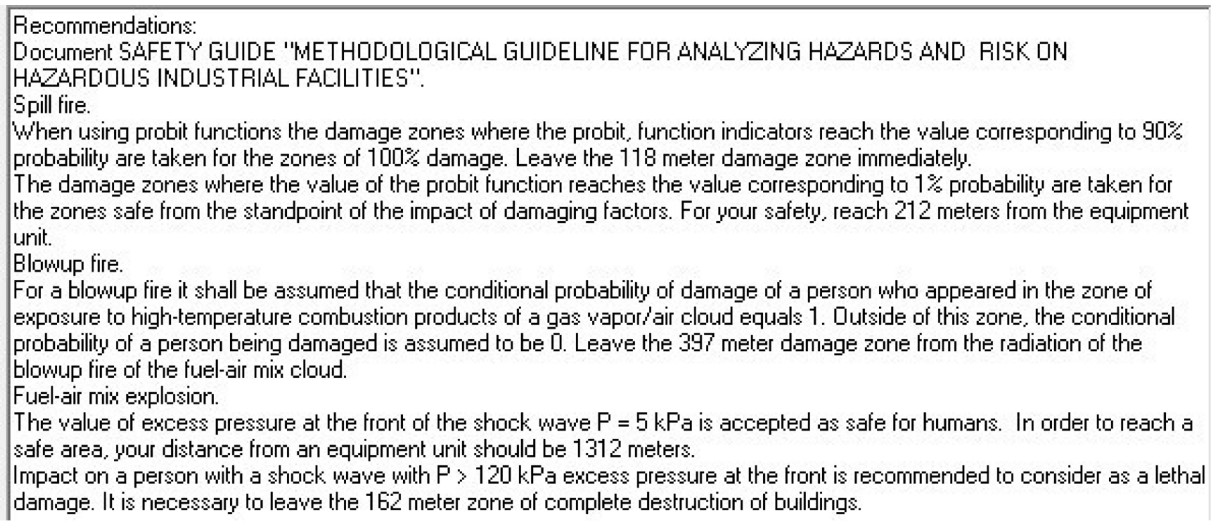

Fig. 7. IMS recommendations for scenario No. 23.

The main components of the system of production rules for managing the issuance of recommendations developed by the IMS based on the methodological document

Parameter	Title
Pr	Spill fire outcome
Vs	Blowup fire outcome
Tv	Fuel-air mix explosion outcome
Di	Dispersion outcome
Pr_1	Zone of thermal radiation probabilistic damage 1%
Pr_{90}	Zone of thermal radiation probabilistic damage 90%
Vs_{LFL}	Zone of lower flammability limit/2 damage
Tv_5	Zone of 5 kPa shock wave damage
Tv_{120}	Zone of 120 kPa shock wave damage
Di_p	Damage zone according to the threshold dose of toxicity
N	Presence
P	Leave
D	Reach

For the selected document, the production rules of the system take the following view:

If Pr=N, then P, Pr_{90}; D, Pr_1;

If Vs=N, then P, Vs_{LFL};

If Tv=N, then P, Tv_{120}; D, Tv_5;

If Di=N, then P, Di_p.

Pressing the "Load data into the database" button allows one to upload new data modeled with the TOXI^{+Risk} software package to the database of computational experiments.

To fill the database of computational experiments, the TOXI^{+Risk} version 5.2 [1] software package was used. Computational experiments were carried out for various substances. Nine substances were used for the current test database: gasoline, chlorine, ammonia, methanol, butane, hexane, chlorine cyan, benzene, diesel fuel. They were selected in order to vary the event trees that characterize the possible outcomes of the scenario. Fig. 8 presents the HPF with one equipment unit (the star), as well as the calculated damage zones for the scenario under identifier No. 23.

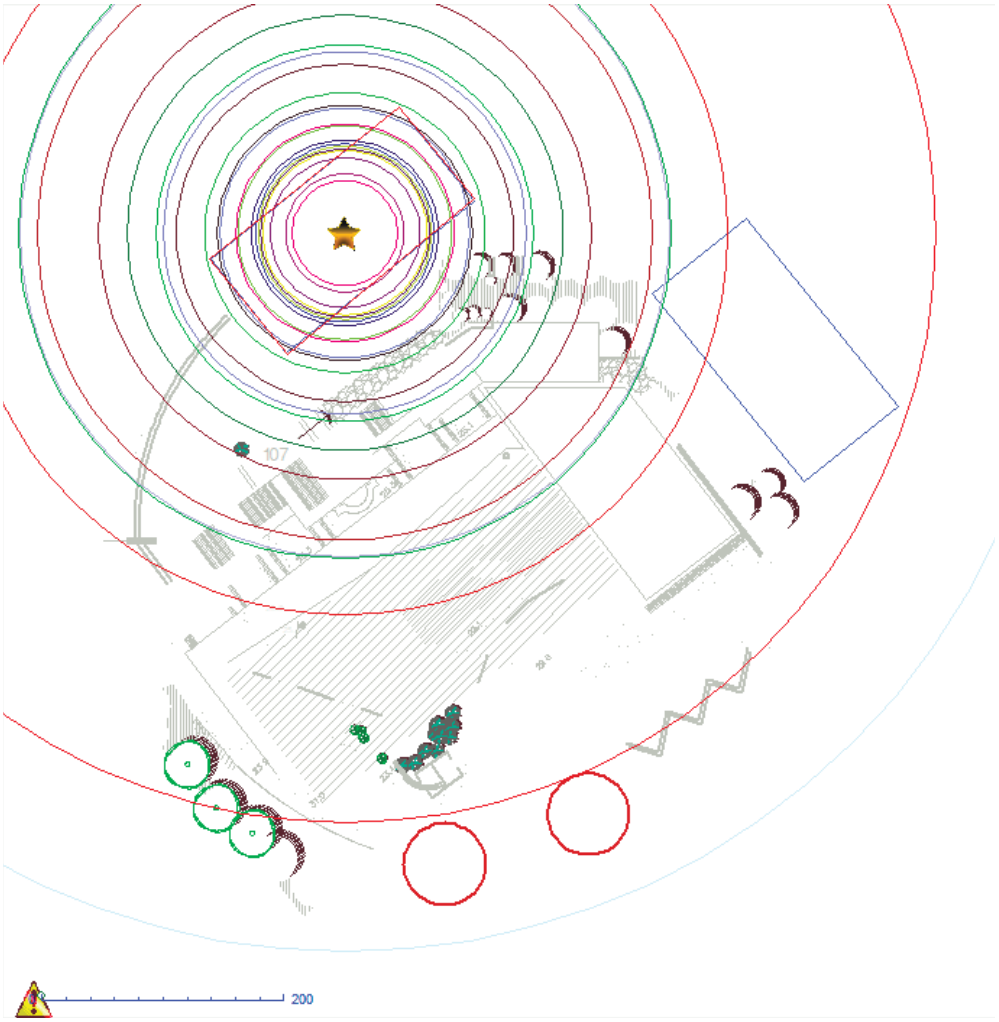

Fig. 8. Calculated damage zones for the selected scenario.

At this stage, the initial data must be input: meteorological parameters, equipment, properties of a hazardous substance, and the choice of an accident development tree. Upon the completion of the input of the initial parameters, the damage zones are calculated for the selected criteria.

After modeling, a file is generated with the results of the scenario of complete equipment destruction (Fig. 9). The criteria for each outcome are divided by page and split into deterministic and probabilistic.

Blowup fire (Ministry of Emergency Situations method)

Site object	Equipment	Status	Hazardous substance	Meteo	Spill area, m2	Hole area, m2	Mass involved in the formation of hazardous factors, kg	Radius of the lower flammability limit/2 zone, m
new areal facility	Tank for LHG 15-1200 -02	Operating status 1	Butane	NE, 1m / s, F, 25 deg. C	7934,31	Complete destruction	0	396,54

Fig. 9. The tab "Blowup fire" for obtaining the file with the results.

As a result, a file with the damage zones was obtained for various criteria of the calculation methods for entering data into the database of computational experiments. Each page of the file represents the results of a particular outcome. The current system includes 51 test experiments with various initial parameters.

Conclusions

1. Analysis was carried out of the relevance of IMS development and the current state of specialized information technologies in Russia and abroad.

2. The functional structure of the IMS was developed. The utilization of this system allows the user to receive recommendations for improving the safety of recipients.

3. The algorithm for the operation of the IMS, schematically representing the order of interaction with the system, is presented.

4. The physical structure of the IMS database was developed; the interactions between the associated tables of the system data were clearly displayed.

5. A system of production rules was developed for managing the issuance of IMS recommendations based on a methodological document.

6. The software implementation of the IMS based on the client-server architecture of the information network was carried out; an example of the system's operation was presented.

7. Scenarios for the total destruction of equipment with various initial parameters were modeled using the TOXI^{+Risk} software package to fill in the server part of the IMS.

In perspective, it is planned to implement scenarios of equipment depressurization to include the flare outcome, add new production rules from other normative documents and fill the CE database with new modeled results.

The authors declare no conflict of interest.

References:

1. Agapov A.A., Lazukina I.O., Marukhlenko S.L., Marukhlenko A.L., Sofin A.S. Using the TOXI^{+RISK} software for assessing fire risk. *Bezopasnost truda v promyshlennosti* [Occupational Safety in Industry]. 2010;(1):46-52 (in Russ.).

2. Kuznetsov A.S., Kornushko V.F. Intelligent control system of chemical-technological processes of structuring of multicomponent elastomer composites based on the production model. *Tonkie Khimicheskie Tekhnologii* = Fine Chemical Technologies. 2017;12(5):88-96 (in Russ.). https://doi.org/10.32362/2410-6593-2017-12-5-88-96

3. Sobolev E.A., Abdulgalimov A.R., Razlivinskaya S.V., Kornyushko V.F. Principles of corporate information system for logistics management of petrochemical enterprises. *Tonkie Khimicheskie Tekhnologii* = Fine Chemical Technologies. 2017;12(1):89-95 (in Russ.). https://doi.org/10.32362/2410-6593-2017-12-1-89-95

4. Kolybanov K.Yu. Principles for design of corporate information system of ecological monitoring of chemical enterprise. Izvestiya vysshikh uchebnykh zavedenii. *Khimiya i khimicheskaya tekhnologiya* = Russian Journal of Chemistry and Chemical Technology. 2008;51(9):103-105 (in Russ.).

5. Kolybanov K.Yu., Kornyushko V.F. Systematic approach to development of data storage of chemical-technological characteristics of recycling processes and air conditioning of radioactive waste. Izvestiya vysshikh uchebnykh zavedenii. *Khimiya i khimicheskaya tekhnologiya* = Russian Journal of Chemistry and Chemical Technology. 2008;51(7):93-96 (in Russ.).

6. Pinoli P., Ceri S., Martinenghi D., Nanni L. Metadata management for scientific databases. *Information Systems.* 2019;81:1-20.

7. Wenjiang Chen, Hongbo Su, Yan Yong, Zhaoji Hua. Decision support system for urban major hazard installations management based on 3DGIS. ScienceDirect. Available at: https://doi.org/10.1016/j.pce.2018.08.008 (accessed March 15, 2019).

8. Borgonovo E., Cappelli V., Maccheroni F., Marinacci M. Risk analysis and decision theory: A bridge. *Eur. J. Operat. Res.* 2018;264(1):280-293.

9. Sumskoy S.I., Agapov A.A., Sofin A.S., Sverchkov A.M.,

Список литературы:

1. Агапов А.А., Лазукина И.О., Марухленко А.Л., Марухленко С.Л., Софьин А.С. Использование программного комплекса ТОКСИ$^{+RISK}$ для оценки пожарного риска // Безопасность труда в промышленности. 2010. № 1. С. 46–52.

2. Кузнецов А.С., Корнюшко В.Ф. Интеллектуальная система управления химико-технологическими процессами и структурирования многокомпонентных эластомерных композитов на основе продукционной модели // Тонкие химические технологии. 2017. Т. 12. № 5. С. 88–96. https://doi.org/10.32362/2410-6593-2017-12-5-88-96

3. Соболев Е.А., Абдулгалимов А.Р., Разливинская С.В, Корнюшко В.Ф. Принципы построения корпоративной информационной системы управления логистическими процессами на предприятиях нефтехимического профиля // Тонкие химические технологии. 2017. Т. 12. № 1. С. 89–95. https://doi.org/10.32362/2410-6593-2017-12-1-89-95

4. Колыбанов К.Ю. Основы построения корпоративных информационных систем экологического мониторинга предприятий химического профиля // Известия высших учебных заведений. Серия: Химия и хим. технология. 2008. Т. 51. № 9. С. 103–105.

5. Колыбанов К.Ю., Корнюшко В.Ф. Системный подход к разработке хранилища данных химико-технологических характеристик процессов переработки и кондиционирования радиоактивных отходов // Известия высших учебных заведений. Серия: Химия и хим. технология. 2008. Т. 51. № 7. С. 93–96.

6. Pinoli P., Ceri S., Martinenghi D., Nanni L. Metadata management for scientific databases // Information Systems. 2019. V. 81. P. 1–20.

7. Wenjiang Chen, Hongbo Su, Yan Yong, Zhaoji Hua. Decision support system for urban major hazard installations management based on 3DGIS [Электронный ресурс]. ScienceDirect: [сайт]. 2018. URL: https://doi.org/10.1016/j.pce.2018.08.008 (дата обращения: 15.03.2019).

8. Borgonovo E., Cappelli V., Maccheroni F., Marinacci M. Risk analysis and decision theory: A bridge // Eur. J. Operat. Res. 2018. V. 264. № 1. P. 280–293.

9. Сумской С.И., Агапов А.А., Софьин А.С., Сверчков

Egorov A.F. Modelling of emergency leaks on the main oil pipelines. *Bezopasnost truda v promyshlennosti* [Occupational Safety in Industry]. 2014;(9):50-53 (in Russ.).

10. Agapov A.A., Khlobystova I.O., Marukhlenko S.L., Marukhlenko A.L., Sofin A.S. "TOXI^{+METEO}" software and hardware complex for assessment of the consequences of possible accidents taking into account data on current weather conditions. *Bezopasnost truda v promyshlennosti* [Occupational Safety in Industry]. 2011;(1):22-25 (in Russ.).

11. Bannikov V.V., Savitskaya T.V. Safety decision support information-modeling system of chemical industry. *Uspekhi v khimii i khimicheskoj tekhnologii* [Journal Adnvances in Chemistry and Chemical Technology]. 2017;31(8):16-18 (in Russ.).

А.М., Егоров А.Ф. Моделирование аварийных утечек на магистральных нефтепроводах // Безопасность труда в промышленности. 2014. № 9. С. 50–53.

10. Агапов А.А., Хлобыстова И.О., Марухленко С.Л., Марухленко А.Л., Софьин А.С. Программно-аппаратный комплекс «ТОКСИ$^{+METEO}$»для оценки последствий возможных аварий с учетом данных о текущих погодных условиях // Безопасность труда в промышленности. 2011. № 1. С. 22–25.

11. Банников В.В., Савицкая Т.В. Информационно-моделирующая система поддержки принятия решений по управлению безопасностью химических производств // Успехи в химии и хим. технологии. 2017. Т. 31. № 8. С. 16–18.

About the authors:

Vladimir V. Bannikov, Postgraduate Student of the Chair of Computer's Integrated Systems in Chemical Technology, D. Mendeleev University of Chemical Technology of Russia (9, Miusskaya pl., Moscow 125047, Russia). E-mail: tiron2007@rambler.ru

Tatyana V. Savitskaya, Dr. of Sci. (Engineering), Professor of the Chair of Computer's Integrated Systems in Chemical Technology, D. Mendeleev University of Chemical Technology of Russia (9, Miusskaya pl., Moscow 125047, Russia). E-mail: savitsk@muctr.ru.

Об авторах:

Банников Владимир Валерьевич, аспирант кафедры компьютерно-интегрированных систем в химической технологии ФГБОУ ВО «Российский химико-технологический университет имени Д.И. Менделеева» (125047, Россия, Москва, Миусская площадь, д. 9). E-mail: tiron2007@rambler.ru

Савицкая Татьяна Вадимовна, доктор технических наук, профессор кафедры компьютерно-интегрированных систем в химической технологии ФГБОУ ВО «Российский химико-технологический университет имени Д.И. Менделеева» (125047, Россия, Москва, Миусская площадь, д. 9). E-mail: savitsk@muctr.ru

For citation: Bannikov V.V., Savitskaya T.V. The development of a decision support information-modeling system for safety in the chemical industry. *Tonkie Khimicheskie Tekhnologii = Fine Chemical Technologies.* 2019;14(4):59-68 (in Russ.). https://doi.org/10.32362/2410-6593-2019-14-4-59-68

Для цитирования: Банников В.В., Савицкая Т.В. Разработка информационно-моделирующей системы поддержки и принятия решений по управлению безопасностью химических производств // Тонкие химические технологии. 2019. Т. 14. № 4. С. 59–68. https://doi.org/10.32362/2410-6593-2019-14-4-59-68

Translated by V. Gusar

Fine Chemical Technologies, 2019, Vol. 14, No. 4, pp. 69–76.
Original Russian Text © Elena V. Burlyaeva, Valery V. Burlyaev, Violetta V. Kononenko, Viktor S. Tsekhanovich, published in Tonkie Khimicheskie Tekhnologii, 2019, Vol. 14, No. 4, pp. 69–76

MATHEMATICS METHODS AND INFORMATION SYSTEMS IN CHEMICAL TECHNOLOGY
МАТЕМАТИЧЕСКИЕ МЕТОДЫ И ИНФОРМАЦИОННЫЕ СИСТЕМЫ В ХИМИЧЕСКОЙ ТЕХНОЛОГИИ

https://doi.org/10.32362/2410-6593-2019-14-4-69-76
UDC 621.311.6:621.3.089.2

CC BY

Verification of functional models of chemical manufacturing

Elena V. Burlyaeva, Valery V. Burlyaev, Violetta V. Kononenko, Viktor S. Tsekhanovich

MIREA – Russian Technological University (M.V. Lomonosov Institute of Fine Chemical Technologies), Moscow 119571, Russia
@ Corresponding author, e-mail: burlyaeva@mirea.ru

A generalized algorithm for the verification of functional models and the rules for the verification of diagrams related by levels of detail were developed in this paper. The algorithm is based on the analysis of a tree which describes the decompose relations in functional diagrams. At each step of the algorithm, a pair consisting of a parent diagram and a functional diagram is selected, and the correlation of the arrows and their roles is checked for both. The formalization of the verification rules was based on the set-theoretic representation of functional diagrams in the form of labeled oriented graphs. The rules make it possible to map the position and roles of the arrows associated with the detailed function block of the parent diagram to the arrows of the child diagram. The following rules for each of the possible arrow roles were established: "input", "output", "control", "mechanism". The use of the logic programming language PROLOG was proposed for the implementation of the algorithm. A knowledge base structure comprised of 3 interrelated predicates to describe the tree of diagrams, nodes and edges of the graphs was suggested. A query to check the verification rules was formed, and methods of binding variables and fixing roles were considered. The analysis and verification of a fragment of a functional model for the production of vinyl acetate from ethylene was conducted as an example. The functional diagrams for the processes "Condensate separation" and "Vinyl acetate isolation" connected by a decompose relation were developed, their set-theoretic models were constructed, and the use of rules for the verification of each type of arrow were considered.

Keywords: *functional modeling, functional model verification, set theory, graph theory, vinyl acetate production.*

Верификация функциональных моделей химических производств

Е.В. Бурляева@, В.В. Бурляев, В.В. Кононенко, В.С. Цеханович

МИРЭА – Российский технологический университет (Институт тонких химических технологий имени М.В. Ломоносова), Москва 119571, Россия
@ Автор для переписки, e-mail: burlyaeva@mirea.ru

Разработан обобщенный алгоритм верификации функциональных моделей и правила проверки связанных отношением детализации диаграмм. Алгоритм основан на анализе дерева, описывающего отношение детализации функциональных диаграмм. На каждом шаге алго-

ритма выбирается пара, состоящая из родительской и функциональной диаграмм, и для этой пары выполняется проверка соответствия стрелок и их ролей. Формализация правил проверки выполнена на основе теоретико-множественного представления функциональных диаграмм в виде помеченных ориентированных графов. Правила позволяют сопоставить положение и роли стрелок, связанных с детализируемым функциональным блоком родительской диаграммы, и стрелок дочерней диаграммы. Построены правила для каждой из возможных ролей стрелки: «вход», «выход», «управление», «механизм». Для реализации построенного алгоритм предложено использование языка логического программирования ПРОЛОГ. Предложена структура базы знаний, включающая 3 взаимосвязанных предиката для описания дерева детализации, вершин и дуг графов, задающих функциональные диаграммы. Сформирован запрос для проверки правил верификации, рассмотрены способы связывания переменных и фиксации ролей. В качестве примера выполнен анализ и верификация фрагмента функциональной модели получения винилацетата из этилена. Приведены функциональные диаграммы для процессов «Разделение конденсата» и «Получение винилацетата», связанных отношением детализации, построены их теоретико-множественные модели, рассмотрено применение правил верификации для каждого типа стрелок.

Ключевые слова: *функциональное моделирование, верификация функциональной модели, теория множеств, теория графов, получение винилацетата.*

Introduction

Enhancing the efficiency of the Russian chemical industry with continuous modernization and the manufacturing improvement is one of the most important and pressing objectives. The methodology of functional modeling is intended for the design, description and analysis of manufacturing systems in order to increase their efficiency [1, 2].

As a rule, the main advantages of functional modeling methodology when compared to other means of describing production and organizational processes are considered to be its convenience for specialists of various profiles, as well as the freedom from restrictions on the level of detail [3–5]. The possibility of a strict formalization of functional models, their analysis and verification are discussed in specialized literature [6, 7] and has been implemented in a set of commercial software products designed to create functional models[1,2] [8]. However, the objective of developing rules and algorithms for checking functional models has not yet been achieved.

Generalized algorithm for functional model verification

According to [9], a functional model is a set of diagrams connected by a decompose relation. The model structure can be represented as a tree. Each branch of this tree presets a pair comprised of a parent and child diagram, the latter detailing one of the parent diagram's functional blocks.

Each arrow associated with the detailed functional block must have a corresponding boundary arrow in the child diagram. Its role is uniquely determined by the role of the corresponding arrow in the parent diagram. In order to check the correctness of the functional model, all the relationships between the parent and child diagrams must be analyzed, and the presence and roles of arrows must be confirmed. A generalized algorithm for functional model verification is shown in Fig. 1.

This algorithm demonstrates a sequential search for diagrams connected by a decompose relation, the choice of arrows that must be displayed in child diagrams and the verification of their roles. (This verification will be discussed below in more detail).

In order to formalize this algorithm, it is necessary to switch from the visual representation of functional models in the form of graphical diagrams to their mathematical descriptions.

The formalization of rules for the verification of functional models based on their set-theoretic representations

In [10] a set-theoretic representation of functional models as a set of special oriented graphs related by levels of detail is proposed in this study. Such a representation allows for the possibility of using the mathematical apparatus accumulated within the framework of graph theory [11] for verifying and analyzing functional diagrams.

A separate functional diagram is not a graph as a diagram can contain boundary and branching arrows, while the edges of a graph connect precisely two of its nodes. It is essential that the semantics of the actions described by a functional diagram is preset not only by

[1]Internet source: https://www.ca.com/us.html
[2]Internet source: https://www.edrawsoft.com/IDEF0-flowcharts.php

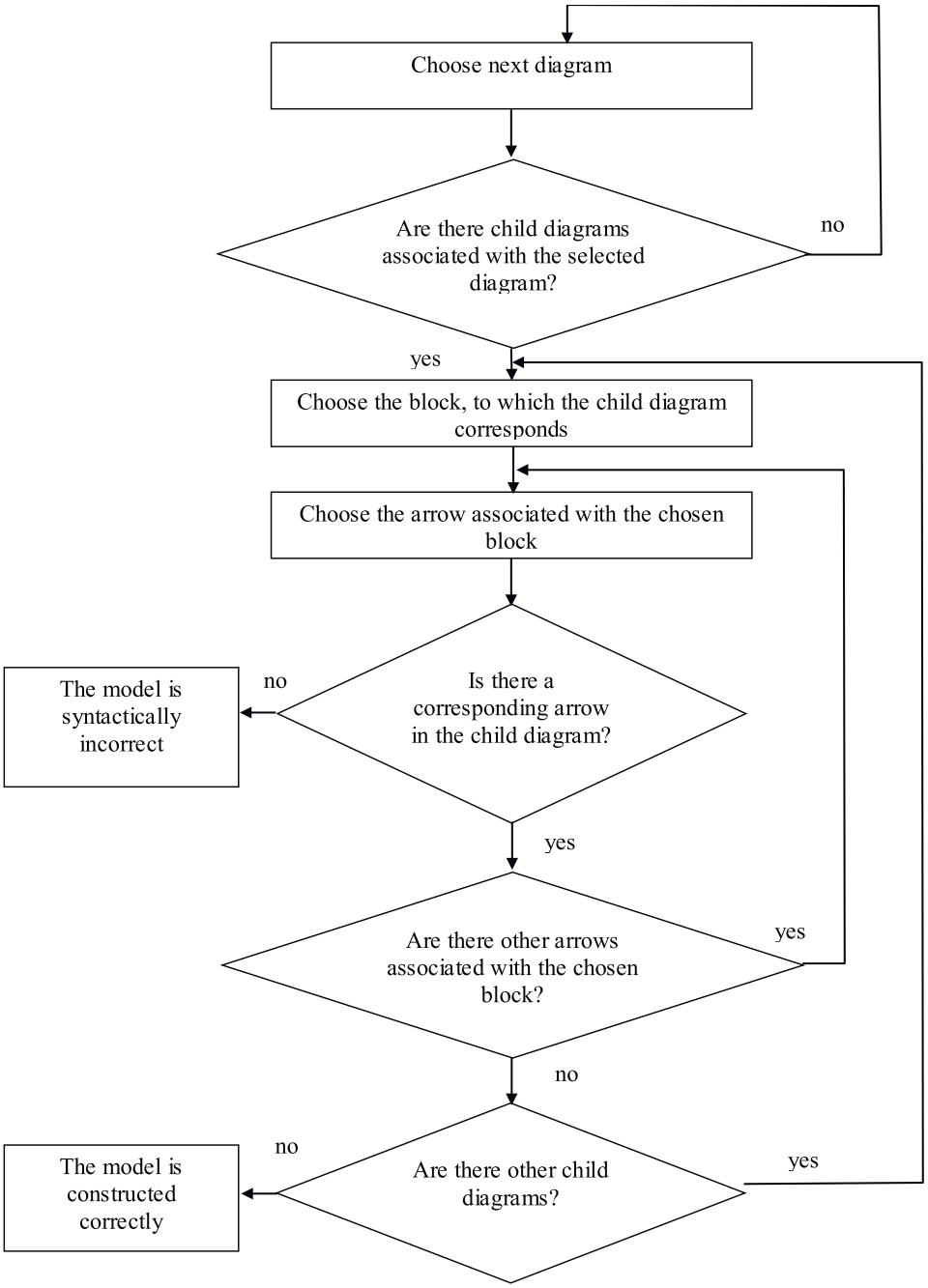

Fig. 1. Algorithm for functional model verification.

the edge name, but also by its position relative to the functional block. A detailed description of a diagram conversion into a graph is given in [10]. Below is a brief list of its main features:

- The diagram is represented as a graph with labeled edges G = (N, L), where N is the set of nodes and L is the set of edges.
- The graph nodes preset functional blocks, diagram boundaries, and the branch points of the arrows.
- Each edge of the graph has a label, which is not necessarily unique.
- When specifying the edges of a graph, both the names of the nodes and their roles must be indicated. Each edge of the graph is described as follows:

edge name (initial_node_role:
initial_node_Name,
end_node_role:
end_node_Name)

In order to formalize the rules of model verification we introduce the following notations:

DP = (NP, LP) is a graph describing the parent diagram;

NP is the set of the DP graph nodes;

LP is the set of the DP graph edges;

(DP, DC, nb) is an element of the decompose relation that describes the decomposition of the nb block of the parent diagram, nb ∈ NP;

DC = (NC, LC) is a graph describing the child diagram;

NC is the set of the DC graph nodes;

LC is the set of the DC graph edges;

np ∈ NP is an element of the NP set, np ≠ nb;

nc ∈ NC is an element of the NC set.

Let us consider the rules, which connect the elements of the LP and LC sets (the edges of graphs describing the parent and child diagrams):

1) Each arrow of the parent diagram, which points to the nb block on the left, has at least one corresponding arrow in the child diagram. The latter arrow has the same label; it goes from the left border of the diagram and points to a block of the child diagram on the left:

if lp(O:np, I:nb) ∈ LP, then lp(O:L, I:nc) ∈ LC

2) Each arrow of the parent diagram, which emerges from the nb block, has at least one corresponding arrow in the child diagram. The latter arrow has the same label; it points to the right border of the diagram from a block of the child diagram:

if lp(O:nb, I:np) ∈ LP, then lp(O:nc, I:R) ∈ LC

3) Each arrow of the parent diagram, which points to the nb block above, has at least one corresponding arrow in the child diagram. The latter arrow has the same label; it goes from the top border of the diagram and points to a block of the child diagram above:

if lp(O:np, C:nb) ∈ LP, then lp(O:U, C:nc) ∈ LC

4) Each arrow of the parent diagram, which points to the nb block below, has at least one corresponding arrow in the child diagram. The latter arrow has the same label; it goes from the bottom border of the diagram and points to some block of the child diagram below:

if lp(O:np, M:nb) ∈ LP, then lp(O:D, M:nc) ∈ LC

The np and nc nodes can describe both blocks of the corresponding functional diagrams and their boundaries or branch points. Note also that one arrow of the parent diagram may correspond to several arrows of the child diagram in cases when the arrow in the child diagram branches without changing its label.

Programming languages, which contain convenient means for describing and analyzing relationships, as well as pattern matching tools, are suitable for the implementation of the functional model verification algorithm. The most convenient logic programming language for this task is PROLOG, which supports predicate notation for storing relations and provides sophisticated means for describing logical rules with related variables [12]. A knowledge base is necessary in order to store a functional model in the PROLOG language. It includes 3 predicates: descriptions of the decompose relation (decompose), of the nodes set (node), and of the edges set (edge). The rules for model verification are a conjunction of these predicates, and constraints are described using role specifying and variable binding. Thus, the first rule describing the correlation between arrows with the "input" role can be verified using the following query:

```
?-decompose(DP,DC,NB),
  edge(LP,o,NP,i,NB),
  edge(LP,o,l,i,NC),
  node(NC,DC).
```

In this query, according to PROLOG rules, the capitalized variables signify:

DP is the parent diagram name;

DC is the child diagram name;

NB is the name of the detailed function block;

LP is the label of the parent diagram edge;

NP is the name of the initial node of the LP edge in the parent diagram;

NC is the name of the final node of the LP edge in the child diagram.

The lowercase letters o and i define the roles of the nodes. The lowercase letter l describes the node corresponding to the diagram left border.

An example of verifying the fragment of a functional model of vinyl acetate production from ethylene

Let us consider the verification of diagram construction using a functional model for vinyl acetate production from ethylene as an example. A generalized technological scheme of this production was given in [13], and its functional and set-theoretic models were built in [10]. For example, let us chose the level A4 "Condensate separation" diagram as a parent diagram (Fig. 2).

The figure shows that this diagram consists of 4 functional blocks. Each of them is decomposed into a separate child diagram. Let us consider the relationship of the "Condensate separation" diagram and the "Vinyl acetate isolation" diagram. The latter describes the preparation of the target product – vinyl acetate. This diagram level is A44, and it represents the result of the decomposition of the last, fourth functional block of the

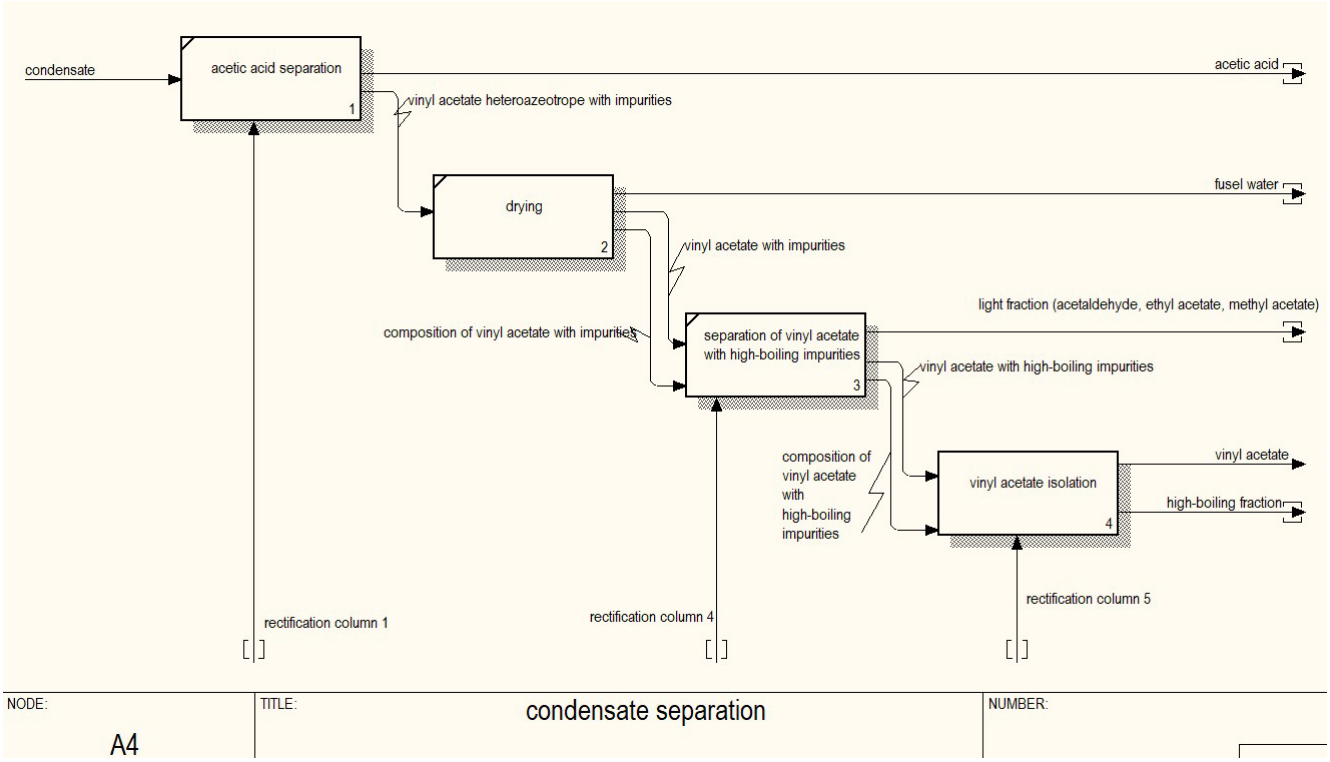

Fig. 2. Parent functional diagram "Condensate separation".

A4 = (N4; L4), where

N4 = {L, R, U, D, Acetic_acid_separation, Drying, Separation_of_vinyl_acetate_with_high-boiling_impurities, ***Vinyl_acetate isolation***}

L4 ⊃ {composition_of_vinyl_acetate_with_high-boiling_impurities
(O:Separation_of_vinyl_acetate_with_high-boiling_impurities,
I: ***Vinyl_acetate_isolation***)

vinyl_acetate_with_high-boiling_impurities
(O: Separation_of_vinyl_acetate_with_high-boiling_impurities,
I: ***Vinyl_acetate_isolation***)

rectification_column_5(*O: D, M:* ***Vinyl_acetate_isolation***)

vinyl_acetate(O: ***Vinyl_acetate_isolation***, I: R)

high-boiling_fraction(O: ***Vinyl_acetate_isolation***, I: R)}

Fig. 3. A set-theoretic representation of the functional diagram "Condensate separation" (fragment).

parent diagram. Thus, we are analyzing an element of the decompose relation

(A4, A44, Vinyl acetate isolation).

Fig. 2 demonstrates that two arrows with the "input" role and one arrow with the "mechanism" role enter the "Vinyl acetate isolation" functional block in the "Condensate separation" diagram. Two arrows with the "exit" role go out of this block. Let us consider a fragment of the set-theoretic description of the parent diagram (Fig. 3). Graph A4 consists of a set of nodes N4 (this set is shown in Fig. 3 completely) and a set of edges L4 (a subset of this set is shown, including edges associated with the "Vinyl acetate isolation" node). For clarity, the edge labels are in italics, and the decomposed node name is in bold italics.

The diagram obtained as a result of the "Vinyl acetate isolation" functional block decomposition is shown in Fig. 4. Let us analyze graph A44 that defines its set-theoretic representation (Fig. 5).

The set of nodes of this graph (N44) includes only 2 nodes corresponding to the diagram functional blocks and 4 service nodes. Since the name of one of the

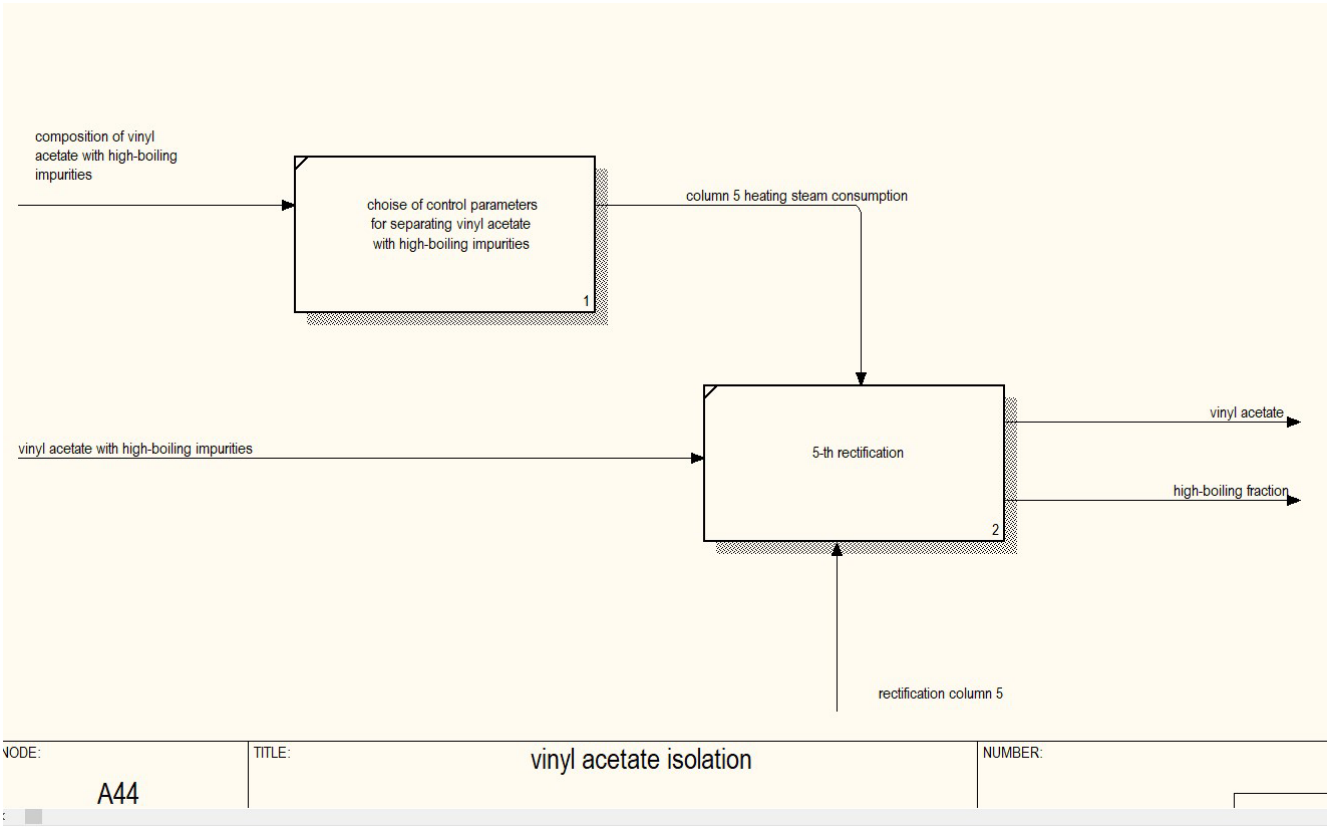

Fig. 4. Child functional diagram
"Vinyl acetate isolation"

A44={N44;L44}, where
N44 = {L, R, U, D, Choice_of_control_parameters, 5th_rectification}
L44 = {*composition_of_vinyl_acetate_with_high-boiling_impurities*
(O:L, I: Choice_of_control_parameters)
vinyl_acetate_with_high-boiling_impurities(O:L, I: 5th_rectification)
rectification_column_5(O:D,M: 5th_rectification)
high-boiling fraction(O: 5th_rectification,I:R)
vinyl_acetate(O: 5th_rectification,I:R)
column_5_heating_steam_consumption
(O: Choice_control_parameters, I: 5th_rectification)}

Fig. 5. A set-theoretic representation of the functional diagram
"Vinyl acetate isolation".

blocks is very long, the name of the node describing it is abbreviated. The set of edges in graph L44 is shown in Fig. 5 completely; as before, the edge labels are in italics.

Let us compare the descriptions of the edges of the parent and child diagrams. In the parent diagram, the "vinyl_acetate_with_high-_boiling_impurities" arrow leads from block 3 to block 4. For the "vinyl acetate isolation" block, this arrow has the "input" role. In the child diagram, this arrow corresponds to the arrow leading from the left border of the diagram to the "Choice_control_parameters" block.

The set-theoretic description of these arrows should correspond to rule 1, where

nb = "Vinyl acetate isolation",

lp = "Vinyl_acetate_with_high-_boiling_impurities",

nc = "Choice_control_parameters".

The verification shows that the rule is obeyed.

Similarly, in the parent diagram, an arrow with the role "mechanism" leads from the bottom border of the

diagram to the "Vinyl acetate isolation" block. In the child diagram, this arrow corresponds to an arrow that also leads from the bottom border to the "5th rectification" function block. The set-theoretic description of these arrows should correspond to rule 4, where

nb = "Vinyl acetate isolation",

lp = "Rectification_column_5",

nc = "5th rectification"

The analysis of the remaining arrows of the parent and child diagrams shows that each edge of the parent diagram corresponds to one edge of the child diagram. The latter corresponds to either rule 1, or rule 2, or rule 4. The child diagram has a single arrow unassociated with the parent diagram: the arrow "column_5_heating_steam_consumption".

Thus, it has been shown that the decomposition of the function block "Vinyl acetate isolation" has been performed correctly.

Conclusion

The algorithm for functional model verification is based on analyzing a tree which describes the level of detail of functional diagrams. At each step of the algorithm, a pair consisting of a parent and child diagrams is selected, and the rules for arrow correlation in these diagrams are checked. To formalize these rules, a set-theoretic representation of the diagrams in the form of graphs is utilized. The rules are implemented with the use of the PROLOG logic programming language.

The authors declare no conflict of interest.

References:

1. Cheremnyh S.V., Semenov I.O., Ruchkin V.S. Modelling and system analysis. IDEF technology. Moscow: Finansy i statistika Publ., 2006. 192 p. (in Russ.).

2. Myshenkov K.S. Justification technique of a choice of CASE-tools for the analysis and design of management systems by enterprise. *Innovatsii* [Innovations]. 2013;10(180):112-122 (in Russ.).

3. Erusheva K., Kolybanov K., Tishaeva I. Functional modeling of the process of choosing the best available technique. *Tonkie Khimicheskie Tekhnologii = Fine Chemical Technologies.* 2017;12(4):98-105 (in Russ.). https://doi.org/10.32362/2410-6593-2017-12-4-98-105

4. Vichugova A.A. Methods and tools for conceptual design of information systems: comparative analysis of structural and object-oriented approaches. *Prikladnaya informatika* [Journal of Applied Informatics]. 2014;1(49):56-65 (in Russ.).

5. Burlyaeva E., Burlyaev V., Frolkova A. Functional simulation of basic organic synthesis production by vinyl acetate manufacturing. *Khimicheskaya tekhnologiya* [Journal of Chemical Technology]. 2016;9:418-423 (in Russ.).

6. Jeong K.-Y., Wu L., Hong J.-D. IDEF method-based simulation model design and development framework. *Journal of Industrial Engineering and Management.* 2009;2(2):337-359. http://dx.doi.org/10.3926/jiem.v2n2.p337-359

7. Repin V., Eliferov V. Process approach to management. Business process modeling. Moscow: Mann, Ivanov and Ferber Publ., 2013. 544 p. (in Russ.).

8. Maklakov S.V. Business process modeling with All Fusion Process Modeler (BPwin 4.1). Moscow: Dialog-MIFI Publ., 2002. 240 p. (in Russ.).

9. Recommendations for standardization. Information technology support the life cycle of product. Methodology of functional modeling. Moscow: Gosstandart Publ., 2001. 19 p. (in Russ.).

10. Burlyaeva E.V., Burlyaev V.V., Tsekhanovich V.S. Set-theoretic description of functional models of chemical manufacturing. *Tonkie Khimicheskie Tekhnologii = Fine Chemical Technologies.* 2017;12(5):71-78 (in Russ.). https://doi.org/10.32362/2410-6593-2017-12-5-71-78

Список литературы:

1. Черемных С.В., Семенов И.О., Ручкин В.С. Моделирование и анализ систем. IDEF-технологии. М.: Финансы и статистика, 2006. 192 с.

2. Мышенков К.С. Методика обоснования выбора CASE-средств для анализа и проектирования систем управления предприятиями // Инновации. 2013. № 10(180). С. 112–122.

3. Ерушева К.И., Колыбанов К.Ю., Тишаева И.Р. Функциональное моделирование процесса выбора наилучшей доступной технологии // Тонкие химические технологии. 2017. Т. 12. № 4. С. 98–105. https://doi.org/10.32362/2410-6593-2017-12-4-98-105

4. Вичугова А.А. Методы и средства концептуального проектирования информационных систем: сравнительный анализ структурного и объектно-ориентированного подходов // Прикладная информатика. 2014. № 1(49). С. 56–65.

5. Бурляева Е.В., Бурляев В.В., Фролкова А.К. Функциональное моделирование производств основного органического синтеза на примере получения винилацетата // Химическая технология. 2016. № 9. С. 418–423.

6. Jeong K.-Y., Wu L., Hong J.-D. IDEF method-based simulation model design and development framework // J. Ind. Eng. & Manag. 2009. V. 2. № 2. P. 337–359. http://dx.doi.org/10.3926/jiem.v2n2.p337-359

7. Репин В.В., Елиферов В.Г. Процессный подход к управлению. Моделирование бизнес-процессов. М.: Манн, Иванов и Фербер, 2013. 544 с.

8. Маклаков С.В. Моделирование бизнес-процессов с AllFusion Process Modeler (BPwin 4.1). М.: Диалог-МИФИ, 2002. 240 с.

9. Рекомендации по стандартизации. Информационные технологии поддержки жизненного цикла продукции. Методология функционального моделирования. М.: Госстандарт России, 2001. 19 с.

10. Бурляева Е.В., Бурляев В.В., Цеханович В.С. Теоретико-множественное представление функциональных моделей химических производств // Тонкие химические технологии. 2017. Т. 12. № 5. С. 71–78. https://doi.org/10.32362/2410-6593-2017-12-5-71-78

11. Алексеев В.Е., Таланов В.А. Графы и алгоритмы. Структуры данных. Модели вычислений. М.: Интуит, Би-

11. Alekseev V., Talanov V. Graphs and algorithms. Data structures. Calculation models. Moscow: Intuit, Binom Publ., 2012. 320 p. (in Russ.).

12. Markov V.N. Modern logical programming in Visual Prolog 7.5. Saint Petersburg: BHV-Peterburg Publ., 2016. 544 p. (in Russ.).

13. Timofeev V.S., Serafimov L.A., Timoshenko A.V. Principles of technology of basic organic and petrochemical synthesis. Moscow: Vysshaya shkola Publ., 2010. 408 p. (in Russ.).

ном, 2012. 320 с.

12. Марков В.Н. Современное логическое программирование на языке Visual Prolog 7.5. СПб.: БХВ-Петербург, 2016. 544 с.

13. Тимофеев В.С., Серафимов Л.А., Тимошенко А.В. Принципы технологии основного органического и нефтехимического синтеза. М.: Высшая школа, 2010. 408 с.

About the authors:

Elena V. Burlyaeva, Dr. of Sci. (Engineering), Professor of the Chair of Information Systems in Chemical Technology, M.V. Lomonosov Institute of Fine Chemical Technologies, MIREA – Russian Technological University (86, Vernadskogo pr., Moscow 119571, Russia). http://orcid.org/0000-0003-1371-1410, Scopus Author ID 36964878300

Valery V. Burlyaev, Cand. of Sci. (Engineering), Professor of the Chair of Information Systems in Chemical Technology, M.V. Lomonosov Institute of Fine Chemical Technologies, MIREA – Russian Technological University (86, Vernadskogo pr., Moscow 119571, Russia). Scopus Author ID 6508353813

Violetta V. Kononenko, Postgraduate Student of the Chair of Information Systems in Chemical Technology, M.V. Lomonosov Institute of Fine Chemical Technologies, MIREA – Russian Technological University (86, Vernadskogo pr., Moscow 119571, Russia).

Viktor S. Tsekhanovich, Postgraduate Student of the Chair of Information Systems in Chemical Technology, M.V. Lomonosov Institute of Fine Chemical Technologies, MIREA – Russian Technological University (86, Vernadskogo pr., Moscow 119571, Russia).

Об авторах:

Бурляева Елена Валерьевна, доктор технических наук, профессор кафедры информационных систем в химической технологии Института тонких химических технологий им. М.В. Ломоносова ФГБОУ ВО «МИРЭА – Российский технологический университет» (Россия, 119571, Москва, пр. Вернадского, д. 86). http://orcid.org/0000-0003-1371-1410, Scopus Author ID 36964878300

Бурляев Валерий Викторович, кандидат технических наук, профессор кафедры информационных систем в химической технологии Института тонких химических технологий им. М.В. Ломоносова ФГБОУ ВО «МИРЭА – Российский технологический университет» (Россия, 119571, Москва, пр. Вернадского, д. 86). Scopus Author ID 6508353813

Кононенко Виолетта Витальевна, аспирант кафедры информационных систем в химической технологии Института тонких химических технологий им. М.В. Ломоносова ФГБОУ ВО «МИРЭА – Российский технологический университет (Россия, 119571, Москва, пр. Вернадского, д. 86).

Цеханович Виктор Сергеевич, аспирант кафедры информационных систем в химической технологии Института тонких химических технологий им. М.В. Ломоносова ФГБОУ ВО «МИРЭА – Российский технологический университет (Россия, 119571, Москва, пр. Вернадского, д. 86).

For citation: Burlyaeva E.V., Burlyaev V.V., Kononenko V.V., Tsekhanovich V.S. Verification of functional models of chemical manufacturing. *Tonkie Khimicheskie Tekhnologii = Fine Chemical Technologies.* 2019;14(4):69-76 (in Russ.). https://doi.org10.32362/2410-6593-2019-14-4-69-76

Для цитирования: Бурляева Е.В., Бурляев В.В., Кононенко В.В., Цеханович В.С. Верификация функциональных моделей химических производств // Тонкие химические технологии. 2019. Т. 14. № 4. С. 69–76. https://doi.org10.32362/2410-6593-2019-14-4-69-76

Translated by M. Povorin

Fine Chemical Technologies, 2019, Vol. 14, No. 4, pp. 77–86.
Original Russian Text © Eduard M. Kartashov published in Tonkie Khimicheskie Tekhnologii, 2019, Vol. 14, No. 4, pp. 77–86

MATHEMATICS METHODS AND INFORMATION SYSTEMS IN CHEMICAL TECHNOLOGY
МАТЕМАТИЧЕСКИЕ МЕТОДЫ И ИНФОРМАЦИОННЫЕ СИСТЕМЫ В ХИМИЧЕСКОЙ ТЕХНОЛОГИИ

https://doi.org/10.32362/2410-6593-2019-14-4-77-86

CC BY

UDC 539.3

Originals of operating images for generalized problems of unsteady heat conductivity

Eduard M. Kartashov

MIREA – Russian Technological University (M.V. Lomonosov Institute of Fine Chemical Technologies), Moscow 119571, Russia
@ Corresponding author, e-mail: kartashov@mitht.ru

A series of operating (Laplace) non-standard images, the originals of which are absent in well-known reference books on operational calculus, are considered. By reducing one of the basic images to the Riemann-Mellin contour integral for the modified Bessel functions and analyzing the corresponding inversion formula using the approaches of the complex variable function theory, an analytical form of the original original is found, which is abrupt in nature with a break point. It is shown that analytical solutions of the corresponding mathematical models using the found originals have a wave character, which is expressed by the presence of the Heaviside step function in the solutions. The latter means that at any time there is a region of physical disturbance to the point of discontinuity and an unperturbed area after the point of discontinuity. The images studied are included in the operational solutions of mathematical models in many areas of applied mathematics. physics, thermomechanics, thermal physics, in particular in the theory of thermal shock of viscoelastic bodies, in the study of the thermal reaction of solids based on the classical Maxwell-Cattaneo-Lykov-Vernott phenomenology, taking into account the final rate of heat propagation. These models are needed to study the thermal reaction of relatively new consolidated structurally sensitive polymeric materials in structures exposed to high-intensity external influences. The analytical relations obtained for the originals and the original improper integrals resulting from them, containing combinations of Bessel functions, can be used in the general methodology of constructing and applying various mathematical models in a wide range of external influences on materials in many fields of science and technology.

Keywords: *originals of operational images, hyperbolic models of unsteady heat conduction, thermal shock.*

Оригиналы операционных изображений для обобщенных задач нестационарной теплопроводности

Э.М. Карташов

МИРЭА – Российский технологический университет (Институт тонких химических технологий имени М.В. Ломоносова), Москва 119571, Россия
@ Автор для переписки, e-mail: kartashov@mitht.ru

Рассмотрена серия операционных (по Лапласу) нестандартных изображений, оригиналы которых отсутствуют в известных справочниках по операционному исчислению. Путем сведения одного из базовых изображений к контурному интегралу Римана-Меллина для модифицированных функций Бесселя и анализа соответствующей формулы обращения с

использованием подходов теории функций комплексного переменного установлен аналитический вид искомого оригинала, имеющего скачкообразный характер с точкой разрыва. Показано, что аналитические решения соответствующих математических моделей с использованием найденных оригиналов имеют волновой характер, что выражается наличием в решениях ступенчатой функции Хевисайда. Последнее означает, что в любой момент времени существует область физического возмущения до точки разрыва и невозмущенная область после точки разрыва. Изученные изображения входят в операционные решения математических моделей во многих областях прикладной математики, физики, термомеханики, теплофизики, в частности в теории теплового удара вязкоупругих тел, при изучении тепловой реакции твердых тел на основе классической феноменологии Максвелла-Каттанео-Лыкова-Вернотта с учетом конечной скорости распространения теплоты. Указанные модели необходимы для изучения термической реакции сравнительно новых консолидированных структурно-чувствительных полимерных материалов в конструкциях, подверженных высокоинтенсивным внешним воздействиям. Полученные для оригиналов аналитические соотношения и вытекающие из них оригинальные несобственные интегралы, содержащие комбинации функций Бесселя, могут быть использованы в общей методологии построения и применения разнообразных математических моделей в широком диапазоне внешних воздействий на материалы во многих областях науки и техники.

Ключевые слова: *оригиналы операционных изображений, гиперболические модели нестационарной теплопроводности, тепловой удар.*

Introduction

Modern structural materials, which are a combination of micro- or nanostructured elements, are often called structurally sensitive materials. The creation of such materials based on nanotechnology is an important direction in the development of modern materials science. Such materials have unique physico-mechanical properties that allow them to be used effectively in structures subject to high-intensity external influences [1, 2]. An important step in the creation and use of these kinds of materials is the construction of appropriate mathematical models to describe their behavior in a wide range of changes in external loads. The general methodology for constructing and studying such models is still far from complete and requires further development. This applies primarily to the mathematical models of a number of physical processes while taking into account spatio-temporal nonlocality.

Classical phenomenological models of transport processes and other phenomena, such as Fourier heat, Nernst mass, Ohm electricity, Newton and Hook voltages, are based on the principle of local thermodynamic equilibrium and the continuous medium hypothesis. The differential equations derived from them for the corresponding physical quantities are local, that is, they do not take into account local non-equilibrium processes; in the process of derivation, an infinite propagation velocity of disturbances is incorporated into them. Moreover, the functions describing these processes are smooth functions of coordinates and time. However, the propagation velocity of the potentials of any physical fields cannot take infinite values. In a real body, the process of their change occurs with a certain delay in time according to the relaxation properties of the material, which are taken into account by relaxation coefficients. Such processes exist in reality. They have so-called front surfaces, passing through which makes the temperature function and its derivatives acquire a discontinuity [3, 4]. These functions are described by hyperbolic differential operators. They include high-intensity non-stationary processes, the flow time of which is comparable to the relaxation time. Examples include heating materials with short laser pulses (duration varies from nano- to femtoseconds); heating processes with friction at a high speed; during a thermal shock; local heating during dynamic propagation of a crack in a transonic mode, etc.

Taking into account the local non-equilibrium embedded in the Maxwell-Cattaneo-Lykov-Vernotte relation for the heat flux (in the one-dimensional case)

$$q(x,t) = -\lambda \frac{\partial T(x,t)}{\partial x} - \tau_r \frac{\partial q(x,t)}{\partial t} \quad (1)$$

together with the energy equation $c\rho\partial T / \partial t = -\partial q / \partial x$ lead to the heat hyperbolic type equation [5]

$$\frac{\partial T(x,t)}{\partial t} = a \frac{\partial^2 T(x,t)}{\partial x^2} - \tau_r \frac{\partial^2 T(x,t)}{\partial t^2} \quad (2)$$

and the corresponding boundary value problems of a generalized type [6]. In this case, τ_r signifies the thermal relaxation time (a measure of the inertia of the heat flux) associated with the rate of heat propagation v_T by the relation $\tau_r = a / v_T^2$ (a – thermal diffusivity). When $v_T \to \infty$, the magnitude $\tau_r \to 0$ and relations (1)–(2) respectively lead to the classical phenomenological law of Fourier heat transfer and the parabolic-type heat equation, which underlies an almost unlimited number of studies on non-stationary heat transfer. The generalized transport problems for equation (2) differ significantly from the classical ones, with it being more difficult to find their analytical solutions. The specificity of such problems lies in the relative simplicity of the original mathematical models and the difficulties of solving them in an analytically closed form. This results in very little success in finding their exact analytical solutions. The main method for solving boundary-value problems of a generalized type for partially bounded domains is the operational one, which leads to complex functional constructions of the Karslow-Jäger type [7] in analytic solutions in the Laplace image space $\overline{T}(x,p) = \int_0^\infty \exp(-pt) T(x,t) dt$. The originals of the aforementioned Karslow-Jäger type constructions do not appear in well-known reference books on operational calculus. Serious computational difficulties arise along this path. The aim of this publication is to consider a series of non-standard images and their originals. In addition to the generalized problems of non-stationary transfer (heat and mass), such images also arise in the description of electric transmission lines, in the study of transient modes of electrical circuits (the propagation of electrical disturbances along the transmission line); in the thermal shock theory of viscoelastic bodies, etc. Let us dwell on the generalized problem for equation (2) in the region $x > 0$, $t > 0$ under the initial condition

$$T(x,t)\big|_{t=0} = T_0, x \geq 0 \tag{3}$$

and boundary conditions of either the first kind (temperature heating or cooling)

$$T(x,t)\big|_{x=0} = T_c, t > 0, \tag{4}$$

or the second kind (thermal heating or cooling)

$$\frac{1}{\tau_r}\int_0^t \frac{\partial T(x,\tau)}{\partial x}\Big|_{x=0} \exp(-\frac{t-\tau}{\tau_r}) d\tau = -\frac{1}{\lambda} q_0, t > 0, \tag{5}$$

or of the third kind (heating or cooling by the environment)

$$\frac{1}{\tau_r}\int_0^t \frac{\partial T(x,t)}{\partial x}\Big|_{x=0} \exp\left(-\frac{t-\tau}{\tau_r}\right) d\tau = \\ = h\left[T(x,t)\big|_{x=0} - T_c\right], t > 0, \tag{6}$$

as well as the constraint condition (in all three cases)

$$\left|T(x,t)\right| < \infty, x \geq 0, t \geq 0. \tag{7}$$

It should be noted that questions of the correct formulation of the boundary conditions for the hyperbolic type equation (2) were considered by the author in [7].

Let consider the next theory: the originals for non-standard images.

Inversion theorems for images

Consider a series of images of the form

$$\overline{f}(p) \exp\left[-x\sqrt{(p+2\alpha)(p+2\beta)}\right],$$

or

$$\begin{cases} \overline{f}(p) \exp\left[-x\overline{\mu}(p)\right] \\ \overline{\mu}(p) = \sqrt{(p+2\alpha)(p+2\beta)}, \end{cases} \tag{8}$$

where $\overline{f}(p)$ – are various combinations of rational and irrational functions of the argument p.

Initially we examine Riemann-Mellin type integral

$$Y_1(x,t) = \frac{1}{2\pi i}\int_{\gamma-i\infty}^{\gamma+i\infty} \frac{1}{\overline{\mu}(p)} \exp\left[pt - x\overline{\mu}(p)\right] dp. \tag{9}$$

The use of the representation of the Bessel function of an imaginary argument $I_n(z)$ in the form of the integral [8]

$$\left(\frac{2}{z}\right)^n I_n(z) = \frac{1}{2\pi i}\int_{\gamma-i\infty}^{\gamma+i\infty} \frac{1}{u^{n+1}} \exp(u + \frac{z^2}{4u}) du \tag{10}$$

and give (9) to a form similar to equation (10). For this, suppose [7]:

$$(p+2\alpha)^{1/2} + (p+2\beta)^{1/2} = \xi^{1/2} \\ (p+2\alpha)^{1/2} - (p+2\beta)^{1/2} = 2\sigma\xi^{-1/2}, \tag{11}$$

the equation leads to

$$p=\frac{1}{4}(\xi+\frac{4\sigma^2}{\xi}-4\rho),\sqrt{(p+2\alpha)(p+2\beta)}=$$
$$=\frac{1}{4}(\xi-\frac{4\sigma^2}{\xi}), \qquad (12)$$

$$\frac{d\xi}{\xi}=\frac{dp}{\sqrt{(p+2\alpha)(p+2\beta)}}. \qquad (13)$$

Here, $\rho=\alpha+\beta, \sigma=\alpha-\beta$. Following this, the integral (9) is transformed by replacing the variable (13). In this case, the straight line ($\gamma-i\infty,\gamma+i\infty$) in the plane p is transformed into a line in the plane ξ. This line is not straight, but by Cauchy's theorem it can be deformed into a line, which is described as ($\gamma'-i\infty,\gamma'+i\infty$). Now, the integral (9) takes the form of

$$Y_1(x,t)=$$
$$=\frac{1}{2\pi i}\int_{\gamma'-i\infty}^{\gamma'+i\infty}\frac{d\xi}{\xi}\exp\left[-\rho t+\frac{1}{4}\xi(t-x)+\frac{\sigma^2}{\xi}(t+x)\right] \qquad (14)$$

If t > x, then, assuming in (14) $(\xi/4)(t-x)=u$ and n = 0 from equation (10) we can derive:

$$Y_1(x,t)=\exp(-\rho t)I_0(\sigma\sqrt{t^2-x^2}),t>x. \qquad (15)$$

If $t < x$, consider the integral (14), taken along a closed contour shown in Figure, which consists of a part of the contour $(\gamma'-i\infty,\gamma'+i\infty)$ and the arc of the circle with the radius R and a center at the start of the coordinates. The integrand function in (14) is regular inside the contour and on the boundary, and it does not contain any poles inside the contour. Afterwards, using the Cauchy theorem, the integral along this contour is equal to zero. It can be demonstrated that for $R \to \infty$ the integral along the arc of the circle turns into zero. Thus, this leads to the following result

$$Y_1(x,t)=0 \text{ for } t<x. \qquad (16)$$

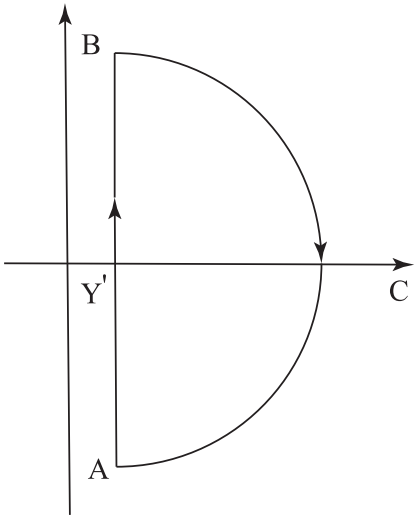

The contour for calculating the integral (14).

Finally, it is possible to derive

$$\frac{1}{\overline{\mu}(p)}\exp\left[-x\overline{\mu}(p)\right]\overleftarrow{*}\exp(-\rho t)I_0(\sigma\sqrt{t^2-x^2})\eta(t-x), \qquad (17)$$

where $\eta(t)$ is the Heaviside function. Further applying the convolution theorem, one can find:

$$\frac{1}{\overline{\mu}(p)}\exp\left[-x\overline{\mu}(p)\right]\overline{f}(p)\overleftarrow{*}\int_0^t f(t-\tau)\exp(-\rho\tau)I_0(\sigma\sqrt{\tau^2-x^2})\eta(\tau-x)d\tau=$$
$$=\int_x^t f(t-\tau)\exp(-\rho\tau)I_0(\sigma\sqrt{\tau^2-x^2})d\tau,t>x, \qquad (18)$$
$$0, \quad t<x, \quad =$$
$$=\left[\int_x^t f(t-\tau)\exp(-\rho\tau)I_0(\sigma\sqrt{\tau^2-x^2})d\tau\right]\eta(t-x).$$

Differentiating (18) with respect to x leads to:

$$\exp\left[-x\overline{\mu}(p)\right]\overline{f}(p)\xleftarrow[*]{*}\begin{cases} f(t-x)\exp(-\rho x)+\sigma x\int_x^t f(t-\tau)\exp(-\rho\tau)\dfrac{I_1(\sigma\sqrt{\tau^2-x^2})}{\sqrt{\tau^2-x^2}}d\tau, t>x. \\ 0, \qquad\qquad t<x. \end{cases} \tag{19}$$

Assuming in (19) that $\overline{f}(p)=1$, then $f(t)=\delta(t)$ is the Dirac function. Thus, from (19) we acquire:

$$\exp\left[-x\overline{\mu}(p)\right]\xleftarrow[*]{*}\begin{cases} \exp(-\rho x)\delta(t-x)+\sigma x\exp(-\rho x)\dfrac{I_1(\sigma\sqrt{t^2-x^2})}{\sqrt{t^2-x^2}}, t>x, \\ 0, \qquad\qquad t<x. \end{cases} \tag{20}$$

Suppose now that in (19) $\overline{f}(p)=\dfrac{1}{p}, f(t)=1$. We can derive the following:

$$\frac{1}{p}\exp\left[-x\overline{\mu}(p)\right]\xleftarrow[*]{*}\begin{cases} \exp(-\rho x)+\sigma x\int_x^t \exp(-\rho\tau)\dfrac{I_1(\sigma\sqrt{\tau^2-x^2})}{\sqrt{\tau^2-x^2}}d\tau, t>x, \\ 0, \qquad\qquad t<x. \end{cases} \tag{21}$$

Assuming $\overline{f}(p)=\dfrac{1}{p}, f(t)=1,$ in (18) then

$$\frac{1}{p\overline{\mu}(p)}\exp\left[-x\overline{\mu}(p)\right]\xleftarrow[*]{*}\begin{cases} \int_x^t \exp(-\rho\tau)I_0(\sigma\sqrt{\tau^2-x^2})d\tau, t>x, \\ 0, \qquad\qquad t<x. \end{cases} \tag{22}$$

Based on that, we can find the original of the following image:

$$\sqrt{\frac{p+2\beta}{p+2\alpha}}\exp\left[-x\overline{\mu}(p)\right]\overline{f}(p)=\frac{p+2\beta}{\overline{\mu}(p)}\exp\left[-x\overline{\mu}(p)\right]\overline{f}(p)=\left\{p\left[\frac{1}{\overline{\mu}(p)}\exp(-x\overline{\mu}(p))\right]\right\}\overline{f}(p)+$$

$$+2\beta\left\{\frac{1}{\overline{\mu}(p)}\exp\left[-x\overline{\mu}(p)\right]\right\}\overline{f}(p)\xleftarrow[*]{*}\int_0^t f(t-\tau)\frac{d}{d\tau}\left[\exp(-\rho\tau)I_0(\sigma\sqrt{\tau^2-x^2})\right]\eta(\tau-x)d\tau+$$

$$+\int_0^t f(t-\tau)\exp(-\rho\tau)I_0(\sigma\sqrt{\tau^2-x^2})\delta(\tau-x)d\tau+2\beta\int_x^t f(t-\tau)\exp(-\rho\tau)I_0(\sigma\sqrt{\tau^2-x^2})d\tau=$$

$$=f(t-x)\exp(-\rho x)-(2\beta-\rho)\int_x^t f(t-\tau)\exp(-\rho\tau)I_0(\sigma\sqrt{\tau^2-x^2})d\tau+$$

$$+\int_x^t f(t-\tau)\exp(-\rho\tau)\left[\frac{\sigma\tau I_1(\sigma\sqrt{\tau^2-x^2})}{\sqrt{\tau^2-x^2}}\right]d\tau=f(t-x)\exp(-\rho x)+$$

$$+\int_x^t f(t-\tau)\exp(-\rho\tau)\left[\frac{\sigma\tau I_1(\sigma\sqrt{\tau^2-x^2})}{\sqrt{\tau^2-x^2}}-\sigma I_0(\sigma\sqrt{\tau^2-x^2})\right]d\tau.$$

Thus:

$$\sqrt{\frac{p+2\beta}{p+2\alpha}}\exp\left[-x\overline{\mu}(p)\right]\overline{f}(p)\xleftarrow[*]{*}f(t-x)\exp(-\rho x)+$$

$$+\int_x^t f(t-\tau)\exp(-\rho\tau)\left[\frac{\sigma\tau I_1(\sigma\sqrt{\tau^2-x^2})}{\sqrt{\tau^2-x^2}}-\sigma I_0(\sigma\sqrt{\tau^2-x^2})\right],t>x. \qquad (23)$$

Assuming in (23) $\overline{f}(p)=\frac{1}{p}$, $f(t)=1$, we obtain

$$\frac{1}{p}\sqrt{\frac{p+2\beta}{p+2\alpha}}\exp\left[-x\overline{\mu}(p)\right]\xleftarrow[*]{*}\exp(-\rho x)+\int_x^t\exp(-\rho\tau)\left[\frac{\sigma\tau I_1(\sigma\sqrt{\tau^2-x^2})}{\sqrt{\tau^2-x^2}}-\sigma I_0(\sigma\sqrt{\tau^2-x^2})\right]d\tau,t>x. \qquad (24)$$

The discovered originals lead to a number of interesting relations for improper integrals containing Bessel functions. Using the inversion theorem for the Laplace transformation, we can transform (17) into:

$$\frac{1}{\overline{\mu}(p)}\exp\left[-x\overline{\mu}(p)\right]=\int_0^\infty\exp(-\rho t-pt)I_0(\sigma\sqrt{t^2-x^2})\eta(t-x)dt=\int_x^\infty\exp\left[-t(p+\rho)\right]I_0(\sigma\sqrt{t^2-x^2})dt\ . \qquad (25)$$

Differentiating both sides of equation (25) with respect to *x*:

$$\exp\left[-x\overline{\mu}(p)\right]=\exp\left[-(\rho+p)x\right]+\sigma x\int_x^\infty\exp\left[-t(\rho+p)\right]\frac{I_1(\sigma\sqrt{t^2-x^2})}{\sqrt{t^2-x^2}}dt. \qquad (26)$$

This operation is justified by the uniform convergence of the integral (26). In addition, both sides of the equation (26) are continuous functions with respect to p, therefore, assuming $p \to 0$ we have:

$$\int_x^\infty \exp(-\rho t)\frac{I_1(\sigma\sqrt{t^2-x^2})}{\sqrt{t^2-x^2}}dt = (1/(\sigma x))\left[\exp(-2x\sqrt{\alpha\beta}) - \exp(-\rho x)\right]. \tag{27}$$

Assuming (25) $p \to 0$, we obtain:

$$\int_x^\infty \exp(-\rho t) I_0(\sigma\sqrt{t^2-x^2})dt = \frac{1}{2\sqrt{\alpha\beta}}\exp(-2x\sqrt{\alpha\beta}). \tag{28}$$

The next class of images, which is of interest for the thermal shock theory of viscoelastic bodies [2], take the form of:

$$\overline{Q}(x,p) = \frac{1}{p}\exp\left[-xp\sqrt{\frac{p+(\beta_1+\beta_2)}{p+\beta_2}}\right], \tag{29}$$

where $\beta_1 > 0, \beta_2 > 0.$ To clarify the possible form of the original (29), we first study the integral

$$\frac{1}{2\pi i}\int_{\gamma-i\infty}^{\gamma+i\infty}\frac{1}{\sqrt{(p+2\alpha)(p+2\beta)}}\exp\left\{\left[-\frac{p}{p+2\beta}x\sqrt{(p+2\alpha)(p+2\beta)}\right]+pt\right\}dp,$$ using the methodology

expressed in (11)–(16) for these purposes. We establish that the original $Q(x, t)$ has the following form:

$$Q(x,t) = F(x,t)\eta(t-x), \tag{30}$$

where $$F(x,t) = \frac{1}{2\pi i}\int_{\gamma-i\infty}^{\gamma+i\infty}\frac{1}{p}\exp\left[-xp\sqrt{\frac{p+(\beta_1+\beta_2)}{p+\beta_2}}+pt\right]dp. \tag{31}$$

The contour integral in (31) has two branch points and is calculated in accordance with the well-known rules of operational calculus [1]. We find that the final result is

$$\frac{1}{p}\exp\left[-xp\sqrt{\frac{p+(\beta_1+\beta_2)}{p+\beta_2}}\right] \xleftarrow{*}{*}$$
$$\xleftarrow{*}{*}\left\{1-\frac{1}{\pi}\int_0^{\beta_1}\frac{1}{y+\beta_2}\exp\left[-(y+\beta_2)t\right]\sin\left[x(y+\beta_2)\sqrt{\frac{\beta_1-y}{y}}\right]dy\right\}\eta(t-x). \tag{32}$$

As follows from (32), the original $Q(x, t)$ allows for a jump when passing through the value $t = x$. The magnitude of this jump is

$$|\Delta| = \lim_{t\to x+0} F(x,t)\eta(t-x) = \lim_{z\to 0} F(x,x+z)\eta(z) = F(x,x) =$$
$$= 1-\frac{1}{\pi}\int_0^{\beta_1}\frac{1}{y+\beta_2}\exp\left[-(y+\beta_2)x\right]\sin\left[x(y+\beta_2)\sqrt{\frac{\beta_1-y}{y}}\right]dy. \quad (33)$$

When calculating the same value $|\Delta|$, using the operational approach, we can see that the ratio for the function (30) is as follows:

$$\lim_{p\to\infty}\left[p\overline{Q}(x,p)\exp(px)\right] = F(x,x). \quad (34)$$

Then, in order to prove (34), we begin with the following:

$$\overline{Q}(x,p) = \int_0^{\infty}\exp(-pt)Q(x,t)dt = \int_x^{\infty}\exp(-pt)F(x,t)dt = \exp(-px)\int_0^{\infty}\exp(-pz)F(x,x+z)dz,$$

from which we acquire $\overline{Q}(x,p)\exp(px) = \int_0^{\infty}\exp(-pz)F(x,x+z)dz.$

Passing to the variable $u = pz$ in the integral, we have

$$p\overline{Q}(x,p)\exp(px) = \int_0^{\infty}\exp(-u)F(x,x+\frac{u}{p})du.$$

The transition to the limit with respect to (29) and (34) while $p \to \infty$ leads to the following relation

$$|\Delta| = \lim_{p\to\infty}\left[p\overline{Q}(x,p)\exp(px)\right] = \exp\left[-(\beta_1 x/2)\right]. \quad (35)$$

Finally, an interesting result is derived from the above calculations and (33):

$$1-\frac{1}{\pi}\int_0^{\beta_1}\frac{1}{y+\beta_2}\exp\left[-(y+\beta_2)x\right]\sin\left[x(y+\beta_2)\sqrt{\frac{\beta_1-y}{y}}\right]dy = \exp\left[-(\beta_1 x/2)\right]. \quad (36)$$

This requires a special explanation (which is supposed to be done in a subsequent publication). From (31), following the rule of differentiating the original $\int_0^t f(\tau)d\tau \xrightarrow[*]{*} (1/p)\overline{f}(p)$ we find another original for the image, which also poses an interest to operational calculus:

$$\exp\left[-xp\sqrt{\frac{p+(\beta_1+\beta_2)}{p+\beta_2}}\right] \xleftarrow[*]{*} \left\{1-\frac{1}{\pi}\int_0^{\beta_1}\frac{1}{y+\beta_2}\exp\left[-(y+\beta_2)t\right]\sin\left[x(y+\beta_2)\sqrt{\frac{\beta_1-y}{y}}\right]dy\right\}\delta(t-x) +$$
$$\left\{\frac{1}{\pi}\int_0^{\beta_1}\exp\left[-(y+\beta_2)t\right]\sin\left[x(y+\beta_2)\sqrt{\frac{\beta_1-y}{y}}\right]dy\right\}\eta(t-x). \quad (37)$$

Finally, we express the operational solutions to the boundary value problems (2)–(7) in generalized variables:

$\xi = \frac{x}{\sqrt{a\tau_r}}, \tau = t/\tau_r, Bi^* = h\sqrt{a\tau_r}, W(\xi,\tau) = \frac{T(x,t)-T_0}{T_c - T_0}$ for the cases (4)–(6) and

$W(\xi,\tau) = \frac{T(x,t)-T_0}{q_0\sqrt{a\tau_r}/\lambda}$ (for the case of (5)).

We discover:

$$\overline{W}(\xi,p) = \overline{f}(p)\exp\left[-\xi\sqrt{p(p+1)}\right], \quad (38)$$

where $\overline{f}(p) = \frac{1}{p}$ in the case of (4), $\overline{f}(p) = \frac{p+1}{p^{3/2}}$ in the case of (5), and $\overline{f}(p) = \frac{Bi^*\sqrt{p+1}}{p(\sqrt{p}+Bi^*\sqrt{p+1})}$ in case (6).

All originals can be found using the above ratios. It was shown in [3] that the originals of images (38) allow for a transition to new functional constructions that are equivalent to those given above and are very convenient for conducting numerical experiments. This is one of the features of the solutions of hyperbolic transport models for partially bounded domains.

Conclusions

The work has presented the originals of non-standard images, which are part of the operational solutions of a wide class of mathematical models in the theory of transfer (heat, mass, momentum), in network analysis, in the thermal shock theory of viscoelastic bodies, etc. A further development of the problem is the use of cylindrical coordinates for the radial gradients of the physical quantities under examination.

The author declares no conflict of interest.

References:

1. Kartashov E.M., Kudinov V.A. Analytical theory of heat conduction and applied thermoelasticity. Moscow: URSS Publ., 2013. 651 p. (in Russ.).

2. Kartashov E.M., Kudinov V.A. Analytical methods of the theory of heat conduction and its applications. Moscow: URSS Publ., 2018. 1080 p. (in Russ.).

3. Kartashov E.M. Analytical solutions of hyperbolic models of unsteady thermal conductivity. *Tonkie Khimicheskie Tekhnologii = Fine Chemical Technologies.* 2018;13(2):81-90 (in Russ.). https://doi.org/10.32362/2410-6593-2018-13-2-81-90

4. Kudinov V.A., Kudinov I.V., Kartashov E.M. (General edition). Methods for solving parabolic and hyperbolic equations for the transfer of heat, mass, momentum. Moscow: URSS Publ., 2016. 336 p. (in Russ.).

5. Lykov A.V. Theory of heat conduction. Moscow: Vysshaya shkola Publ., 1967. 600 p. (in Russ.).

6. Kartashov E.M. Analytical solutions of hyperbolic models of transfer. *Inzhenerno-Fizicheskii zhurnal = Journal of Engineering Physics and Thermophysics.* 2014;87(5):1072-1082. (in Russ.).

7. Karslow H., Eger D. Operational methods in applied mathematics. Moscow: Inostrannaya literatura Publ., 1948. 294 p. (in Russ.).

8. Ango A. Mathematics for electrical and radio engineers. Moscow: Nauka Publ., 1964. 772 p. (in Russ.).

Список литературы:

1. Карташов Э.М., Кудинов В.А. Аналитическая теория теплопроводности и прикладной термоупругости. М.: URSS, 2013. 651 с.

2. Карташов Э.М., Кудинов В.А. Аналитические методы теории теплопроводности и ее приложений. М.: URSS, 2018. 1080 с.

3. Карташов Э.М. Аналитические решения гиперболических моделей нестационарной теплопроводности // Тонкие химические технологии. 2018. Т. 13. № 2. С. 81–90. https://doi.org/10.32362/2410-6593-2018-13-2-81-90

4. Кудинов В.А., Кудинов И.В., Карташов Э.М. (Общая редакция). Методы решения параболических и гиперболических уравнений переноса тепла, массы, импульса. М.: URSS, 2016. 336 с.

5. Лыков А.В. Теория теплопроводности. М.: Высшая школа, 1967. 600 с.

6. Карташов Э.М. Аналитические решения гиперболических моделей переноса // Инжен.-физич. журнал. 2014. Т. 87. № 5.С. 1072–1082.

7. Карслоу Х., Егер Д. Операционные методы в прикладной математике. М.: Иностранная Литература, 1948. 294 с.

8. Анго А. Математика для электро- и радиоинженеров. М.: Наука, 1964. 772 с.

About the author:

Eduard M. Kartashov, Dr. of Sci. (Physics and Mathematics), Professor of the Chair of Higher and Applied Mathematics, M.V. Lomonosov Institute of Fine Chemical Technologies, MIREA – Russian Technological University (86, Vernadskogo pr., Moscow 119571, Russia).

Об авторе

Карташов Эдуард Михайлович, доктор физико-математических наук, профессор кафедры высшей и прикладной математики Института тонких химических технологий им. М.В. Ломоносова ФГБОУ ВО «МИРЭА – Российский технологический университет» (119571, Россия, Москва, пр-т Вернадского, д. 86).

For citation: Kartashov E.M. Originals of operating images for generalized problems of unsteady heat conductivity. *Tonkie Khimicheskie Tekhnologii = Fine Chemical Technologies.* 2019;14(4):77-86 (in Russ.). https://doi.org/10.32362/2410-6593-2019-14-4-77-86

Для цитирования: Карташов Э.М. Оригиналы операционных изображений для обобщенных задач нестационарной теплопроводности // Тонкие химические технологии. 2019. Т. 14. № 4. С. 77–86. https://doi.org/10.32362/2410-6593-2019-14-4-77-86

Translated by S. Durakov

Author Guidelines

The scientific and technical reviewed journal Fine Chemical Technologies is issued 6 times a year and publishes original experimental and theoretical works in form of unabridged articles, brief reports, reviews by the authors and also predictive and analytical articles in the field of fine chemical technologies and related sciences. The main sections of the journal are

- Theoretical bases of chemical technologies
- Chemistry and technology of organic substances
- Chemistry and technology of medicinal compounds and biologically active substances
- Synthesis and processing of polymeric composites
- Chemistry and technology of inorganic materials
- Analytical methods in chemistry and chemical technology
- Mathematics methods and information systems in chemical technologies
- Review articles

The papers are submitted in English or Russian and are published in the original language. We recommend authors to submit their manuscript strictly online, via the e-mail address *vestnik@mitht.ru*.

Liability of the authors

The authors who present their works for publication in the Fine Chemical Technologies journal shall guarantee that the papers are original (have not been published in other media in the present form or similar to it in content), the works are not under consideration in editorial boards of other publications, and all potential conflicts of interest relating to the copyright and publication of the respective articles have been settled.

Liability of the Editorial Board:

All manuscripts are accepted for publication on the grounds of the results of the review thereof. It is a custom in the journal to provide a single-blind review by two independent experts. At this point in time, there is a move towards a double-blind review. Members of the Editorial Board and external experts who specialize in areas close to those of the reviewed works are engaged for the purpose.

The Editorial board is liable for the quality of the research articles, takes measures not to allow inadequate actions on the part of the authors and reviewers, and oversees that norms of publishing ethics be complied with.

The manuscript of a research article received by the journal's Editorial Board is reviewed by the Editor-in-Chief as to its conformity to the profile of the journal and the requirements set to the text layout and formatting. Articles that fail to meet the profile of the journal or the requirements set thereto are rejected by the Editorial Board without any review.

It is the prerogative of the Editorial Board to select the reviewer (the names of the reviewers are not be disclosed). Articles accepted for the publication are thoroughly edited. Minor amendments and corrections of stylistic, formal and editor's list nature are entered into the article without the approval of the authors. If due to the review or editing more serious corrections are needed, the article will be sent back to the authors for finalization. The authors will have to incorporate all the amendments necessary to be made from their viewpoint and make comments regarding all he critical remarks in a response letter to the Editorial Board. The finalized manuscript should be returned to the Editorial Board within a maximally short time (not exceeding 10 working days) together with the previous version of the article and the electronic version of the finalized text.

Submitting articles to the Editorial Board

Manuscripts are accepted either in Russian or in English and are published in the original language. The recommended length of the manuscript of an original study is 10 to 15 pages of the A4 format (up to 27000 symbols with spaces), a review article – 30 to 35 pages of the A4 format (up to 60000 symbols with spaces) together with tables and references.

The following materials should be also presented to the Editorial Board in the scanned format addressed to *vestnik@mitht.ru*

- The manuscript signed by all the authors of the article;
- The expert opinion;
- A cover letter on behalf of the organization where the work was fulfilled;
- Statement of the authors regarding absence of conflicts of interest;
- Completed contract on the transfer of rights to use the creative work.

Apart from that, it is necessary to provide the above manuscript of the article in Microsoft Word format to the above e-mail address and provide the names of the potential reviewers (at least three experts) specifying their full names, affiliation and e-mail addresses. The suggested reviewers should not be working in the same organization with the authors and there should be no conflicts of interest. The editors reserve the right to choose reviewers and appoint reviewers at their discretion.

Requirements to the layout and format of the manuscript

The text of the manuscript should be executed in Microsoft Office Word and saved in doc, docx, rtf formats. The end-to-end numbering is adopted for the manuscript. Lettering in Times New Roman is preferable in all cases (font size 12 pt with 1.5 line spacing and 2 cm margins). All the materials should be aggregated in a single complete file with all figures, tables and any additional supplemental materials. Please organize your text in the following sequence:

Writing an abstract (Russian block follows English one):

- UDC;
- Title of the article (semi-bold);
- Authors and their affiliated institutions, linked by superscript numbers, should be listed beneath the title on the opening page of the manuscript.
- E-mail address of the author engaged in correspondence (@Corresponding author, e-mail address);
- An abstract in a structured format that should briefly repeat the main sections of the article (the aim, methods, results and conclusions described in the article amounting to 250-300 words). An abstract should be clear for understanding without the reader having to turn to the very text of the article.
- Keywords (from 5 to 10 words or word combinations separated by comma, which characterize the content of the article).
- Glossary of all the English terms used in the article.

The body of the text

The authors of the articles should necessarily stick to the following structure of the text (IMRAD structure – Introduction, Methods, Results and Discussion):

- brief information about the status of the issue under consideration and setting the objective to be achieved in the article;
- method to achieve the objectives set in the article and accepted assumptions;
- the main content of the article (for instance, the description of the essence of processes and phenomena, proof of the ideas stated in the article, source and target mathematical formulae, mathematical computations and transformations, experiments and calculations, examples and illustrations);
- discussion of the results received and comparing thereof with the previously known;
- conclusions and recommendations.

Acknowledgments

Acknowledgments section may be presented in Russian, English or both languages. It should comprise the following:

- **Clarification regarding any potential or actual conflicts of interest of the authors.** Any affiliations, financial relations, financial or political interests in the manuscript, including employment and other liabilities that may result in withholding or deliberate corruption of data or adversely influenced interpretation, are

considered a conflict of interest and must be explicitly stated as such. Please note that conflicts of interest do not impede a publication, though failure to disclose one does.

• **A brief list of funding sources** for the results reported in the paper, as well as the publication process itself (*e.g.* a commercial organization, a foundation or government grant, *etc.*).

• An optional note describing **the roles or responsibilities of the authors**. You may also place here an acknowledgment for any individuals or organizations that assisted in your work.

References

References are placed in the end of the article (starting with a new page) and are presented in conformity with the requirements given below. References should be numbered in the order in which they are cited. Within the body of the text references should be provided in Arabic numerals enclosed in square brackets. The reference list should be formed by hand without the use of the List function.

List of references should be organized according to the guidelines by U.S. National Information Standards Organization NISO Z39.29-2005 [R2010] in **Vancouver style**. In references to cited literature it is necessary to specify for the journal the names and initials of all the authors, the title of the article, the name of the journal, the year, number, volume, page numbers (from and to), DOI of the article (if any); for book publications: place of publication (city), name of the publishing house, year of publication, total number of pages or cited pages (from and to). It is not advisable to make references to author's abstracts and theses, anonymous sources in the Internet, statistical reports, articles in sociopolitical newspapers and magazines, textbooks and manuals. Self-citation should not exceed 20%. All references should be verified carefully.

References:

1. Ivanov A.E., Zubov V.P. Smart polymers as surface modifiers for bioanalytical devices and biomaterials: theory and practice. *Russ. Chem. Rev.* 2016;85(6):565-584. https://doi.org/10.1070/RCR4567

2. Zeidler J., Baraniak D., Ostrowski T. Bioactive nucleoside analogues possessing selected five-membered azaheterocyclic bases. *Eur. J. Med. Chem.* 2015;97:409-418. https://doi.org/10.1016/j.ejmech.2014.11.057

3. Rukk N.S., Zakalyukin R.M., Skryabina A.Yu. Lantanide oxyiodides. *Tonkie Khimicheskie Tekhnologii = Fine Chemical Technologies.* 2016;11(1):5-22 (in Russ.). https://doi.org/10.32362/2410-6593-2016-11-1-5-22

4. Tret'yakov Yu.D., Martynenko L.I., Grigor'ev A.N., Tsivadze A.Yu. Inorganic Chemistry. Moscow: Khimiya Publ., 2001. V. 1. 472 p. (in Russ.).

Information about the authors:

In the very end of the article, information about all the authors should be provided in conformity with the sample attached. The authors should specify the ORCID number as well as Researcher ID and Scopus Author ID (if any). The BSI standard is fit for the transliteration of the authors' names.

About the authors:

Irina S. Silina, Postgraduate Student of the Chair of General Chemical Technology, M.V. Lomonosov Institute of Fine Chemical Technologies, MIREA – Russian Technological University (86, Vernadskogo pr., Moscow 119571, Russia). ResearcherID (if any), Scopus Author ID (if any), ORCID. E-mail.

Yuriy A. Treger, Dr. of Sci. (Chemistry), Professor, Advisor of General Director, LLC Scientific Research Engineering Center Sintez (86, Vernadskogo pr., Moscow 119571, Russia). ResearcherID (if any), Scopus Author ID (if any), ORCID. E-mail.

Full name and the contact number of the author who is to be negotiated with on the issue of publication should be specified on a separate page.

Additional requirements to the layout and format of the text, figures, graphs and tables:

It is allowed to archive text documents and figures (rar, zip).

When working on the layout of the manuscript it is advised to observe the following requirements:

• automatic hyphenation should not be used;

• the following signs «…» should be used as inverted commas;

• the sign «–» (dash) should be separated by spaces, the signs "minus", "interval" or "chemical bond" are not separated by spaces;

- only «×» should be used as a multiplication sign;
- in decimals used in the text and in figures point should be used to separate the whole from the fraction part (0.25 instead of 0,25);
- letters of Latin and Greek alphabets should be used in formulas;
- use SI system when selecting units of measure;
- abbreviations used in the article should be deciphered when first used in the text (with the exception of commonly used abbreviations);
- it is not allowed to duplicate the data in the text, tables and figures.

Tables should have titles and running numbers which are referenced to in the text. If there is only one table in the text, it is not numbered. Tables should include only necessary numerical data. The use of data which is not discussed in the text is not permitted. The width of a table should not exceed 75 mm (when placed in a single column), or 160 mm (if placed across the width of the page). The alignment of horizontal lines and vertical columns in the table should be strictly observed.

Illustrations (figures, graphs) should be presented in the format fit for direct reproduction.

All the figures should have inscriptions. All the figures should be numbered in Arabic numerals in the order in the text and the text should contain a note to the figure. If there is only one picture in the text, it is not numbered.

Figures are placed in the text of the manuscript. Inscriptions to figures are placed under the figures and are not duplicated in the figure file. Also, the figures are presented in separate files in the tiff or png format with the definition of at least 300 dpi, archived if necessary. The name of the file should contain the name of the first author in Latin type and the number of the figure which should be the same as the number of the figure in the text (for instance, Demidov_Fig.2.tif). Each file should contain only one figure.

Illustrations in color which will be available in electronic versions of the articles placed on the website of the journal and e-library.ru are also allowed. Should it be necessary to place vector drawings, they should be presented in the format of the program used when they were made: Adobe Illustrator or in the EPS format. The creation of graphs with the Microsoft Excel may be also possible with subsequent saving in the aforementioned formats. It is strongly unadvisable to use Microsoft Graph, Microsoft Draw (supplied together with Microsoft Word), PaintBrush (Windows component) and Paint (Windows 95 component).

Figures and photographs should have contrast images. The size of the figure should be no more than 75 mm broad (when placed in a single column), or not exceed 150 mm (when placed across the page.

Formulas are typed in the formula editor Microsoft Equation 3.0 or Math Type program. The use of other programs should be approved by the Editorial Board. Font Sizes in mathematical editor are as follows: Equation editor: regular symbol 10pt, large index – 8pt, small index – 6pt, large symbol 12pt, small symbol – 8pt. If several formulas (equations) are used in the text, they should be numbered in sequence.

The size of the formula in width should be no longer than 75 mm (if placed in one column), or no longer than 150 mm (when placed across the width of the page); formulas should be presented in the format suitable for direct reproduction.

Structural chemical formulas and reaction schemes should be located in the text and performed in the ChemWindow program. The following settings are recommended: link length 14.4 PT (0.508 cm), line thickness 0.6 PT (0.021 cm). The fonts Arial or Helvetica, 9 PT, are preferred in formulas. Chemical compounds in the schemes are numbered in bold Arabic numerals without brackets (Arial Bold 9 PT). In the text, the number of the full title of a connection is given in brackets, in other cases without them, but with obligatory explanation. The size of the chemical formula should be no more than 75 mm broad (when placed in a single column), or not exceed 150 mm (when placed across the page. Chemical formulas and schemes should be presented in the format fit for direct reproduction. The scheme number and the explanatory inscription should be placed under the scheme in the center and separated from the subsequent text by one empty line.

Footnotes

Footnotes are numbered in Arabic numerals. Footnotes may contain links to anonymous sources on the Internet, statistical reports, articles in socio-political newspapers and magazines, textbooks and manuals, references to abstracts and theses, and comments of the authors.

Submission of a manuscript for publication suggests that all the authors accept the given instructions.

Address of the Editorial Office: 86, Vernadskogo pr., Moscow 119571, Russian Federation.
Phone number: +7(495)246-05-55 (# 2-88)
E-mail: *vestnik@mitht.ru*
Chief of the editorial staff: Galina D. Seredina

Printed in MIREA – Russian Technological University.
78, Vernadskogo pr., Moscow, 119454, Russian Federation.
Signed to print on August 30, 2019.
Format 60×90/8. Digital print.
C.p.l. 11,5.
100 copies. Order no. 905.
Price: RUR 1061,30

Отпечатано в МИРЭА – Российском технологическом университете.
119454, РФ, г. Москва, пр-кт Вернадского, д. 78.
Подписано в печать 30.08.2019 г.
Формат 60×90/8. Печать цифровая.
Уч.-изд. листов 11,5.
Тираж 100 экз. Заказ № 905.
Цена 1061,30 руб.

ИОНХ РАН

Черняев 2019

Dear Colleagues,

We are pleased to invite you to participate in the **XXII International Chernyaev Conference on Chemistry, Analytics, and Technology of Platinum Metals** that will be held from **November 18 to November 22, 2019** in Moscow, Russia at the **Kurnakov Institute of General and Inorganic Chemistry, Russian Academy of Sciences,** and **MIREA – Russian Technological University.**

The Conference aims to summarize the results of fundamental and applied research in the field of chemistry, analysis, technology, application of platinum metals and gold, compounds and materials based on them; to discuss general trends and prospects.

The information about the Conference is available on the website www.chernyaev2019.ru

Program

Section 1. Chemistry of compounds of platinum metals and gold
Section 2. Analytical chemistry of platinum metals and gold
Section 3. Technology of processing of raw materials and production of platinum metals and gold
Section 4. Application of platinum metals and gold

The conference will be accompanied by an exhibition of instruments, equipment, reagents, and standard samples.

Sponsors:

РФФИ

Российская Академия Наук

ЛАБТЕСТ LABTEST

КРАСЦВЕТМЕТ

plaurum
Екатеринбургский завод по обработке цветных металлов

КОРТЭК

Information partners:

ЖУРНАЛ НЕОРГАНИЧЕСКОЙ ХИМИИ

ЖУРНАЛ «КООРДИНАЦИОННАЯ ХИМИЯ»

ТОНКИЕ ХИМИЧЕСКИЕ ТЕХНОЛОГИИ Fine Chemical Technologies

ТЕХНОСФЕРА
Аналитика www.j-analytics.ru
НАУЧНО-ТЕХНИЧЕСКИЙ ЖУРНАЛ

Химия и жизнь
научно-популярный журнал
издается с 1965 года

ДМДК